

Top-K Pairwise Ranking: Bridging the Gap Among Ranking-Based Measures for Multi-Label Classification

Zitai Wang^{1,2}, Qianqian Xu^{3*}, Zhiyong Yang⁴, Peisong Wen^{3,4}, Yuan He⁵,
Xiaochun Cao⁶, Qingming Huang^{4,3,7*}

¹IIE, Chinese Academy of Sciences, Beijing, 100093, Beijing, China.

²SCS, University of Chinese Academy of Sciences, Beijing, 100049, Beijing, China.

³IIP, ICT, Chinese Academy of Sciences, Beijing, 100190, Beijing, China.

⁴SCST, University of Chinese Academy of Sciences, Beijing, 100049, Beijing, China.

⁵Alibaba Group, Hangzhou, 311121, Zhejiang, China.

⁶SCST, Shenzhen Campus of Sun Yat-sen University, Shenzhen, 518107, Guangdong, China.

⁷BDKM, University of Chinese Academy of Sciences, Beijing, 101408, Beijing, China.

*Corresponding author(s). E-mail(s): xuqianqian@ict.ac.cn; qmhuang@ucas.ac.cn;

Contributing authors: wangzitai@iie.ac.cn; yangzhiyong21@ucas.ac.cn;
wenpeisong20z@ict.ac.cn; heyuan.hy@alibaba-inc.com; caoxiaochun@mail.sysu.edu.cn;

Abstract

Multi-label ranking, which returns multiple top-ranked labels for each instance, has a wide range of applications for visual tasks. Due to its complicated setting, prior arts have proposed various measures to evaluate model performances. However, both theoretical analysis and empirical observations show that a model might perform inconsistently on different measures. To bridge this gap, this paper proposes a novel measure named Top-K Pairwise Ranking (TKPR), and a series of analyses show that TKPR is compatible with existing ranking-based measures. In light of this, we further establish an empirical surrogate risk minimization framework for TKPR. On one hand, the proposed framework enjoys convex surrogate losses with the theoretical support of Fisher consistency. On the other hand, we establish a sharp generalization bound for the proposed framework based on a novel technique named data-dependent contraction. Finally, empirical results on benchmark datasets validate the effectiveness of the proposed framework.

Keywords: Image Classification, Multi-Label Classification, Model Evaluation, Top-K Ranking.

1 Introduction

In many real-world visual tasks, the instances are intrinsically multi-labeled [Boutell et al \(2004\)](#); [Carneiro et al \(2007\)](#); [Wang et al \(2016\)](#); [Chen et al \(2019\)](#). For example, a photo taken on a coast might consist of multiple objects such as the sea,

beach, sky, and cloud. Hence, Multi-Label Classification (MLC) has attracted rising attention in recent years [Liu et al \(2022b\)](#); [Wei et al \(2022\)](#); [Ding et al \(2023\)](#); [Wu et al \(2023\)](#); [Kim et al \(2023\)](#); [Liu et al \(2023\)](#); [Chen et al \(2023\)](#).

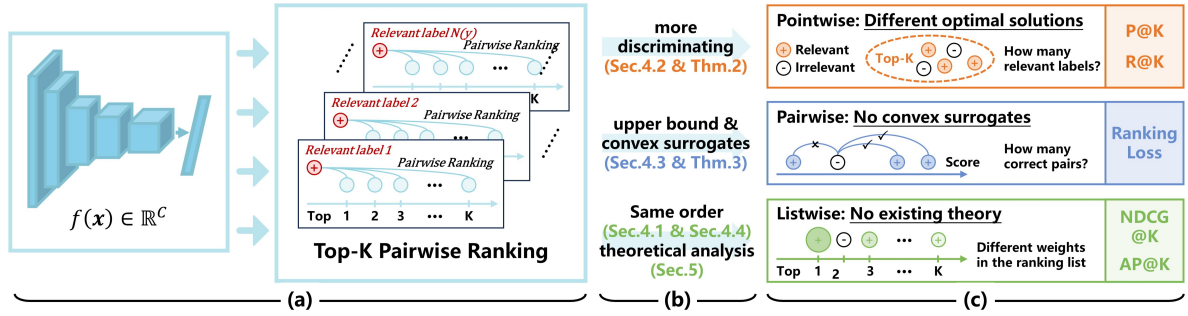


Fig. 1 Overview of measure comparison: (a) the definition of the proposed TKPR measure, (b) the advantages of TKPR over existing ranking-based measures, and (c) representative ranking-based measures and their limitations.

Due to the complicated setting, a number of measures are proposed to evaluate the model performance Zhang and Zhou (2014); Wu and Zhou (2017); Liu et al (2022b). Generally speaking, existing MLC measures can be divided into two groups: the threshold-based ones and the ranking-based ones. The former ones, such as the Hamming loss Dembczynski et al (2012b); Wu and Zhu (2020), the subset accuracy Wu and Zhu (2020); Gerych et al (2021), and the F-measure Tsoumakas et al (2011a); Ye et al (2012); Waegeman et al (2014), require predefined thresholds to decide whether each label is relevant. Although these measures are widely used due to its intuitive nature, the optimal thresholds might vary according to the decision conditions in the test phase, and thus predefined thresholds could produce systematic biases. By contrast, the ranking-based ones only check whether the relevant labels are top-ranked, which is insensitive to the selection of thresholds. In view of this, this paper focuses on the ranking-based measures and their optimization, which is also known as Multi-Label Ranking (MLR) Dembczynski et al (2012a); Li et al (2017b); Wu et al (2021).

As shown in Fig.1(c), existing ranking-based measures fall into the following three categories, according to the taxonomy in Learning-to-Rank Liu (2009): (1) Pointwise approaches, such as precision@K and recall@K Wydmuch et al (2018); Menon et al (2019), reduce MLC to multiple single-label problems and check whether each relevant label is ranked higher than K. (2) Pairwise approaches, such as the ranking loss Dembczynski et al (2012a); Gao and Zhou (2013); Wu and Zhu (2020); Wu et al (2021) and AUC Wu and Zhou (2017), transforms MLC into a series of pairwise problems that checks whether the relevant label

is ranked higher than the irrelevant one. (3) Listwise approaches, such as Average Precision (AP) Wu et al (2020); Ridnik et al (2021) and Normalized Discounted Cumulative Gain (NDCG) Prabhu and Varma (2014); Kalina and Krzysztow (2018), do not have such transformation.

Faced with these measures, prior arts have provided a series of theoretical and empirical insights Gao and Zhou (2013); Wu and Zhou (2017); Kalina and Krzysztow (2018); Menon et al (2019); Wu and Zhu (2020); Wu et al (2021). However, two important problems remain open. On one hand, the Bayes optimal solutions to different measures might be different. Consequently, **optimizing a specific measure does not necessarily induce better model performances in terms of the others**. For example, Menon et al (2019) theoretically shows that no multiclass reduction can be optimal for both precision@K and recall@K. Empirically, as shown in Fig.2(a), the model performances on different measures show different trends when optimizing the ranking loss. One potential remedy is to optimize the more discriminating listwise measures. However, the connection among these measures has not been well studied, though some literature has compared the measures within the same category Kalina and Krzysztow (2018); Menon et al (2019); Wu and Zhu (2020). On the other hand, **efficient optimization on these complicated measures is still challenging**. For instance, Gao and Zhou (2013) shows that convex surrogate losses are inconsistent with the ranking loss. Although Dembczynski et al (2012a) presents a consistent surrogate, its generalization property and empirical performance are not satisfactory Wu et al (2021). Hence, a natural question arises:

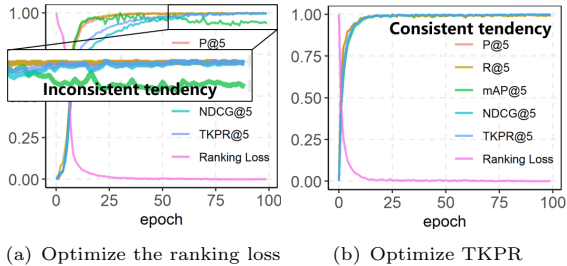


Fig. 2 Normalized ranking-based measures *w.r.t.* the training epoch on the Pascal VOC 2007 dataset in the MLC setting. (a) When optimizing the ranking loss, the changes in different measures are inconsistent. (b) By contrast, when optimizing TKPR, the changes are highly consistent.

Whether there exists a measure that is **(A)** compatible with other measures and also **(B)** easy to optimize?

To answer this question, as shown in Fig.1(a), we construct a novel measure named Top-K Pairwise Ranking (TKPR) by integrating the intelligence of existing ranking-based measures. As shown in Sec.4.1, TKPR has three equivalent formulations that exactly correspond to the aforementioned three categories of measures. On top of the pointwise formulation, the analysis in Sec.4.2 shows that TKPR is more discriminating than precision@K and recall@K. Then, Sec.4.3 shows that the pairwise formulation of TKPR is the upper bound of the ranking loss. Finally, based on the listwise formulation, Sec.4.4 shows that TKPR has the same order as a cut-off version of AP. To sum up, as shown in Fig.2(b), **TKPR is compatible with existing ranking-based measures**, which answers **(A)**.

Considering these advantages, it is appealing to construct an Empirical Risk Minimization (ERM) framework for TKPR, as an answer to **(B)**. As shown in Sec.5, the original objective has the following abstract formulation:

$$\min_f \mathbb{E}_{(\mathbf{x}, \mathbf{y})} \left[\sum_i \sum_k \ell_{i,k}(f; \mathbf{x}) \right], \quad (1)$$

where the loss $\ell_{i,k}$ takes the model prediction $f(\mathbf{x})$, a relevant label i , and the top- k label as inputs.

First, in Sec.5.1, we replace the discrete loss $\ell_{i,k}$ with differentiable surrogate losses. One basic

requirement for such surrogates is Fisher Consistency, *i.e.*, optimizing the surrogate objective should recover the solution to Eq.(1). In this direction, prior arts Wydmuch et al (2018); Menon et al (2019); Wang et al (2023) assume that no ties exist in the conditional distribution $\mathbb{P}[y_i = 1 | \mathbf{x}]$. By contrast, we adopt a more practical with-tie assumption since some labels could be highly correlated in the multi-label setting. Under this assumption, we first present a necessary and sufficient condition for the Bayes optimal solution to Eq.(1) in Sec.5.1.1. On top of this, a sufficient condition is established for TKPR Fisher consistency in Sec.5.1.2, which indicates that **common convex losses are all reasonable surrogates**.

Then, we turn to minimize the unbiased estimation of the surrogate objective over the training data sampled from the distribution. But, whether the performance on training data can generalize well to unseen data? First, in Sec.5.2.1, we show that, based on the traditional techniques Wu and Zhu (2020); Wu et al (2021), the proposed framework can achieve a generalization bound proportional to \sqrt{K} , where K is a hyperparameter determined by the largest ranking position of interest. For scenarios requiring a large K , this bound is rather unfavorable. To fix this issue, in Sec.5.2.2, we extend the traditional definition of Lipschitz continuity and propose a novel technique named data-dependent contraction. On top of this, we can **obtain informative generalization bounds** that not only eliminate the dependence on K , but also become sharper under an imbalanced label distribution. What’s more, the proposed framework also achieves sharper bounds on the pairwise ranking loss. Eventually, in Sec.5.2.3, we show that the novel technique is applicable to both kernel-based models and convolutional neural networks by presenting the corresponding practical results.

Finally, the empirical results presented in Sec.6 validate the effectiveness of the learning algorithm induced by the ERM framework and the theoretical results.

To sum up, the contribution of this paper is four-fold:

- **New measure with detailed comparison:** We propose a novel measure named TKPR that is compatible with existing ranking-based MLC

measures such as precision@K, recall@K, the ranking loss, NDCG@K, and AP@K.

- **ERM framework with consistent convex surrogates:** An ERM framework for TKPR optimization is established with convex surrogate losses, supported by Fisher consistency.
- **Technique for generalization analysis:** A novel technique named data-dependent contraction provides sharp and informative generalization bounds.
- **Induced Algorithm and Empirical Validation:** The empirical results not only speak to the effectiveness of the learning algorithm induced by the ERM framework, but also validate the theoretical results.

2 Related Work

2.1 Multi-Label Classification

In this part, we outline existing methods and some common settings for multi-label classification.

According to the taxonomy presented in [Zhang and Zhou \(2014\)](#), traditional methods for MLC fall into two categories. The first category, named **problem transformation**, transforms MLC into other well-studied problems. For example, one-vs-all approaches treat the prediction on each label as a binary classification problem [Boutell et al \(2004\)](#); [Dembczynski et al \(2010, 2012b\)](#). Ranking-based approaches optimize the pairwise ranking between relevant and irrelevant labels [Fürnkranz et al \(2008\)](#); [Gao and Zhou \(2013\)](#). And [Tsoumakas et al \(2011a\)](#); [Boutell et al \(2004\)](#); [Jernite et al \(2017\)](#); [Menon et al \(2019\)](#) reduce MLC to multiple multiclass problems, where each problem consists of a relevant label. The second category, named **algorithm adaptation**, utilizes traditional learning techniques to model multi-label data such as decision tree [Clare and King \(2001\)](#) and SVM [Elisseeff and Weston \(2001\)](#).

In the era of deep learning, algorithm adaptation methods utilize the high learning capability of neural networks to model the correlation between classes. For example, [Wang et al \(2016\)](#); [Chen et al \(2019\)](#); [Tang et al \(2020\)](#) utilize Recurrent Neural Networks (RNNs) or Graph Convolutional Networks (GCNs) to exploit the higher-order dependencies among labels. [Wang et al \(2017\)](#); [You et al \(2020\)](#); [Ye et al \(2020\)](#) capture the attentional regions of the image by exploiting the information

hidden in the label dependencies. As an orthogonal direction, **loss-oriented methods**, which follow the inspiration of problem transformation, aims to boost the learning process with well-designed loss functions. For example, [Wu et al \(2020\)](#) proposes a weighted binary loss to handle the imbalanced label distribution. [Ridnik et al \(2021\)](#) designs an adaptive weight scheme for the binary loss to pay more attention to hard-negative labels. Recently, [Liu et al \(2022a\)](#) employs causal inference to eliminate the contextual bias induced by co-occurrence but out-of-interest objects in images.

In another direction, an emerging trend is to learn with partial annotations since fully-annotated multi-label datasets are generally expensive. However, the definition of partial annotation still lacks consensus. For example, MLML [Sun et al \(2010\)](#); [Cole et al \(2021\)](#); [Zhou et al \(2022\)](#); [Chen et al \(2023\)](#) assumes that only a part of relevant labels, even only a single relevant label, is available. This setting is correlated to extreme multi-label learning, where an extremely large number of candidate labels is of interest [Liu et al \(2017\)](#); [Wydmuch et al \(2018\)](#); [Kalina and Krzysztof \(2018\)](#); [Wei et al \(2022\)](#). As a comparison, the other MLML setting assumes that a part of irrelevant labels is also available [Wu et al \(2014, 2018\)](#); [Baruch et al \(2022\)](#). And PML [Xu et al \(2019\)](#); [Xie and Huang \(2022\)](#) requires all relevant labels and assumes that extra false positive labels exist.

In this paper, the proposed framework belongs to both problem transformation and loss-oriented methods. Besides, this framework is naturally applicable to MLML since the objective does not require irrelevant labels as inputs. Thus, we also provide the empirical results under the MLML setting in Sec.6.

2.2 Optimization on Ranking-Based Measures

In this part, we briefly review the optimization methods on ranking-based measures. Note that **the scenario is not limited to multi-label classification**. In fact, a significant part of methods in this direction focuses on the binary case, where the top-ranked instances are of interest, rather than labels.

2.2.1 Top-K Optimization

The top-K measure, which checks whether the ground-truth label is ranked higher than K, is a popular metric for multiclass classification when semantic ambiguity exists among the classes [Xu et al \(2014\)](#); [Russakovsky et al \(2015\)](#); [He et al \(2016\)](#). The key issue of top-K optimization is its Bayes optimal solution. To be specific, the early work [Lapin et al \(2015\)](#) simply relaxes the multi-class hinge loss. However, [Lapin et al \(2016, 2018\)](#) point out that the induced objective is inconsistent with the top-K measure. In other words, optimizing the relaxed objective does not necessarily recover the solution to the original one. To fix this issue, [Yang and Koyejo \(2020\)](#) establishes a sufficient and necessary condition for top-K consistency, that is, the top-K preserving property.

Faced with multi-label data, [Menon et al \(2019\)](#) shows that the pointwise measures, precision@K and recall@K, is equivalent to the top-K measure averaged on relevant labels. In [Sec.4](#), we show that TKPR has a similar but more discriminating pointwise formulation.

2.2.2 Multi-Label AUC Optimization

As a representative pairwise ranking measure, AUC measures the probability that the positive instance is ranked higher than the negative one in each pair [Ling et al \(2003\)](#). In multi-label learning, AUC has three formulations that average correctly-ranked pairs on each label, each instance, and prediction matrix, named macro-AUC, instance-AUC, and micro-AUC, respectively [Wu and Zhou \(2017\)](#). Formally, the ranking loss is equivalent to instance-AUC. However, the theoretical analyses cannot simply adapt from the single-labeled AUC [Yang et al \(2022\)](#); [Wang et al \(2022\)](#); [Yang and Ying \(2023\)](#); [Yang et al \(2023\)](#); [Dai et al \(2023\)](#) to the ranking loss. To be specific, [Gao and Zhou \(2013\)](#) points out that no convex surrogate loss is consistent with the ranking loss. To address this issue, [Dembczynski et al \(2012a\)](#); [Wu et al \(2021\)](#) propose pointwise convex surrogates for the ranking loss. Unfortunately, neither the theoretical generalization bound nor the empirical results of these surrogates is satisfactory.

As shown in [Sec.3.2.2](#) and [Sec.5.2](#), the proposed framework provides a promising solution to minimizing the ranking loss. And the empirical analysis in [Sec.6](#) also validates its effectiveness.

2.2.3 AP & NDCG Optimization

AP and NDCG are two popular performance measures for ranking systems, particularly in the fields of information retrieval [Xu and Li \(2007\)](#); [Radlinski and Craswell \(2010\)](#) and recommender systems [Xu et al \(2012\)](#); [Huang et al \(2015\)](#). AP is adaptable to largely skewed datasets since it is an asymptotically-unbiased estimation of AUPRC, which is insensitive to the data distribution [Davis and Goadrich \(2006\)](#). On the other hand, NDCG considers the graded relevance values, which allows it performs beyond the relevant/irrelevant scenario.

To the best of our knowledge, existing work on AP & NDCG optimization generally focuses on the setting of retrieval, where the ranking of instances is of interest [Mohapatra et al \(2018\)](#); [Ramzi et al \(2021\)](#); [Brown et al \(2020\)](#); [Wen et al \(2022a\)](#); [Swezey et al \(2021\)](#); [Qiu et al \(2022\)](#). By contrast, multi-label learning focuses on the ranking of labels [Wu et al \(2020\)](#); [Ridnik et al \(2021\)](#); [Prabhu and Varma \(2014\)](#); [Kalina and Krzysztof \(2018\)](#). In this direction, although random forest algorithms can directly optimize NDCG-based losses [Prabhu and Varma \(2014\)](#), it is not applicable to neural networks.

In [Sec.4](#), we show that optimizing TKPR is also favorable to the model performance on both NDCG@K and AP@K.

3 Preliminaries

In this section, we first present basic notations and common settings for MLC, as summarized in [Tab.1](#). Then, as shown in [Fig.1](#), we review existing ranking-based measures and point out their limitations.

3.1 Notations and Settings

Let \mathcal{X} be the input space, and $\mathcal{L} := \{1, 2, \dots, C\}$ denotes the set of possible labels. In MLC, each input $\mathbf{x} \in \mathcal{X}$ is associated with a label vector $\mathbf{y} \in \mathcal{Y} := \{0, 1\}^C$. Traditional MLC interprets $y_i = 1$ or 0 as the relevance/irrelevance of label i to the instance \mathbf{x} , respectively. Since fully-annotated data are generally expensive, MLC with Missing Labels (MLML) has gained rising attention, where $y_i = 0$ means that the annotation of the label y_i is missing [Sun et al \(2010\)](#); [Ibrahim et al \(2020\)](#); [Cole et al \(2021\)](#); [Wei et al \(2022\)](#); [Liu et al](#)

Table 1 Some important Notations used in this paper.

Notation	Description
\mathcal{X}, \mathcal{Y}	the input space and output space
C	the number of classes
\mathcal{L}	the set of possible labels
K	the hyperparameter of TKPR
\mathcal{D}	the joint distribution defined on $\mathcal{Z} := \mathcal{X} \times \mathcal{Y}$
(\mathbf{x}, \mathbf{y})	a sample belonging to \mathcal{Z}
\mathcal{S}	the dataset <i>i.i.d.</i> sampled from \mathcal{D}
$\eta(\mathbf{x})_i$	the conditional probability $\mathbb{P}[y_i = 1 \mathbf{x}]$
$\mathcal{P}(\mathbf{y}), \mathcal{N}(\mathbf{y})$	the relevant/irrelevant label set of \mathbf{y}
$N(\mathbf{y}), N_-(\mathbf{y})$	the number of relevant/irrelevant labels of \mathbf{y}
$\pi_{\mathbf{s}}(i)$	the index of s_i when sorting $\mathbf{s} \in \mathbb{R}^C$ descendingly
$\sigma(\mathbf{s}, k)$	the index of the top- k entry in $\mathbf{s} \in \mathbb{R}^C$
$s^{[k]}$	the top- k entry in $\mathbf{s} \in \mathbb{R}^C$
$\text{Tie}_k(\mathbf{s})$	the indices of the entries that equals to $s^{[k]}$
$\text{Top}_k(\mathbf{s})$	the indices of the top-1 to top- k entries in $\mathbf{s} \in \mathbb{R}^C$
f	a score function mapping \mathcal{X} to \mathbb{R}^C
\mathcal{F}	the set of score functions
$m(f)$	the measure defined on \mathcal{D} , <i>i.e.</i> , $\mathbb{E}_{\mathbf{z} \sim \mathcal{D}} [m(f(\mathbf{x}), \mathbf{y})]$
$m(f \mathbf{x})$	the conditional measure, <i>i.e.</i> , $\mathbb{E}_{\mathbf{y} \mathbf{x}} [m(f(\mathbf{x}), \mathbf{y})]$
$m(f, \mathbf{y})$	the measure defined on a sample, <i>i.e.</i> , $m(f(\mathbf{x}), \mathbf{y})$
$\hat{m}(f, \mathcal{S})$	the empirical measure defined on \mathcal{S}
$m_{\text{MC}}, m_{\text{ML}}$	Abstract multiclass/multi-label measures
α	the weighting terms for pointwise measures
$\alpha_1, \alpha_2, \alpha_3$	weighting terms for TKPR (refer to Prop.2)
$\text{reg}(f; m)$	the regret of f <i>w.r.t.</i> the measure m
ℓ_{0-1}, ℓ	the 0-1 loss and its surrogate loss
$\hat{\mathcal{C}}_{\mathcal{S}}(\mathcal{F})$	the empirical complexity of \mathcal{F}

(2022b). In other words, let $\mathcal{P}(\mathbf{y}) := \{i \in \mathcal{L} \mid y_i = 1\}$ denote the relevant label set of \mathbf{y} . Then, in traditional MLC, the number of relevant labels can be directly obtained by $N(\mathbf{y}) := |\mathcal{P}(\mathbf{y})| = \sum_{i \in \mathcal{L}} y_i$. While in MLML, we only know that the number of relevant labels is no less than $N(\mathbf{y})$.

Let \mathcal{D} be the joint distribution defined on $\mathcal{Z} := \mathcal{X} \times \mathcal{Y}$. Given a sample $(\mathbf{x}, \mathbf{y}) \in \mathcal{Z}$,

$$\eta(\mathbf{x})_i := \mathbb{P}[y_i = 1 | \mathbf{x}] = \sum_{\mathbf{y}: y_i=1} \mathbb{P}[\mathbf{y} | \mathbf{x}] \quad (2)$$

represents the conditional probability of the class i according to \mathcal{D} . Some prior arts assume that no ties exist among the conditional probabilities Wydmuch et al (2018); Menon et al (2019); Wang et al (2023). That is, given an input $\mathbf{x} \in \mathcal{X}$, for any $i \neq j \in \mathcal{L}, \eta(\mathbf{x})_i \neq \eta(\mathbf{x})_j$. However, this no-tie assumption might be a little strong since some labels might be highly correlated in the multi-label setting. In the following discussion, we will adopt the following with-tie assumption:

Assumption 1. Given an input $\mathbf{x} \in \mathcal{X}$, we assume that ties might exist in the conditional distribution $\eta(\mathbf{x})$. That is,

$$\forall \mathbf{x} \in \mathcal{X}, i \neq j \in \mathcal{L}, \mathbb{P}[\eta(\mathbf{x})_i = \eta(\mathbf{x})_j] > 0. \quad (3)$$

Given the training data sampled from \mathcal{D} , our goal is to learn a score function $f : \mathcal{X} \rightarrow \mathbb{R}^C$ such that the relevant labels can be ranked higher than the irrelevant ones. Then, one can adopt the top-ranked labels as the final decision results. Following the prior arts Yang and Koyejo (2020); Wang et al (2023), we adopt the worst case assumption when ties exist between the scores:

Assumption 2. Ties might exist in $f(\mathbf{x})$, and all the ties will be wrongly broken. In other words, given $i, j \in \mathcal{L}$ such that $\eta(\mathbf{x})_i > \eta(\mathbf{x})_j$, if $f(\mathbf{x})_i = f(\mathbf{x})_j$, then we have $\pi_f(i) > \pi_f(j)$, where $\pi_f(i) \in \mathcal{L}$ denotes the index of $f(\mathbf{x})_i$ when $f(\mathbf{x}) \in \mathbb{R}^C$ is sorted in descending order.

Corollary 1. Given a relevant label i and an irrelevant label j such that $f(\mathbf{x})_i = f(\mathbf{x})_j$, we have $\pi_f(i) > \pi_f(j)$.

Remark 1. Asm.2 will be used when the conditional distribution $\eta(\mathbf{x})$ is available, such as the proofs of Prop.4 and Thm.3. And Cor.1 applies to the case where the relevant and irrelevant labels are given, such as the proof of Prop.3.

3.2 Ranking-based MLC Measures

To evaluate model performances in multi-label setting, prior arts have proposed various measures. According to the taxonomy in Learning-to-Rank Liu (2009), we classify existing ranking-based measures into three categories: the pointwise ones, the pairwise ones, and the listwise ones.

3.2.1 Pointwise Measures

Essentially, pointwise measures reduce the multi-label problem to $N(\mathbf{y})$ multiclass classification problems. Abstractly, given a sample $(\mathbf{x}, \mathbf{y}) \in \mathcal{Z}$, we have

$$m_{\text{ML}}(f, \mathbf{y}) = \frac{1}{\alpha} \sum_{y \in \mathcal{P}(\mathbf{y})} m_{\text{MC}}(f, y), \quad (4)$$

where $m_{\text{MC}} : \mathbb{R}^C \times \mathcal{L} \rightarrow \mathbb{R}_+$ denotes a measure for multiclass classification, and α is a weighting term designed for different scenarios. As shown

in Menon et al (2019), when selecting the top-K measure Lapin et al (2016, 2018); Yang and Koyejo (2020) as m_{MC} , m_{ML} will be exactly equivalent to two pointwise measures: precision@K and recall@K.

Proposition 1. Let $\mathbf{1}[\cdot]$ denote the indicator function. Given the top-K measure $m_K(f, \mathbf{y}) = \mathbf{1}[\pi_f(\mathbf{y}) \leq K]$. When $\alpha = K$, m_{ML} is equivalent to

$$P@K(f, \mathbf{y}) := \frac{1}{K} \sum_{k=1}^K y_{\sigma(f,k)}; \quad (5)$$

when $\alpha = N(\mathbf{y})$, m_{ML} is equivalent to

$$R@K(f, \mathbf{y}) := \frac{1}{N(\mathbf{y})} \cdot \sum_{k=1}^K y_{\sigma(f,k)}, \quad (6)$$

where $\sigma(f, k) \in \mathcal{L}$ denotes the top-k class in $f(\mathbf{x})$.

Cor.4 of Menon et al (2019) shows that, under the no-tie assumption, the Bayes optimal solutions to optimizing P@K and R@K are generally inconsistent. In other words, optimizing one measure cannot guarantee the performance on the other one. We will update this corollary under Asm.1 in Appendix A. In Sec.4.4, we show that optimizing our proposed measure, *i.e.*, TKPR can boost both precision and recall performance.

3.2.2 Pairwise Measures

Pairwise measures check whether in each label pair, the relevant label is ranked higher than the irrelevant one. Similar inspiration exists in many paradigms such as contrastive learning Khosla et al (2020); Aljundi et al (2023). For multi-label learning, the ranking loss, which is essentially equivalent to instance-AUC Wu and Zhou (2017), calculates the fraction of mis-ranked pairs for each sample Gao and Zhou (2013):

$$L_{\text{rank}}(f, \mathbf{y}) := \frac{1}{N(\mathbf{y})N_-(\mathbf{y})} \sum_{i \in \mathcal{P}(\mathbf{y})} \sum_{j \in \mathcal{N}(\mathbf{y})} \ell_{0-1}(s_i - s_j), \quad (7)$$

where $\mathbf{s} := f(\mathbf{x})$ denotes the output of the score function, $\ell_{0-1}(t) := \mathbf{1}[t \leq 0]$ is the 0-1 loss, $\mathcal{N}(\mathbf{y}) := \{j \in \mathcal{L} \mid y_j = 0\}$ is the irrelevant label set, and $N_-(\mathbf{y}) := |\mathcal{N}(\mathbf{y})|$ is the number of irrelevant labels.

To optimize the ranking loss, one should replace the non-differentiable 0-1 loss with a differentiable surrogate loss ℓ , which induces the following surrogate objective:

$$L_{\text{rank}}^\ell(f, \mathbf{y}) := \frac{1}{N(\mathbf{y})N_-(\mathbf{y})} \sum_{i \in \mathcal{P}(\mathbf{y})} \sum_{j \in \mathcal{N}(\mathbf{y})} \ell(s_i - s_j). \quad (8)$$

However, as pointed out in Wu and Zhou (2017), under Asm.1, $L_{\text{rank}}^\ell(f, \mathbf{y})$ induced by any convex surrogate loss is inconsistent with $L_{\text{rank}}(f, \mathbf{y})$, and we have to select a non-convex one to optimize. Although Dembczynski et al (2012a) proposes a consistent surrogate, its generalization property is not satisfactory Wu et al (2021), which is summarized later in Tab.2.

To address this issue, in Sec.4.3, we show that the TKPR loss is the upper bound of the ranking loss. Furthermore, Sec.5.2 shows that the Empirical Risk Minimization framework for TKPR also enjoys a sharp generalization on the ranking loss.

3.2.3 Listwise Measures

Listwise measures assign different weights to labels according to their positions in the ranking list. In this way, these measures pay more attention to the top-ranked labels. For example, Normalized Discounted Cumulative Gain at K (NDCG@K) Wei et al (2022), weighs the importance of different positions with a specified decreasing discount functions:

$$\begin{aligned} \text{DCG@K}(f, \mathbf{y}) &:= \sum_{k=1}^K D(k) y_{\sigma(f,k)}, \\ \text{IDCG@K}(\mathbf{y}) &:= \max_f \text{DCG@K}(f, \mathbf{y}) = \sum_{k=1}^{N_K(\mathbf{y})} D(k), \\ \text{NDCG@K}(f, \mathbf{y}) &:= \frac{\text{DCG@K}(f, \mathbf{y})}{\text{IDCG@K}(\mathbf{y})}, \end{aligned}$$

where $N_K(\mathbf{y}) := \min\{K, N(\mathbf{y})\}$, and $D(k)$ is the discount function. Here, we consider two common choices Wang et al (2013):

$$\begin{aligned} D_{\log}(k) &:= 1/\log_2(k+1), \\ D_l(k) &:= K+1-k. \end{aligned} \quad (9)$$

As another example, Average Precision (AP) Wu and Zhou (2017); Wu et al (2020); Ridnik et al (2021); Wen et al (2022b, 2024) averages the precision performance at different recall performances:

$$\text{AP}(f, \mathbf{y}) := \frac{1}{C} \sum_{k=1}^C y_{\sigma(f,k)} \cdot \text{P@k}(f, \mathbf{y}). \quad (10)$$

In this paper, we consider its cut-off version Li et al (2017a):

$$\text{AP@K}(f, \mathbf{y}) := \frac{1}{N_K(\mathbf{y})} \sum_{k=1}^K y_{\sigma(f,k)} \cdot \text{P@k}(f, \mathbf{y}). \quad (11)$$

As shown in Sec.2.2.3, existing work on NDCG & AP optimization generally focuses on the ranking of instances, rather than that of labels. In Sec.4.1 and Sec.4.4, we will show that optimizing TKPR can also boost the model performance on the two measures.

4 TKPR and its Advantages

In this section, we begin by the definition of TKPR. Then, detailed analyses illustrate how this measure is compatible with existing ranking-based measures, whose outline is shown in Fig.1.

4.1 Three formulations of TKPR

To bridge the gap among existing ranking-based measures, we average the ranking results between relevant labels and the top-ranked ones:

$$\text{TKPR}(f, \mathbf{y}) := \frac{1}{\alpha K} \sum_{y \in \mathcal{P}(\mathbf{y})} \sum_{k \leq K} \mathbf{1}[s_y > s_{[k]}], \quad (12)$$

where $s_{[k]}$ denotes the k -largest entry in \mathbf{s} , and α denotes the weighting terms.

At the first glance, Eq.(12) has a pairwise formulation. But if we review Eq.(4), it is not difficult to find that TKPR also enjoys a pointwise formulation:

$$\text{TKPR}(f, \mathbf{y}) = \frac{1}{\alpha} \sum_{y \in \mathcal{P}(\mathbf{y})} \left[\frac{1}{K} \sum_{k \leq K} m_k(f, y) \right], \quad (13)$$

Besides, TKPR also exhibit a listwise formulation, whose proof can be found in Appendix B.1.

Proposition 2. Given a score function f and $(\mathbf{x}, \mathbf{y}) \in \mathcal{Z}$,

$$\text{TKPR}^\alpha(f, \mathbf{y}) = \begin{cases} \frac{1}{K} \cdot \text{DCG-l@K}(f, \mathbf{y}), & \alpha = \alpha_1, \\ \frac{1}{K} \cdot \text{DCG-ln@K}(f, \mathbf{y}), & \alpha = \alpha_2, \\ \frac{1}{K} \cdot \text{NDCG-l@K}(f, \mathbf{y}), & \alpha = \alpha_3, \end{cases}$$

where $\text{DCG-l@K}, \text{NDCG-l@K}$ represent the NDCG measures equipped with the linear discount function D_l defined in Eq.(9), respectively;

$$\text{DCG-ln@K}(f, \mathbf{y}) := \frac{1}{N_K(\mathbf{y})} \cdot \text{DCG-l@K}(f, \mathbf{y}). \quad (14)$$

denotes the linear DCG@K with a linear weighting term; $\alpha_1 = 1$, $\alpha_2 := N_K(\mathbf{y})$, $\alpha_3 := N_K(\mathbf{y})\tilde{N}_K(\mathbf{y})$, and

$$\tilde{N}_K(\mathbf{y}) := [2K + 1 - N_K(\mathbf{y})] / 2.$$

Hence, optimizing TKPR is favorable to the model performance on the NDCG measures. Next, on top of these formulations, we will show how TKPR is compatible with other ranking-based measures.

4.2 TKPR v.s. P@K and R@K

Intuitively, TKPR is more discriminating than P@K and R@K. That is, TKPR can distinguish finer-grained differences on model performances. For example, given $K = 4$ and a sample with

$$\mathbf{y} = (1 \ 1 \ 0 \ 0 \ 0 \ 0),$$

let $\mathbf{s}_1 = f_1(\mathbf{x})$ and $\mathbf{s}_2 = f_2(\mathbf{x})$ be two predictions such that

$$\begin{aligned} \mathbf{s}_1 &= (0.8 \ 0.8 \ 0.9 \ 0.9 \ 0.2 \ 0.2), \\ \mathbf{s}_2 &= (0.9 \ 0.9 \ 0.8 \ 0.8 \ 0.2 \ 0.2). \end{aligned}$$

It is clear that f_2 performs better than f_1 since the relevant labels are ranked higher. However, P@K fails to distinguish this difference:

$$\begin{aligned} \text{P@K}(f_1, \mathbf{y}) &= \frac{2}{4} = \frac{2}{4} = \text{P@K}(f_2, \mathbf{y}), \\ \text{TKPR}^{\alpha_1}(f_1, \mathbf{y}) &= \frac{2+1}{4} < \frac{4+3}{4} = \text{TKPR}^{\alpha_1}(f_2, \mathbf{y}). \end{aligned}$$

Although this example aligns with our intuitive understanding, there are evident instances of

counterexamples. Given another prediction $\mathbf{s}_3 = f_3(\mathbf{x})$ such that

$$\mathbf{s}_3 = (0.8 \ 0.1 \ 0.9 \ 0.2 \ 0.2 \ 0.2),$$

TKPR fails to distinguish the difference:

$$\begin{aligned} \text{P@K}(f_1, \mathbf{y}) &= \frac{2}{4} > \frac{1}{4} = \text{P@K}(f_3, \mathbf{y}), \\ \text{TKPR}^{\alpha_1}(f_1, \mathbf{y}) &= \frac{2+1}{4} = \frac{3}{4} = \text{TKPR}^{\alpha_1}(f_3, \mathbf{y}). \end{aligned}$$

In view of this, we present a precise definition of statistical discriminancy, which enables us to conduct a comprehensive comparison between measures.

Definition 1 (Statistical discriminancy [Ling et al \(2003\)](#)). *Given two measures m_1 and m_2 and two predictions \mathbf{s}, \mathbf{s}' , let*

$$\begin{aligned} P &:= \{(\mathbf{s}, \mathbf{s}') \mid m_1(\mathbf{s}) > m_1(\mathbf{s}'), m_2(\mathbf{s}) = m_2(\mathbf{s}')\}, \\ S &:= \{(\mathbf{s}, \mathbf{s}') \mid m_1(\mathbf{s}) = m_1(\mathbf{s}'), m_2(\mathbf{s}) > m_2(\mathbf{s}')\}. \end{aligned}$$

Then, the degree of discriminancy between m_1 and m_2 is defined by $\text{Dis}(m_1, m_2) := |P| / |S|$. We say m_1 is statistically more discriminating if and only if $\text{Dis}(m_1, m_2) > 1$. In this case, m_1 could discover more discrepancy that m_2 fails to distinguish.

Then, the following theorem validates our conjunction, whose details can be found in [Appendix B.2](#).

Theorem 1. *Given $K > 1$, TKPR is statistically more discriminating than P@K and R@K.*

Proof Sketch. *The proof is based on the concept of partition number in combinatorial mathematics [Andrews \(1998\)](#). To be concise, we first define a partition number $pn_K(a, b)$ that exactly equals to the number of predictions with $\text{P@K}(f, \mathbf{y}) = b/K$, $\text{TKPR}^{\alpha_1}(f, \mathbf{y}) = a/K$. Then, $|P| - |S|$ can be denoted as the function of $pn_K(a, b)$. We further construct a recurrence formula for $pn_K(a, b)$, which helps complete the proof.*

4.3 TKPR v.s. the ranking loss

To compare TKPR with the ranking loss, we have the following equivalent formulation of [Eq.\(13\)](#), where the indicator function is replaced by the 0-1 loss. The corresponding proof can be found in [Appendix B.3](#).

Proposition 3. *Under [Asm.2](#), maximizing TKPR is equivalent to minimizing the TKPR loss*

$$L_K^\alpha(f, \mathbf{y}) := \frac{1}{\alpha K} \sum_{y \in \mathcal{P}(\mathbf{y})} \sum_{k \leq K+1} \ell_{0-1}(s_y - s_{[k]}), \quad (15)$$

Furthermore, the following inequality holds:

$$L_{\text{rank}}(f, \mathbf{y}) \leq \frac{\alpha}{N(\mathbf{y})} L_K^\alpha(f, \mathbf{y}). \quad (16)$$

Since L_K^α is the upper bound of L_{rank} , minimizing L_K^α will boost the performance on L_{rank} . Besides, the TKPR loss has the following advantages:

- **(Scenario).** L_{rank} can only be applied to traditional MLC since the irrelevant labels are explicitly required. Whereas, L_K^α loss is applicable to both traditional MLC and MLML.
- **(Complexity).** L_{rank} suffers from a high computational burden $\mathcal{O}(C^2)$ [Wu et al \(2021\)](#). By contrast, L_K^α enjoys a complexity of $\mathcal{O}(CK)$.
- **(Theoretical results).** Further analysis in [Sec.5.1](#) and [Sec.5.2](#) shows that L_K^α has some other superior properties, which is summarized in [Tab.2](#).

4.4 TKPR v.s. AP@K

The following theorem shows that benefiting from the linear discount function, TKPR has the same order as AP@K. In other words, optimizing TKPR can help improve the model performance on AP@K, whose proof can be found in [Appendix B.4](#).

Theorem 2. *Given a score function f and $(\mathbf{x}, \mathbf{y}) \in \mathcal{Z}$, there exists a constant $\rho > 0$ such that*

$$\begin{aligned} \rho \cdot \text{TKPR}^{\alpha_2}(f, \mathbf{y}) &\leq \text{AP@K}(f, \mathbf{y}) \\ &\leq K \cdot \text{TKPR}^{\alpha_1}(f, \mathbf{y}), \end{aligned} \quad (17)$$

where the upper bound of ρ is bounded in

$$[1/(K+1), K \ln(K+1)].$$

Remark 2. *Abstractly, the upper bound of ρ has two parts:*

$$\rho \leq U_1(f, K) \cdot U_2(f, K), \quad (18)$$

where U_1 is increasing w.r.t. $\text{P@K}(f, \mathbf{y})$ but is not monotonic w.r.t. the ranking performance of the

model; U_2 is also increasing w.r.t. $P@K(f, \mathbf{y})$. We present the concrete formulations and the corresponding analysis in Appendix B.4.

The training process generally improves both P@K and the ranking performance. According to Rem.2, TKPR will bound AP@K more tightly when P@K increases. While this bound might alternate between becoming tighter and looser when the learning process only improves the ranking performance. Fortunately, the empirical results in Fig.2 show that optimizing TKPR can consistently boost AP@K, and more results can be found in Sec.6.

5 ERM Framework for TKPR

So far, we have known that optimizing TKPR will be compatible with existing ranking-based measures. Thus, it becomes appealing to construct an Empirical Risk Minimization (ERM) framework for TKPR. To this end, we first present the following risk minimization problem based on Eq.(15):

$$\begin{aligned} (OP_1) \min_f \mathcal{R}_K^\alpha(f) &:= \mathbb{E}_{\mathbf{z} \sim \mathcal{D}} [L_K^\alpha(f, \mathbf{y})], \\ &= \mathbb{E}_{\mathbf{z} \sim \mathcal{D}} \left[\frac{1}{\alpha K} \sum_{\mathbf{y} \in \mathcal{P}(\mathbf{y})} \sum_{k \leq K+1} \ell_{0-1}(s_{\mathbf{y}} - s_{[k]}) \right], \end{aligned} \quad (19)$$

According to Eq.(19), the main challenges for directly minimizing $\mathcal{R}_K^\alpha(f)$ are two-fold:

- (C1) The loss function ℓ_{0-1} is not differentiable, making gradient-based methods infeasible;
- (C2) The data distribution \mathcal{D} is unavailable, making it impossible to calculate the expectation.

Next, we will tackle the challenges (C1) and (C2) in Sec.5.1 and Sec.5.2, respectively.

5.1 Consistency Analysis of the ERM Framework

To tackle (C1), one common strategy is to replace ℓ_{0-1} with a differentiable surrogate loss $\ell : \mathbb{R} \rightarrow \mathbb{R}_+$. Let

$$L_K^{\alpha, \ell}(f, \mathbf{y}) := \frac{1}{\alpha K} \sum_{\mathbf{y} \in \mathcal{P}(\mathbf{y})} \sum_{k \leq K+1} \ell(s_{\mathbf{y}} - s_{[k]}) \quad (20)$$

Then, we have the following surrogate objective:

$$(OP_2) \min_f \mathcal{R}_K^{\alpha, \ell}(f) := \mathbb{E}_{(\mathbf{x}, \mathbf{y}) \sim \mathcal{D}} [L_K^{\alpha, \ell}(f, \mathbf{y})]. \quad (21)$$

As mentioned in Sec.3.2.2, convex surrogate losses are inconsistent with the ranking loss L_{rank}^ℓ . In view of this, a question naturally arises: whether a convex surrogate objective (OP_2) is consistent with the original one? In other words,

Given a convex ℓ , can optimizing (OP_2) recover the solution to (OP_1)?

To answer this question, we first present the definition of TKPR consistency:

Definition 2 (TKPR Fisher consistency). *The surrogate loss $\ell : \mathbb{R} \rightarrow \mathbb{R}_+$ is Fisher consistent with TKPR if for any sequence $\{f^{(t)}\}_{t=1}^\infty$,*

$$\text{reg}(f^{(t)}; \mathcal{R}_K^{\alpha, \ell}) \rightarrow 0 \implies \text{reg}(f^{(t)}; \mathcal{R}_K^\alpha) \rightarrow 0, \quad (22)$$

where

$$\text{reg}(f; m) := \mathbb{E}_{(\mathbf{x}, \mathbf{y})} [m(f(\mathbf{x}), \mathbf{y})] - \inf_g \mathbb{E}_{(\mathbf{x}, \mathbf{y})} [m(g(\mathbf{x}), \mathbf{y})]$$

represents the regret of f w.r.t. the measure m .

Next, we present the Bayes optimal solution to (OP_1) in Sec.5.1.1. On top of this, a sufficient condition for TKPR consistency, which consists of convexity, is established in Sec.5.1.2.

5.1.1 TKPR Bayes Optimality

We first define the Bayes optimal solution to TKPR optimization:

Definition 3 (TKPR Bayes optimal). *Given the joint distribution \mathcal{D} , the score function $f^* : \mathcal{X} \rightarrow \mathbb{R}^C$ is TKPR Bayes optimal if*

$$f^* \in \arg \inf_f \mathcal{R}_K^\alpha(f). \quad (23)$$

In other words, our goal is to find the solution to Eq.(23). The following property is necessary for further analysis.

Definition 4 (Top- K ranking-preserving property with ties). *Given $\mathbf{a}, \mathbf{b} \in \mathbb{R}^C$, we say that \mathbf{b} is top- K ranking-preserving with ties w.r.t. \mathbf{a} , denoted as $\text{RPT}_K(\mathbf{b}, \mathbf{a})$, if for any $k \leq K-1$,*

$$\text{Tie}_k(\mathbf{b}) = \text{Tie}_k(\mathbf{a}),$$

and

$$\text{Tie}_K(\mathbf{b}) \subset \text{Tie}_K(\mathbf{a}),$$

where $\text{Tie}_k(\mathbf{a}) := \{i \in \mathcal{L} \mid a_i = a_{[k]}\}$ returns the labels having ties with $a_{[k]}$.

Then, the following proposition reveals the sufficient and necessary condition for TKPR optimization, whose proof can be found in Appendix C.1.

Proposition 4 (Bayes optimality of TKPR). *The score function $f : \mathcal{X} \rightarrow \mathbb{R}^C$ is TKPR Bayes optimal if and only if for an input \mathbf{x} , the prediction $f(\mathbf{x})$ is top- K ranking-preserving w.r.t. $\Delta(\mathbf{x}) \in \mathbb{R}^C$, where*

$$\Delta(\mathbf{x})_i := \sum_{\mathbf{y}: y_i=1} \frac{\mathbb{P}[\mathbf{y} \mid \mathbf{x}]}{\alpha}. \quad (24)$$

Corollary 2. *Given $\alpha = \alpha_1$, the Bayes optimal solution of TKPR is top- K ranking preserving w.r.t. $\eta(\mathbf{x})$. Given $\alpha = \alpha_2$, if the hyperparameter K is large enough, the Bayes optimal solution of TKPR is top- K ranking preserving w.r.t. $\eta'(\mathbf{x})$, which is defined in Appendix A.*

Benefiting from the additional consideration on the ranking among the top- K labels, RPT is stricter than the Bayes optimalities of P@K and R@K described in Appendix A. Thus, this corollary again validates that TKPR is more discriminating than P@K and R@K.

5.1.2 Consistency of the Surrogate Objective

So far, we have known the Bayes optimal solution to TKPR optimization. On top of this, we can further present the following sufficient condition for TKPR consistency, which is much easier to check than the top- K ranking-preserving property. Please refer to Appendix C.2 for the details.

Theorem 3. *The surrogate loss $\ell(t)$ is TKPR Fisher consistent if it is bounded, differentiable, strictly decreasing, and convex.*

Proof Sketch. *The key point is to show that if $\neg\text{RPT}(\mathbf{s}, \Delta)$, \mathbf{s} will not be an optimal solution to (OP_2) . Given a prediction \mathbf{s} and $i, j \in \mathcal{L}$, $\neg\text{RPT}(\mathbf{s}, \Delta)$ consists of three cases: (1) $\Delta_i = \Delta_j$ but $s_i \neq s_j$; (2) $\Delta_i \neq \Delta_j$ but $s_i = s_j$; (3) $\Delta_i < \Delta_j$ but $s_i > s_j$. We obtain the result in each case by a contradiction.*

In Thm.3, we have discussed the consistency w.r.t. all measurable functions. However, common surrogate losses are not bounded. To this end, we next restrict the functions within a special function set \mathcal{F} , which induces the concept of \mathcal{F} -consistency:

Definition 5 (TKPR \mathcal{F} -consistency). *The surrogate loss $\ell : \mathbb{R} \rightarrow \mathbb{R}_+$ is \mathcal{F} -consistent with TKPR if for any sequence $\{f^{(t)}\}_{n=1}^\infty, f \in \mathcal{F}$,*

$$\text{reg}(f^{(t)}; \mathcal{R}_K^{\alpha, \ell}) \rightarrow 0 \implies \text{reg}(f^{(t)}; \mathcal{R}_K^\alpha) \rightarrow 0, \quad (25)$$

Then, we can find that common convex surrogate losses are all \mathcal{F} -consistent with TKPR:

Corollary 3. *Let \mathcal{F} denote the set of functions whose outputs are bounded in $[0, 1]$. Then, the surrogate loss $\ell(t)$ is \mathcal{F} -consistent with TKPR if it is differentiable, strictly decreasing, and convex in $[0, 1]$. Thus, we can conclude that the square loss $\ell_{sq}(t) = (1-t)^2$, the exponential loss $\ell_{exp}(t) = \exp(-t)$, and the logit loss $\ell_{logit}(t) = \log(1 + \exp(-t))$ are all \mathcal{F} -consistent with TKPR.*

As pointed out in Gao and Zhou (2013), any convex surrogate losses are inconsistent with the ranking loss L_{rank} . Although Dembczynski et al (2012a) proposes a consistent surrogate, its generalization bound is not satisfactory Wu et al (2021), as shown in Tab.2. In the next part, we show that the ERM framework for multi-label also enjoys a sharp generalization bound on the ranking loss.

5.2 Generalization Analysis of the ERM Framework

To tackle (C2), we turn to optimize its empirical estimation based on the given dataset $\mathcal{S} = \{\mathbf{z}^{(n)}\}_{n=1}^N$ sampled *i.i.d.* from \mathcal{D} . For the sake of convenience, let $s_y^{(n)}$ denote the score of the class $y \in \mathcal{L}$ on the n -th sample. Then, we have the following empirical optimization problem:

$$\begin{aligned} (OP_3) \quad \min_{f \in \mathcal{F}} \hat{\mathcal{R}}_K^{\alpha, \ell}(f) &:= \frac{1}{N} \sum_{n \leq N} L_K^{\alpha, \ell}(f(\mathbf{x}^{(n)}), \mathbf{y}^{(n)}) \\ &= \frac{1}{NK} \sum_{n \leq N} \sum_{y \in \mathcal{P}(\mathbf{y}^{(n)})} \sum_{k \leq K+1} \frac{1}{\alpha} \cdot \ell\left(s_y^{(n)} - s_{[k]}^{(n)}\right). \end{aligned} \quad (26)$$

In Sec.5.1, we know that optimizing (OP_2) can recover the solution to (OP_1) . Then,

Can optimizing (OP_3) approx.
the solution to (OP_2)?

In other words, it requires that the model performance on \mathcal{S} can generalize well to unknown data. In Sec.5.2.1, we first follow the techniques used in prior arts [Wu and Zhu \(2020\)](#); [Wu et al \(2021\)](#) and present a coarse-grained result. To obtain a more fine-grained result, in Sec.5.2.2, we extend the definition of Lipschitz continuity and propose a novel contraction technique that relies on the data distribution. On top of this, the proposed ERM framework enjoys a sharper generalization bound under mild conditions. Finally, in Sec.5.2.3, we present some practical results for kernel-based models and convolutional neural networks.

5.2.1 Generalization Bounds with Traditional Techniques

In this part, our analysis is based on the traditional Lipschitz continuity property and the following assumption:

Definition 6 (Lipschitz continuity). *We say the loss function $L(f, \mathbf{x})$ is μ -Lipschitz continuous, if $\forall f, f' \in \mathcal{F}$, $|L(f, \mathbf{y}) - L(f', \mathbf{y})| \leq \mu \|f(\mathbf{x}) - f'(\mathbf{x})\|$, where $\|\cdot\|$ denotes the 2-norm.*

Assumption 3. *We assume that (1) the surrogate loss ℓ is μ_ℓ -Lipschitz continuous, has an upper bound M_ℓ , and satisfies the conditions in [Thm.3](#); (2) the hyperparameter $K \geq \max_{\mathbf{z} \sim \mathcal{D}} N(\mathbf{y})$.*

Remark 3. *According to [Cor.3](#), we should normalize the outputs of the surrogate loss ℓ with a bounded function such as [Softmax](#). Note that [Softmax](#) is $1/\sqrt{2}$ -Lipschitz continuous [Yang et al \(2022\)](#), which will not affect the order of the generalization bound. Thus, we will omit [Softmax](#) for the sake of conciseness.*

Following the techniques in prior arts [Wu and Zhu \(2020\)](#); [Wu et al \(2021\)](#), we have the following lemma:

Lemma 1 (Basic lemma for generalization analysis [Mohri et al \(2012\)](#)). *Given the function set \mathcal{F} and a loss function $L : \mathbb{R}^C \times \mathcal{Y} \rightarrow [0, M]$, let $\mathcal{G} = \{L \circ f : f \in \mathcal{F}\}$. Then, for any $\delta \in (0, 1)$, with probability at least $1 - \delta$ over the training set \mathcal{S} , the following generalization bound holds for all the $g \in \mathcal{G}$:*

$$\mathbb{E}_{\mathbf{z} \sim \mathcal{D}} [g(\mathbf{z})] \lesssim \Phi(L, \delta) + \hat{\mathcal{C}}_{\mathcal{S}}(\mathcal{G}), \quad (27)$$

where

$$\Phi(L, \delta) := \frac{1}{N} \sum_{n=1}^N g(\mathbf{z}^{(n)}) + 3M \sqrt{\frac{\log 2/\delta}{2N}}, \quad (28)$$

consists of the empirical risk and a δ -dependent term,

$$\hat{\mathcal{C}}_{\mathcal{S}}(\mathcal{G}) := \mathbb{E}_{\xi} \left[\sup_{f \in \mathcal{F}} \frac{1}{N} \sum_{n=1}^N \xi^{(n)} g(\mathbf{z}^{(n)}) \right], \quad (29)$$

denotes an empirical complexity measure for the function set \mathcal{G} , $\xi := (\xi^{(1)}, \xi^{(2)}, \dots, \xi^{(N)})$ are the independent random variables for the complexity measure, and \lesssim is the asymptotic notation helps omit constants and undominated terms:

$$f(t) \lesssim g(t) \iff \exists \text{ a constant } C, f(t) \leq C \cdot g(t).$$

Remark 4. *Different random variables ξ will induce different complexity measures. For example, given uniform random variables taking values from $\{-1, +1\}$, it becomes Rademacher complexity, denoted as $\mathfrak{R}_{\mathcal{S}}(\mathcal{G})$. Given the standard normal distribution, it turns to Gaussian complexity, denoted as $\mathfrak{G}_{\mathcal{S}}(\mathcal{G})$.*

According to [Lem.1](#), our task is to bound $\hat{\mathcal{C}}_{\mathcal{S}}(\mathcal{G})$. To this end, the following contraction lemma can help us obtain the result directly:

Lemma 2 (Vector Contraction Inequality [Maurer \(2016\)](#)). *Assume that the loss function $L(f, \mathbf{x})$ is μ -Lipschitz continuous. Then, the following inequality holds:*

$$\hat{\mathcal{C}}_{\mathcal{S}}(\mathcal{G}) \leq \sqrt{2} \mu \hat{\mathcal{C}}_{\mathcal{S}}(\mathcal{F}). \quad (30)$$

According to [Lem.2](#), we present the Lipschitz constant of the TKPR loss $L_K^{\alpha, \ell}$, whose proof can be found in [Appendix D.1.1](#).

Proposition 5. *Under [Asm.3](#), the TKPR surrogate loss $L_K^{\alpha, \ell}$ is $\mu_\ell \mu_K$ -Lipschitz continuous and bounded by M_K , where*

- $\mu_K = \frac{K+1}{\sqrt{K}} + \sqrt{K+1}$, $M_K = (K+1)M_\ell$ when $\alpha = \alpha_1$;
- $\mu_K = \frac{K+1}{\sqrt{K}} + \frac{\sqrt{K+1}}{K}$, $M_K = (K+1)M_\ell$ when $\alpha = \alpha_2$;
- $\mu_K = \frac{K+1}{K^2} + \frac{2}{K\sqrt{K+1}}$, $M_K = \frac{K+1}{K} M_\ell$ when $\alpha = \alpha_3$.

Finally, combining Lem.1-2 and Prop.5, we obtain the generalization bound of the proposed ERM framework, whose proof is presented in Appendix D.1.2.

Proposition 6. *Under Asm.3, for any $\delta \in (0, 1)$, with probability at least $1 - \delta$ over the training set \mathcal{S} , the following generalization bound holds for all the $f \in \mathcal{F}$:*

$$\mathcal{R}_K^{\alpha, \ell}(f) \lesssim \Phi(L_K^{\alpha, \ell}, \delta) + \begin{cases} \mathcal{O}(\sqrt{K}) \cdot \hat{\mathcal{C}}_{\mathcal{S}}(\mathcal{F}), & \alpha \in \{\alpha_1, \alpha_2\}, \\ \mathcal{O}(1/K) \cdot \hat{\mathcal{C}}_{\mathcal{S}}(\mathcal{F}), & \alpha = \alpha_3. \end{cases}$$

Furthermore, combining Prop.3, we show that optimizing TKPR can provide a sharp generalization bound for the ranking loss, whose proof can be found in Appendix D.1.3.

Proposition 7. *Under Asm.3, let*

$$\mathcal{R}_{rank}^{\ell}(f) := \mathbb{E}_{(\mathbf{x}, \mathbf{y}) \sim \mathcal{D}} [L_{rank}^{\ell}(f, \mathbf{y})] \quad (31)$$

denote the generalization error of the traditional ranking loss. Then, for any $\delta \in (0, 1)$, with probability at least $1 - \delta$ over the training set \mathcal{S} , the following generalization bound holds for all the $f \in \mathcal{F}$:

$$\mathcal{R}_{rank}^{\ell}(f) \lesssim \begin{cases} \Phi(L_K^{\alpha, \ell}, \delta) + \mathcal{O}(\sqrt{K}) \cdot \hat{\mathcal{C}}_{\mathcal{S}}(\mathcal{F}), & \alpha \in \{\alpha_1, \alpha_2\}, \\ K \cdot \Phi(L_K^{\alpha, \ell}, \delta) + \mathcal{O}(1) \cdot \hat{\mathcal{C}}_{\mathcal{S}}(\mathcal{F}), & \alpha = \alpha_3. \end{cases}$$

5.2.2 Sharper Bounds with Data-dependent Contraction

Although Prop.6 and Prop.7 have provided sharp generalization bounds than prior arts Dembczynski et al (2012a); Wu et al (2021), the results under α_1 and α_2 suffer an order of \sqrt{K} , which is unfavorable in the scenarios requiring a large K . After rethinking the proofs, we find that the root cause lies in the simple relaxation of the term $\frac{1}{N(\mathbf{y})}$ to 1. Note that the distribution of relevant labels is generally imbalanced, with only a small subset of instances having a large number of labels, and the majority of instances only having a few labels. This insight motivates us to extend the traditional Lipschitz continuity property:

Definition 7 (Local Lipschitz continuity). *Let $\{\mathcal{S}_q\}_{q=1}^Q$ be a partition of \mathcal{S} . We say the loss function $L(f, \mathbf{y})$ is local Lipschitz continuous with the partition $\{\mathcal{S}_q\}_{q=1}^Q$ and constants $\{\mu_q\}_{q=1}^Q$ if for any $f, f' \in \mathcal{F}, q \in \{1, 2, \dots, Q\}$,*

$$|L(f, \mathbf{y}) - L(f', \mathbf{y})| \leq \mu_q \cdot \|f(\mathbf{x}) - f'(\mathbf{x})\|, (\mathbf{x}, \mathbf{y}) \in \mathcal{S}_q. \quad (32)$$

Then, the following data-dependent contraction inequality helps us obtain a sharper bound under the following assumption, whose proof can be found in Appendix D.2.1.

Assumption 4. *Next, we assume that $\hat{\mathcal{C}}_{\mathcal{S}}(\mathcal{F}) \sim \mathcal{O}(1/\sqrt{N})$. Note that this result holds for kernel-based models with traditional techniques Wu and Zhu (2020); Wu et al (2021) and neural networks with latest techniques Golowich et al (2018); Long and Sedghi (2020).*

Proposition 8 (Data-dependent contraction inequality). *Under Asm.4, if the loss function $L(f, \mathbf{y})$ is local Lipschitz continuous with a partition \mathcal{S}_Q and constants $\{\mu_q\}_{q=1}^Q$. Let $\pi_q := \frac{N_q}{N}$ be the ratio of \mathcal{S}_q in \mathcal{S} , where $N_q = |\mathcal{S}_q|$. Then,*

$$\hat{\mathcal{C}}_{\mathcal{S}}(\mathcal{G}) \leq \hat{\mathcal{C}}_{\mathcal{S}}(\mathcal{F}) \sum_{q=1}^Q \sqrt{\pi_q} \mu_q. \quad (33)$$

Remark 5. *Eq.(33) is favorable when π_q is decreasing w.r.t. μ_q . In this case, a sharper generalization bound might be available. However, if local Lipschitz continuity degenerates to Def.6, this inequality becomes a little loose since $\sum_{q=1}^Q \sqrt{\pi_q} > 1$.*

Similar to Prop.5, we partition the dataset \mathcal{S} and calculate the Lipschitz constants for $L_K^{\alpha, \ell}(f, \mathbf{y})$ as follows, whose proof can be found in Appendix D.2.2.

Proposition 9. *Let $\mathcal{S}_q := \{\mathbf{z} \in \mathcal{S} : N(\mathbf{y}) = q\}$. That is, all the samples in \mathcal{S}_q have q relevant labels. Then, under Asm.3, $L_K^{\alpha, \ell}(f, \mathbf{y})$ is local Lipschitz continuous with constants $\{\mu_q\}_{q=1}^Q$ such that*

$$\mu_q = \frac{\mu_{\ell} [(K+1)\sqrt{q} + q\sqrt{K+1}]}{\alpha(q)K}, \quad (34)$$

where $\alpha(q) \in \{1, q, q(2K+1-q)/2\}$ and $q \leq K$.

Table 2 Systematic comparison between the TKPR loss and the ranking loss, as well as its pointwise surrogates. For *Generalization*, we assume that $\pi_i \propto e^{-\lambda i}$, and more details can be found in Prop.10. For *Consist.*, \checkmark and \times mean that a convex surrogate loss can be consistent with the original objective or not, respectively. *Complexity* represents the time complexity for each sample. And for *MLML*, \checkmark and \times mean that the loss is applicable to MLML or not, respectively.

Loss	Generalization	Consist.	Complexity	MLML
L_{rank} Gao and Zhou (2013)	$\mathcal{O}(\sqrt{\frac{C}{N}})$	\times	$\mathcal{O}(C^2)$	\times
L_{u_1} Dembczynski et al (2012a)	$\mathcal{O}(\sqrt{\frac{C^2}{N}})$	\times	$\mathcal{O}(C)$	\times
L_{u_2} Dembczynski et al (2012a)	$\mathcal{O}(\sqrt{\frac{C^2}{N}})$	\checkmark	$\mathcal{O}(C)$	\times
L_{u_3} Wu et al (2021)	$\mathcal{O}(\sqrt{\frac{C}{N}})$	\times	$\mathcal{O}(C)$	\times
L_{u_4} Wu et al (2021)	$\mathcal{O}(\sqrt{\frac{C^2}{N}})$	\times	$\mathcal{O}(C)$	\times
$L_K^{\alpha, \ell}$ (Ours)	$\mathcal{O}(\sqrt{\frac{C}{Ne^\lambda}})$	\checkmark	$\mathcal{O}(CK)$	\checkmark

Table 3 The concrete formulations of $\mathfrak{g}(K)$ under an exponential distribution and a multinomial distribution, parameterized by λ .

$\alpha(q)$	$\pi_q \propto e^{-\lambda q}$	λ	$\pi_q \propto q^{-\lambda}$
1	$\frac{1}{\lambda^2}$	(0, 3)	$K^{(3-\lambda)/2}$
		[3, 5)	$\ln K$
		[5, ∞)	1
q	$\frac{1}{e^{\lambda/2}}$	(0, 1)	$K^{(1-\lambda)/2}$
		[1, 3)	$\ln K$
		[3, ∞)	1
$\frac{q(2K+1-q)}{2}$	$\frac{1}{Ke^{\lambda/2}}$	(0, 1)	$K^{-(1+\lambda)/2}$
		[1, 3)	$K^{-1} \ln K$
		[3, ∞)	K^{-1}

Combining Lem.1 and Prop.9, we obtain the following generalization bound of TKPR optimization, whose proof can be found in Appendix D.2.3.

Theorem 4. Under Asm.3 and Asm.4, for any $\delta \in (0, 1)$, with probability at least $1 - \delta$ over the training set \mathcal{S} , the following generalization bound holds for all $f \in \mathcal{F}$:

$$\mathcal{R}_K^{\alpha, \ell}(f) \lesssim \Phi(L_K^{\alpha, \ell}, \delta) + \hat{\mathcal{C}}_{\mathcal{S}}(\mathcal{F})\mathcal{O}(\mathfrak{g}(K)), \quad (35)$$

where $\mathfrak{g}(K)$ relies on the distribution of π_q . In Tab.3, we present the results under an exponential distribution and a multinomial distribution, parameterized by λ .

Proof Sketch. When π_q follows an exponential distribution, we relax the bound with the definite integral from 1 to K . When π_q follows a multinomial distribution, we relax the bound with Riemann zeta function Titchmarsh et al (1986). Note that the order of Riemann zeta function is out of the scope of this paper. Thus, we only provide a coarse-grained result, and more fine-grained results can be found in Fokas and Lenells (2022).

Compared with the results in Prop.6, we have the following observations:

- When $\pi_q \propto e^{-\lambda q}$, we generally obtain a sharper bound, where \sqrt{K} is replaced with λ^{-2} and $e^{-\lambda/2}$. This property is appealing since λ is independent of the selection of the hyperparameter K , and the bound will become sharper as the distribution becomes more imbalanced.
- When $\pi_q \propto q^{-\lambda}$, if $\alpha(q) = 1$, a sharper bound is available when $\lambda > 2$. If $\alpha(q) = q$, a sharper bound is consistently available under any $\lambda > 0$. As λ increases, *i.e.*, the distribution becomes more imbalanced, that is, the generalization bound will become sharper.
- For $\alpha(q) = q(2K + 1 - q)/2$, the data-dependent contraction technique fails to provide a sharper bound *w.r.t.* K . However,

when $\pi_q \propto e^{-\lambda q}$, the result becomes more informative due to the additional term $e^{-\lambda/2}$.

Similarly, we can obtain a sharper generalization bound for the ranking loss, whose proof can be found in Appendix D.2.4.

Proposition 10. *Let $\tilde{L}_K^\ell(f, \mathbf{y}) := \frac{\alpha}{N(\mathbf{y})} \cdot L_K^{\alpha, \ell}(f, \mathbf{y})$. Then, under Asm.3 and Asm.4, for any $\delta \in (0, 1)$, with probability at least $1 - \delta$ over the training set \mathcal{S} , the following generalization bound holds for all the $f \in \mathcal{F}$:*

- When $\pi_q \propto e^{-\lambda q}$,

$$\mathcal{R}_{\text{rank}}^\ell(f) \lesssim \Phi(\tilde{L}_K^\ell, \delta) + \mathcal{O}(e^{-\lambda/2}) \cdot \hat{\mathcal{C}}_{\mathcal{S}}(\mathcal{F}).$$

- When $\pi_q \propto q^{-\lambda}$,

$$\mathcal{R}_{\text{rank}}^\ell(f) \lesssim \Phi(\tilde{L}_K^\ell, \delta) + \begin{cases} \mathcal{O}(K^{(1-\lambda)/2}) \cdot \hat{\mathcal{C}}_{\mathcal{S}}(\mathcal{F}), & \lambda \in (0, 1), \\ \mathcal{O}(\ln K) \cdot \hat{\mathcal{C}}_{\mathcal{S}}(\mathcal{F}), & \lambda \in [1, 3), \\ \mathcal{O}(1) \cdot \hat{\mathcal{C}}_{\mathcal{S}}(\mathcal{F}), & \lambda \in [3, \infty). \end{cases}$$

Compared with the results in Prop.7, we have the following observations:

- When $\pi_q \propto e^{-\lambda q}$, a sharper bound is consistently available for any choice of α , and the bound will become sharper as the distribution becomes more imbalanced.
- When $\pi_q \propto q^{-\lambda}$, a sharper bound is available for $\alpha \in \{\alpha_1, \alpha_2\}$. However, it does not hold for $\alpha = \alpha_3$.
- For $\alpha(q) = q(2K + 1 - q)/2$, $\Phi(\tilde{L}_K^\ell, \delta)$ is smaller than $K \cdot \Phi(L_K^{\alpha, \ell}, \delta)$, which is also favorable.

5.2.3 Practical Bounds for Common Models

Next, we show that the proposed contraction technique is applicable to common models, such as kernel-based models and neural networks. Note that we omit the cases where π_q follows the multinomial distribution for the sake of conciseness.

Practical Bounds for Kernel-Based Models. Let \mathbb{H} be a reproducing kernel Hilbert space (RKHS) with the kernel function κ , where $\kappa : \mathcal{X} \times \mathcal{X} \rightarrow \mathbb{R}$ is a Positive Definite Symmetric (PSD) kernel. The set of kernel-based models can

be defined as:

$$\mathcal{F}_{\mathbb{H}} := \{\mathbf{x} \rightarrow \mathbf{W}^T \phi(\mathbf{x}) : \|\mathbf{W}\|_{\mathbb{H}, 2} \leq \Lambda\}, \quad (36)$$

where $\phi : \mathcal{X} \rightarrow \mathbb{H}$ is a feature mapping associated with κ , $\mathbf{W} = (\mathbf{w}_1, \mathbf{w}_2, \dots, \mathbf{w}_C)^T$ represents the model parameters, and $\|\mathbf{W}\|_{\mathbb{H}, 2} := (\sum_{j=1}^C \|\mathbf{w}_j\|_{\mathbb{H}}^2)^{1/2}$. Assume that $\exists r > 0$ such that $\kappa(\mathbf{x}, \mathbf{x}) \leq r^2$ for all $\mathbf{x} \in \mathcal{X}$. Then, we have the following propositions, whose proof can be found in Appendix D.3.1:

Proposition 11. *Under Asm.3 and Asm.4, for any $\delta \in (0, 1)$, with probability at least $1 - \delta$ over the training set \mathcal{S} , the following generalization bound holds for all the $f \in \mathcal{F}_{\mathbb{H}}$:*

$$\mathcal{R}_K^{\alpha, \ell}(f) \lesssim \Phi(L_K^{\alpha, \ell}, \delta) + \begin{cases} \mathcal{O}(\sqrt{\frac{C\Lambda^2 r^2}{N\lambda^4}}), & \alpha = \alpha_1 \\ \mathcal{O}(\sqrt{\frac{C\Lambda^2 r^2}{Ne^\lambda}}), & \alpha = \alpha_2 \\ \mathcal{O}(\sqrt{\frac{C\Lambda^2 r^2}{NK^2 e^\lambda}}), & \alpha = \alpha_3. \end{cases}$$

Proposition 12. *Under Asm.3 and Asm.4, for any $\delta \in (0, 1)$, with probability at least $1 - \delta$ over the training set \mathcal{S} , the following generalization bound holds for all the $f \in \mathcal{F}_{\mathbb{H}}$:*

$$\mathcal{R}_{\text{rank}}^\ell(f) \lesssim \Phi(\tilde{L}_K^\ell, \delta) + \mathcal{O}(\sqrt{\frac{C\Lambda^2 r^2}{Ne^\lambda}}).$$

In Tab.2, we compare the TKPR loss with the ranking loss systematically, as well as its pointwise surrogates. The results show that only the TKPR loss has both convex consistent surrogate losses and a sharp generalization bound on the ranking loss. Furthermore, the TKPR loss also enjoys a comparable computational complexity and more wider application scenarios. We will validate these observations in Sec.6.

Practical Bounds for CNNs. Next, we consider a family of neural networks, which consists of N_c convolutional layers and N_f fully-connected layers. To be specific, in each convolutional layer, a convolution operation is followed by an activation function and an optional pooling operation. All the convolutions utilize zero-padding Goodfellow et al (2016) with the kernel $KN^{(l)}$ for layer $l \in \{1, \dots, N_c\}$. In each fully-connected layer, a fully-connected operation, parameterized by $V^{(l)}$, is followed by an activation function.

All the activation functions and pooling operations are 1-Lipschitz continuous. Finally, Let $\Theta = \{KN^{(1)}, \dots, KN^{(N_c)}, V^{(1)}, \dots, V^{(N_f)}\}$ represent the parameter set of the networks.

Meanwhile, we assume that the inputs and parameters are all regularized. Concretely, the input $\mathbf{x} \in \mathbb{R}^{d \times d \times c}$ satisfies $\|\text{vec}(\mathbf{x})\| \leq \chi$, where $\text{vec}(\cdot)$ denotes the vectorization operation defined on \mathcal{X} . The initial parameters, denoted as Θ_0 , satisfy

$$\begin{aligned} \|\text{mt}(KN_0^{(l)})\|_2 &\leq 1 + \nu, l = 1, \dots, N_c, \\ \|V_0^{(l)}\|_2 &\leq 1 + \nu, l = 1, \dots, N_f, \end{aligned}$$

where $\text{mt}(\cdot)$ denotes the operator matrix of the given kernel;. And the distance from Θ_0 to the current parameters Θ is bounded:

$$\beta \geq \|\Theta - \Theta_0\| := \sum_{l=1}^{N_c} \|\text{mt}(KN^{(l)}) - \text{mt}(KN_0^{(l)})\|_2 + \sum_{l=1}^{N_f} \|V^{(l)} - V_0^{(l)}\|_2$$

Let $\mathcal{F}_{\beta, \nu, \chi}$ denote the set of convolutional neural networks described above. Then, we have the following propositions, whose proof can be found in Appendix D.3.2.

Proposition 13. *Under Asm.3 and Asm.4, for any $\delta \in (0, 1)$, with probability at least $1 - \delta$ over the training set \mathcal{S} , the following generalization bound holds for all the $f \in \mathcal{F}_{\beta, \nu, \chi}$:*

$$\mathcal{R}_K^{\alpha, \ell}(f) \lesssim \Phi(L_K^{\alpha, \ell}, \delta) + \begin{cases} \mathcal{O}\left(\frac{d \log(B_{\beta, \nu, \chi} N)}{\sqrt{N \chi^2}}\right), & \alpha = \alpha_1, \\ \mathcal{O}\left(\frac{d \log(B_{\beta, \nu, \chi} N)}{\sqrt{N e^\lambda}}\right), & \alpha = \alpha_2, \\ \mathcal{O}\left(\frac{d \log(B_{\beta, \nu, \chi} N)}{\sqrt{N e^\lambda K}}\right), & \alpha = \alpha_3, \end{cases}$$

where $B_{\beta, \nu, \chi} := \chi \beta (1 + \nu + \beta / N_a)^{N_a}$, $N_a := N_c + N_f$.

6 Experiment

In this section, we perform a series of experiments on benchmark datasets to validate the effectiveness of the proposed framework and the theoretical results. The induced learning algorithm, which contains a warm-up strategy, is summarized in Appendix E.

6.1 Efficiency Validation

In this part, we aim to validate this argument, we conduct an additional experiment, and such a superiority is also observed. Specifically, we use ResNet50 and swin-transformer as the backbone. For ResNet50, we set the input size as 448×448 , the batch size as 16, and K as 15. For swin-transformer, we adjust the input size to 384×384 . The number of classes C is set as $\{100, 1000, 5000, 10000\}$. To exclude the impact of implementation, we also report the results of the official pytorch loss `torch.nn.MultiLabelMarginLoss`, whose complexity is also $\mathcal{O}(C^2)$, denoted by `torch.ml`. We run 300 trials and report the results averaged over the latter 200 ones. All the experiments are conducted on an Nvidia(R) A100 GPU with a fixed random seed and a synchronized setup. Tab.4 presents the time of forward-propagation, loss computation, and back-propagation, from which we have the following observations:

- The complexity has little effect on the time of forward-propagation but has a significant impact on the loss computation and back-propagation.
- For small models such as ResNet50, the effect of complexity is significant even with small C .
- For large models such as swin-transformer, the effect is not so significant until C is large enough.
- The computation time of pointwise surrogates, *i.e.*, $L_{u_1}, L_{u_2}, L_{u_3}, L_{u_4}$ is insensitive to C . The time with $C = 10,000$ is almost the same as that with $C = 100$.
- The proposed TKPR loss $L_K^{\alpha, \ell}$, which enjoys a complexity of $\mathcal{O}(CK)$, achieves comparable results with the pointwise surrogates.
- The ranking loss L_{rank} and the official implementation `torch.ml` suffer from the high complexity. Their time of loss computation and back-propagation scales fast as C increases, becoming a significant part of the overall training time.
- Our implementation is efficient since the ranking loss L_{rank} has comparable or better results than the official implementation `torch.ml`.

Table 4 Empirical results of time complexity, where the seconds are averaged over 200 trials.

	Forward	Loss	Backward	Total	Forward	Loss	Backward	Total
ResNet50, C=100				Swin-transformer, C=100				
torch.ml	0.0170	0.0001	0.0334	0.0504	0.1506	0.0003	0.3077	0.4586
L_{rank}	0.0166	0.0066	0.0377	0.0609	0.1515	0.0067	0.3136	0.4718
L_{u_1}	0.0170	0.0002	0.0335	0.0508	0.1510	0.0004	0.3087	0.4601
L_{u_2}	0.0170	0.0002	0.0336	0.0508	0.1507	0.0004	0.3078	0.4589
L_{u_3}	0.0170	0.0003	0.0336	0.0510	0.1512	0.0005	0.3092	0.4609
L_{u_4}	0.0171	0.0002	0.0336	0.0509	0.1519	0.0013	0.3099	0.4631
$L_K^{\alpha, \ell}$ (Ours)	0.0167	0.0062	0.0369	0.0598	0.1512	0.0063	0.3125	0.4700
ResNet50, C=1,000				Swin-transformer, C=1,000				
torch.ml	0.0169	0.0013	0.0351	0.0533	0.1506	0.0014	0.3092	0.4611
L_{rank}	0.0166	0.0067	0.0410	0.0643	0.1516	0.0068	0.3157	0.4741
L_{u_1}	0.0170	0.0002	0.0336	0.0508	0.1507	0.0004	0.3081	0.4592
L_{u_2}	0.0171	0.0002	0.0336	0.0510	0.1510	0.0005	0.3088	0.4602
L_{u_3}	0.0171	0.0003	0.0337	0.0511	0.1516	0.0005	0.3099	0.4619
L_{u_4}	0.0171	0.0002	0.0336	0.0510	0.1509	0.0005	0.3086	0.4600
$L_K^{\alpha, \ell}$ (Ours)	0.0167	0.0062	0.0369	0.0598	0.1505	0.0063	0.3102	0.4671
ResNet50, C=5,000				Swin-transformer, C=5,000				
torch.ml	0.0165	0.0256	0.0706	0.1127	0.1502	0.0270	0.3408	0.5180
L_{rank}	0.0165	0.0103	0.0894	0.1162	0.1509	0.0109	0.3607	0.5226
L_{u_1}	0.0170	0.0002	0.0336	0.0509	0.1513	0.0004	0.3083	0.4600
L_{u_2}	0.0171	0.0002	0.0337	0.0511	0.1514	0.0004	0.3088	0.4607
L_{u_3}	0.0171	0.0003	0.0338	0.0512	0.1517	0.0005	0.3093	0.4615
L_{u_4}	0.0171	0.0002	0.0338	0.0512	0.1518	0.0004	0.3095	0.4617
$L_K^{\alpha, \ell}$ (Ours)	0.0167	0.0064	0.0378	0.0609	0.1515	0.0067	0.3122	0.4704
ResNet50, C=10,000				Swin-transformer, C=10,000				
torch.ml	0.0164	0.0966	0.1777	0.2907	0.1496	0.0989	0.4388	0.6873
L_{rank}	0.0165	0.0254	0.1887	0.2306	0.1505	0.0261	0.4623	0.6389
L_{u_1}	0.0171	0.0002	0.0337	0.0510	0.1507	0.0004	0.3073	0.4584
L_{u_2}	0.0171	0.0002	0.0338	0.0512	0.1514	0.0005	0.3090	0.4608
L_{u_3}	0.0172	0.0003	0.0340	0.0514	0.1518	0.0005	0.3098	0.4621
L_{u_4}	0.0172	0.0002	0.0339	0.0513	0.1511	0.0005	0.3083	0.4598
$L_K^{\alpha, \ell}$ (Ours)	0.0168	0.0070	0.0394	0.0632	0.1508	0.0074	0.3130	0.4712

6.2 Multi-Label Classification

6.2.1 Protocols

Datasets. We conduct the MLC experiments on three benchmark datasets:

- Pascal VOC 2007 [Everingham et al \(2010\)](#) is a widely-used multi-label dataset for computer vision tasks. This dataset consists of 10K images coming from 20 different categories. There are 5,011 images and 4,952 images in the training set and the test set, respectively. Each image in

the training set contains an average of 1.4 labels, with a maximum of 6 labels.

- MS-COCO [Lin et al \(2014\)](#) is another popular dataset for multi-label recognition tasks, which consists of 122,218 images and 80 object categories. The dataset is split into a training set, consisting of 82,081 images, and a test set, consisting of 40,137 images. On average, each image in the training set contains 2.9 labels, with a maximum of 13 labels.
- NUSWDIE [Chua et al \(2009\)](#) is a large-scale multi-label dataset containing 269,648 Flickr

Table 5 The empirical results of the ranking-bases losses and TKPR on MS-COCO, where the backbone is ResNet101. The best and runner-up results on each metric are marked with red and blue, respectively. The best competitor on each measure is marked with underline.

Type	Metrics	P@K		R@K		mAP@K		NDCG@K		TKPR ^{α1}		TKPR ^{α2}		TKPR ^{α3}		Ranking Loss	
		K	3	5	3	5	3	5	3	5	3	5	3	5	3		5
Ranking Loss	L_{rank}		.540	.424	.673	.821	.473	.514	.687	.734	1.143	1.492	.533	.618	.226	.148	.034
	L_{u_1}		.571	.424	.705	.817	.609	.621	.706	.730	1.204	1.538	.549	.626	.234	.150	.037
	L_{u_2}		.535	.419	.668	.814	.473	.512	.680	.726	1.135	1.478	.527	.611	.223	.146	.035
	L_{u_3}		.536	.414	.663	.804	.511	.542	.676	.717	1.138	1.472	.524	.605	.223	.145	.033
	L_{u_4}		<u>.615</u>	<u>.443</u>	<u>.753</u>	<u>.846</u>	<u>.663</u>	<u>.665</u>	<u>.753</u>	<u>.765</u>	<u>1.288</u>	<u>1.631</u>	<u>.591</u>	<u>.664</u>	<u>.251</u>	<u>.159</u>	<u>.032</u>
	L_{LSEP}		.522	.420	.648	.816	.419	.469	.650	.711	1.078	1.444	.498	.594	.211	.142	.045
	L_{TKML}		.522	.393	.654	.775	.540	.554	.667	.697	1.135	1.435	.521	.594	.222	.141	.045
TKPR (Ours)	α_1		.578	.423	.712	.816	<u>.730</u>	<u>.733</u>	<u>.795</u>	<u>.811</u>	<u>1.319</u>	<u>1.605</u>	<u>.629</u>	<u>.672</u>	<u>.264</u>	<u>.160</u>	.029
	α_2		<u>.587</u>	<u>.432</u>	<u>.724</u>	<u>.832</u>	<u>.752</u>	<u>.758</u>	<u>.813</u>	<u>.831</u>	<u>1.356</u>	<u>1.646</u>	<u>.645</u>	<u>.688</u>	<u>.271</u>	<u>.163</u>	<u>.024</u>
	α_3		.575	.428	.710	.825	.716	.726	.782	.805	1.310	1.608	.619	.670	.260	.159	<u>.025</u>

Table 6 The empirical results of state-of-the-art MLC methods and TKPR on MS-COCO, where the backbone is ResNet101. The best and runner-up results on each metric are marked with red and blue, respectively. The best competitor on each measure is marked with underline.

Type	Metrics	P@K		R@K		mAP@K		NDCG@K		TKPR ^{α1}		TKPR ^{α2}		TKPR ^{α3}		Ranking Loss	
		K	3	5	3	5	3	5	3	5	3	5	3	5	3		5
Loss Oriented	ASL [†]		.668	.474	.800	.885	.879	.868	.910	.910	1.536	1.841	.722	.754	.305	.181	.015
	DB-Loss		<u>.676</u>	<u>.475</u>	<u>.807</u>	<u>.886</u>	<u>.892</u>	<u>.877</u>	<u>.919</u>	<u>.915</u>	<u>1.554</u>	<u>1.856</u>	<u>.730</u>	<u>.759</u>	<u>.308</u>	<u>.182</u>	<u>.015</u>
	CCD [†]		.654	.463	.783	.868	.860	.848	.894	.893	1.510	1.803	.709	.740	.299	.177	.018
	Hill [†]		.643	.462	.775	.868	.829	.826	.874	.881	1.467	1.774	.692	.731	.292	.175	.019
	SPLC [†]		.619	.457	.757	.866	.754	.768	.835	.855	1.389	1.715	.660	.711	.277	.170	.020
TKPR (Ours)	α_1		.678	.476	<u>.810</u>	.889	<u>.895</u>	.880	.889	.918	1.558	<u>1.862</u>	.732	.762	.309	.183	.014
	α_2		<u>.678</u>	<u>.477</u>	.810	<u>.889</u>	.894	<u>.880</u>	<u>.922</u>	<u>.918</u>	1.558	1.860	<u>.733</u>	<u>.762</u>	<u>.309</u>	<u>.183</u>	<u>.015</u>
	α_3		<u>.678</u>	<u>.477</u>	<u>.810</u>	<u>.890</u>	<u>.895</u>	<u>.881</u>	<u>.922</u>	<u>.918</u>	<u>1.558</u>	<u>1.862</u>	<u>.732</u>	<u>.762</u>	<u>.309</u>	<u>.183</u>	<u>.014</u>

images and 81 object categories. On average, each image in the training set contains 2.4 labels, with a maximum of 11 labels.

Backbone and Optimization Method. For CNN backbone, we utilize ResNet101 He et al (2016) pre-trained on ImageNet Deng et al (2009) as the backbone, as used in Wu et al (2020); Ridnik et al (2021). The model is optimized by Stochastic Gradient Descent (SGD) with Nesterov momentum of 0.9 and a weight decay value of 1e-4 Sutskever et al (2013). And an 1-cycle learning rate policy is utilized with the max learning rate searched in {0.1, 0.01, 0.001, 0.0001}. All input images are rescaled to 448×448, and the batch size is searched in {32, 64, 128}. For transformer backbone, we select swin-transformer Liu et al (2021) pre-trained on ImageNet-22k as the backbone. As suggested by Liu et al (2022a), we use Adam as the optimizer with a weight decay of 1e-4, a batch size of 32, a learning rate searched in {5e-5, 1e-6} with an 1-cycle policy, and the input images are rescaled to 384×384. More details can be found in Appendix E.

Evaluation Metric. We evaluate the model performances on TKPR^α, where $\alpha \in \{\alpha_1, \alpha_2, \alpha_3\}$. Meanwhile, we also report the results on P@K, R@K, mAP@K, NDCG@K, and the ranking loss, where $K \in \{3, 5\}$. Note that NDCG@K adopts a logarithmic discount function, and mAP@K summarizes the AP@K performance on different samples.

Competitors. On one hand, we focus on ranking-based losses. Note that the pointwise surrogates of the ranking loss are also selected to validate Prop.3 and the generalization analyses in Sec.5.2:

- L_{rank} Gao and Zhou (2013) is exactly the loss defined in Eq.(7).
- L_{u_1} Dembczynski et al (2012a) has an abstract formulation $\frac{1}{C} \sum_i \ell_i$, where ℓ_i denotes the loss on the i -th class. While primarily designed for optimizing the Hamming loss, this loss also serves as a traditional surrogate for L_{rank} .
- L_{u_2} Dembczynski et al (2012a) is a consistent surrogate for L_{rank} , which can be formulated as $\frac{1}{N(\mathbf{y})N_-(\mathbf{y})} \sum_i \ell_i$.

- L_{u_3}, L_{u_4} Wu et al (2021) are two reweighted surrogate pointwise losses, which can be formulated as $\frac{\sum_i \ell_i^+}{N(\mathbf{y})} + \frac{\sum_i \ell_i^-}{N_-(\mathbf{y})}$ and $\frac{\sum_i \ell_i}{\min\{N(\mathbf{y}), N_-(\mathbf{y})\}}$, respectively, where ℓ_i^- and ℓ_i^+ denote the loss on relevant and irrelevant labels, respectively.
- LSEP Li et al (2017b) employs a smooth approximation of pairwise ranking to make the objective easier to optimize. Additionally, negative sampling techniques are used to reduce the computational complexity.
- TKML Hu et al (2020) aims to maximize the score difference between the top- $(k+1)$ score of all the labels and the lowest prediction score of all the relevant labels.

On the other hand, we also compare several state-of-the-art loss-oriented MLC methods:

- DB-Loss Wu et al (2020) modifies the binary cross-entropy loss to tackle the imbalanced label distribution, which is achieved by rebalancing the weights of the co-occurrence of labels and restraining the dominance of negative labels.
- The ASymmetric Loss (ASL) Ridnik et al (2021) dynamically adjusts the weights to focus on hard-negative samples while keeping attention on positive samples.
- Hill, SPLC Zhang et al (2021) are two simple loss functions designed for both MLC and MLML. The Hill loss is a robust loss that can re-weight negatives to avoid the effect of false negatives. And the Self-Paced Loss Correction (SPLC) is derived from the maximum likelihood criterion under an approximate distribution of missing labels.
- The Causal Context Debiasing (CCD) Liu et al (2022a) incorporates the casual inference to eliminate the contextual hard-negative objects and highlight the hard-positive objects.

6.2.2 Overall Performance

Here, we report the results on MS-COCO with the CNN backbone. The results on the transformer backbone and those on Pascal VOC 2007 and NUSWDIE can be found in Appendix F. From Tab.5 and Tab.6, we have the following observations:

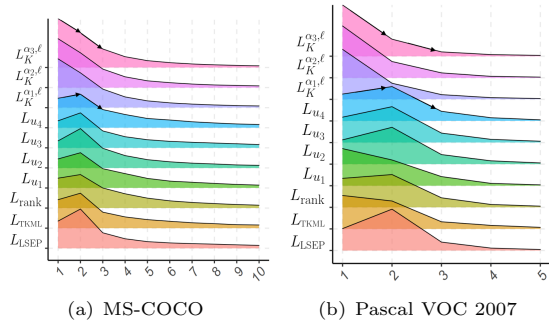


Fig. 3 According to the model predictions, we visualize the rank distributions of relevant labels on MS-COCO and Pascal VOC 2007. The results show that the proposed methods can rank more relevant labels on the top-1 position, which explains why the proposed methods can improve the ranking-based measures.

Compared with the ranking-based losses, the proposed algorithm for TKPR optimization can significantly improve the model performances on $\mathbf{mAP@K}$, $\mathbf{NDCG@K}$, the ranking loss, and the TKPR measures. For example, the performance gap between the proposed methods and the runner-up method is 9.3%, 6.3%, 5.4%, and 6% in terms of $\mathbf{mAP@3}$, $\mathbf{NDCG@3}$, $\mathbf{TKPR}^{\alpha_2@3}$, and ranking loss, respectively. Notably, the performance gains on $\mathbf{mAP@K}$, $\mathbf{NDCG@K}$, the ranking loss not only validate our theoretical analyses in Sec.4 and Sec.5.2 but also show the proposed learning algorithm can be a promising solution to optimizing existing ranking-based measures.

However, the performances on $\mathbf{P@K}$ and $\mathbf{R@K}$ are not so impressive. To explain this counter-intuitive phenomenon, we visualize the rank distribution of relevant labels in Fig.3. It is clear that the proposed methods rank most relevant labels at the top-1 position, while the competitors rank most relevant labels at the top-2 position. On one hand, this difference explains how the pairwise/listwise measures are improved under similar $\mathbf{P@K}$ and $\mathbf{R@K}$ performances. On the other hand, the rank distribution is consistent with the Bayes optimality presented in Sec.5.1.1, which again validate the effectiveness of the proposed framework.

Compared with the state-of-the-art methods, the proposed methods achieve the best performances consistently on all the measures, which again validate the effectiveness of the proposed framework.

[†]Official implementation.

Table 7 The empirical results of the ranking-based losses and TKPR on MS-COCO-MLML, where the backbone is ResNet50. The best and runner-up results on each metric are marked with red and blue, respectively. The best competitor on each measure is marked with underline.

Type	Metrics	P@K		R@K		mAP@K		NDCG@K		TKPR $^{\alpha 1}$		TKPR $^{\alpha 2}$		TKPR $^{\alpha 3}$		Ranking loss	
		K	3	5	3	5	3	5	3	5	3	5	3	5	3		5
Ranking loss	L_{rank}		.517	.402	.639	.781	.544	.570	.660	.702	1.102	1.426	.513	.590	.217	.141	.0417
	L_{u_1}		.519	.360	.658	.728	.686	.673	.748	.749	1.246	1.447	.602	.626	.251	.148	.0643
	L_{u_2}		.512	.358	.652	.724	.677	.668	.738	.742	1.225	1.431	.594	.620	.247	.146	.0671
	L_{u_3}		<u>.570</u>	<u>.426</u>	<u>.700</u>	<u>.815</u>	.664	.677	.745	<u>.770</u>	1.252	<u>1.569</u>	.585	<u>.646</u>	.247	<u>.155</u>	<u>.0312</u>
	L_{u_4}		.531	.371	.671	.745	<u>.700</u>	<u>.688</u>	<u>.761</u>	<u>.763</u>	<u>1.268</u>	1.482	<u>.611</u>	.637	<u>.255</u>	.150	.0714
	L_{LSEP}		.542	.414	.672	.800	.575	.596	.696	.730	1.168	1.493	.543	.617	.230	.147	.0346
	L_{TKML}		.536	.387	.668	.764	.575	.575	.687	.701	1.167	1.442	.540	.600	.229	.143	.0452
TKPR (Ours)	α_1		<u>.627</u>	<u>.449</u>	<u>.763</u>	<u>.854</u>	<u>.820</u>	<u>.814</u>	<u>.864</u>	<u>.871</u>	<u>1.451</u>	<u>1.741</u>	<u>.688</u>	<u>.722</u>	<u>.289</u>	<u>.172</u>	<u>.0228</u>
	α_2		.626	.446	.762	.850	.820	.813	.864	.869	1.450	1.734	.687	.721	.288	.171	.0249
	α_3		<u>.628</u>	<u>.450</u>	<u>.763</u>	<u>.854</u>	<u>.821</u>	<u>.815</u>	<u>.865</u>	<u>.871</u>	<u>1.453</u>	<u>1.741</u>	<u>.687</u>	<u>.722</u>	<u>.289</u>	<u>.172</u>	<u>.0234</u>

6.2.3 Fine-grained Analysis

To further validate the theoretical results in Sec. 4, we visualize the normalized measures *w.r.t.* the training epoch on the Pascal VOC 2007 dataset. Specifically, given a sequence of measures $\mathcal{M} := \{m^{(t)}\}_{t=1}^T$, where T is the maximum number of epochs, we normalize these measures by

$$\tilde{m}^{(t)} := \frac{\max\{\mathcal{M}\} - m^{(t)}}{\max\{\mathcal{M}\} - \min\{\mathcal{M}\}}.$$

As shown in Fig. 4, we have the following observations: (1) For the competitors, *i.e.*, in (a)-(c), different measures reach the peak values at different epochs. In other words, the tendency of different measures are inconsistent when optimizing these losses. (2) Optimizing the ranking loss and its surrogates fails to guarantee the model performances on the other measures. For example, in (a), mAP@5 even shows a decreasing trend at the late epochs. (3) By contrast, when optimizing TKPR, all the measures display a similar increasing trend, which is consistent with the our analyses in Sec. 4.

6.3 Multi-Label Classification with Missing Labels

6.3.1 Protocols

Datasets. The experiments are conducted on MS-COCO Lin et al (2014) and Pascal VOC 2012 Everingham et al (2010). VOC 2012 contains 20 classes and 5,717 training images, which are non-overlapping with the Pascal VOC 2007 dataset. To simulate the MLML setting, we randomly select one positive label for each training example, as

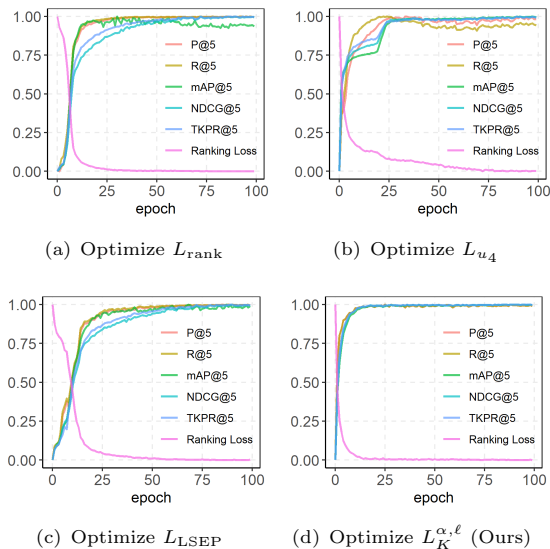


Fig. 4 Normalized ranking-based measures *w.r.t.* the training epoch on the Pascal VOC 2007 dataset in the MLC setting. (a)-(c) When optimizing the competitors, the changes in different measures are inconsistent. (d) By contrast, when optimizing TKPR, the changes are highly consistent, which validates our analyses in Sec. 4.

performed in Cole et al (2021); Zhou et al (2022); Kim et al (2022).

Backbone and Optimization Method. Following the prior arts (Cole et al, 2021; Zhou et al, 2022; Kim et al, 2022), we use ResNet50 (He et al, 2016) pre-trained on ImageNet (Deng et al, 2009) as the backbone and Adam as the optimizer, with a weight decay of $1e-4$, a batch size of 64, a learning rate searched in $\{1e-4, 1e-5\}$ with an 1-cycle policy. The input images are rescaled to 448×448 . More details can be found in Appendix E.

Table 8 The empirical results of state-of-the-art MLML methods and TKPR on MS-COCO-MLML, where the backbone is ResNet50. The best and runner-up results on each metric are marked with red and blue, respectively. The best competitor on each measure is marked with underline.

Type	Metrics	P@K		R@K		mAP@K		NDCG@K		TKPR $^{\alpha 1}$		TKPR $^{\alpha 2}$		TKPR $^{\alpha 3}$		Ranking loss
	K	3	5	3	5	3	5	3	5	3	5	3	5	3	5	
Loss Oriented	ROLE †	.618	.439	.752	.837	.812	.801	.858	.860	1.441	1.715	.683	.713	.287	.170	.0415
	EM+APL †	<u>.638</u>	<u>.456</u>	<u>.772</u>	<u>.862</u>	<u>.838</u>	<u>.831</u>	<u>.879</u>	<u>.883</u>	<u>1.478</u>	<u>1.770</u>	<u>.699</u>	<u>.732</u>	<u>.294</u>	<u>.175</u>	.0265
	Hill †	.594	.424	.726	.816	.775	.768	.825	.832	1.386	1.652	.658	.690	.276	.164	.0296
	SPLC †	.599	.424	.731	.814	.784	.773	.833	.836	1.402	1.662	.664	.693	.279	.165	.0319
	LL-R †	.501	.349	.761	.850	.708	.741	.768	.807	1.184	1.389	.637	.710	.252	.158	<u>.0250</u>
	LL-Ct †	.500	.348	.761	.849	.709	.741	.768	.807	1.185	1.389	.638	.710	.253	.158	.0251
	LL-Cp †	.495	.345	.755	.842	.702	.734	.762	.801	1.177	1.378	.633	.704	.251	.157	.0272
TKPR (Ours)	α_1	<u>.642</u>	<u>.456</u>	<u>.776</u>	<u>.863</u>	<u>.843</u>	<u>.834</u>	<u>.882</u>	<u>.885</u>	<u>1.485</u>	<u>1.775</u>	<u>.701</u>	<u>.733</u>	<u>.295</u>	<u>.175</u>	<u>.0200</u>
	α_2	<u>.643</u>	<u>.457</u>	<u>.777</u>	<u>.864</u>	<u>.845</u>	<u>.835</u>	<u>.883</u>	<u>.885</u>	<u>1.488</u>	<u>1.778</u>	<u>.702</u>	<u>.734</u>	<u>.296</u>	<u>.176</u>	<u>.0196</u>
	α_3	.640	.453	.774	.859	.842	.831	.881	.882	1.483	1.769	.701	.732	.295	.175	.0215

Competitors. Besides the ranking-based losses, Hill, and SPLC, we select the following state-of-the-art MLML methods as the competitors:

- ROLE Cole et al (2021) proposes a regularization that constrains the number of expected relevant labels to tackle the single-relevant problem.
- EM+APL Zhou et al (2022) combines the entropy-maximization (EM) loss and an asymmetric pseudo-labeling (APL) scheme to address the single-relevant problem.
- LL-R, LL-Ct, and LL-Cp Kim et al (2022) belong to the Large-Loss-Matter framework, where the missing labels are regarded as noises. Based on this observation, these methods reject or correct samples with large losses to prevent the model from memorizing the noisy labels.

6.3.2 Overall Performance

Here, we report the results on MS-COCO. The results on Pascal VOC 2012 and the corresponding fine-grained analyses can be found in Appendix F.3. From Tab.7 and Tab.8, we have the following observations:

Compared with the ranking-based losses, the proposed methods demonstrate consistent improvements. For example, the performance gap between the proposed methods and the runner-up method increases to 12.1%, 10.4%, 7.7%, 8.4% in terms of mAP@3, NDCG@3, TKPR $^{\alpha 2}$ @3, and the ranking loss, respectively. This phenomenon is not surprising since the competitors explicitly require irrelevant labels as inputs. Consequently, the missing relevant labels will bias the learning process

and degenerate the model performance. By contrast, the proposed framework only takes the relevant labels as inputs and thus alleviates the negative impact of the missing labels.

Compared with the state-of-the-art MLML methods, the proposed methods also achieve consistent improvements. For example, the performance gap between the proposed methods and the runner-up method is 0.7%, 0.4%, 0.3%, and 5.4% in terms of mAP@3, NDCG@3, TKPR $^{\alpha 2}$ @3, and ranking loss, respectively. It is worth mentioning that although EM+APL achieves superior performance on top-ranking measures, it fails to outperform LL-R and LL-Ct on the ranking loss. This phenomenon validates the inconsistency among different measures. Hence, it is necessary to optimize compatible measures such as the proposed TKPR.

6.3.3 Sensitivity Analysis

Next, we investigate the sensitivity of the proposed methods to the hyperparameters K and E_w . The results are shown in Fig.5 and Fig.6, where we adopt L_{rank} as the warm-up loss. From the results, we have the following observations:

For K , the best performances of the proposed methods are achieved when $K \in \{4, 6\}$. A small K will lead to a lack of supervision, while a large K means ranking positions that are out of interest are optimized. Hence, both of them will degrade the performance. Besides, the best TKPR@K performances are achieved when K is close to 5, which is consistent with the expectation of the proposed framework.

For E_w , a larger E_w leads to more stable performances. However, as E_w increases, the effect of the proposed methods becomes weaker, inducing

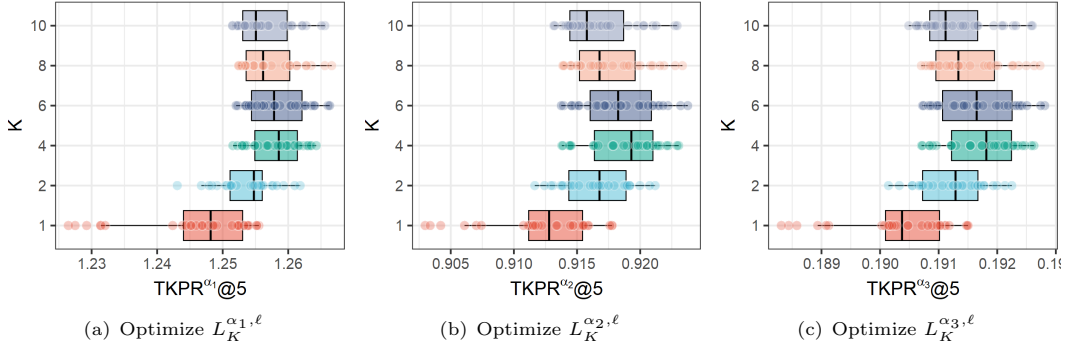


Fig. 5 Sensitivity analysis of the proposed methods on Pascal VOC 2012-MLML. The y-axis denotes the values of the hyperparameter K , and the x-axis represents the value of TKPR@5 under the corresponding K .

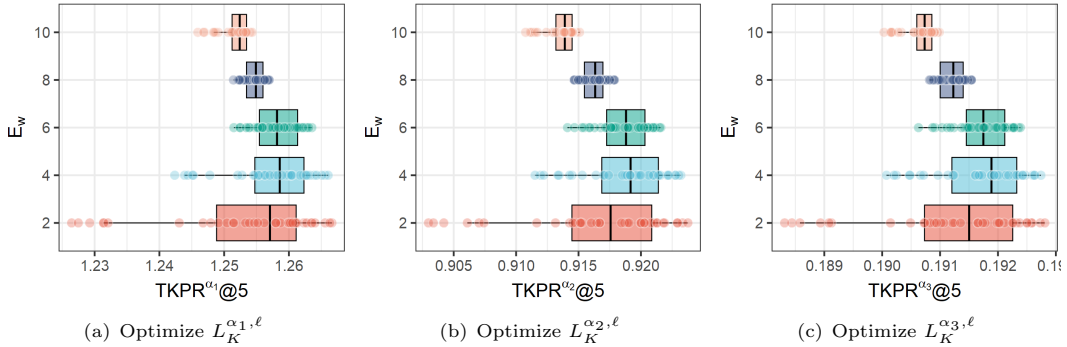


Fig. 6 Sensitivity analysis of the proposed methods on Pascal VOC 2012-MLML. The y-axis denotes the values of the hyperparameter E_w , and the x-axis represents the value of TKPR@5 under the corresponding E_w .

a significant performance degradation. Hence, a moderate E_w is preferred to balance the learning between the global pattern and the local ranking.

7 Conclusion, Limitation, and Future Work

This paper proposes a novel measure for multi-label ranking named TKPR. A series of analyses show that optimizing TKPR is compatible with existing ranking-based measures. In view of this, an empirical surrogate risk minimization framework is further established for TKPR with theoretical support. On one hand, this ERM framework enjoys convex surrogate losses. On the other hand, a novel technique, named data-dependent contraction, helps the proposed framework achieve a sharp generalization bound on both TKPR and the ranking loss. Finally, experimental results on different benchmark datasets and settings speak

to the effectiveness of the proposed framework, as well as the theoretical analyses.

TKPR is closely related to: 1) the scenarios where the top-ranking performance is of interest. As shown in Sec.4, TKPR is more discriminating than P@K and R@K. Although one can select a suitable K such that P@K and R@K can find the performance difference on a specific sample, the number of ground-truth labels differs among samples, making the selection of K rather challenging. Hence, TKPR is a better choice in such scenarios. Of course, AP@K and NDCG@K are also reasonable options, but it is challenging to perform direct optimization on these measures. 2) the scenarios where multiple ranking-based measures are important. As shown in Sec.4, if the model achieves a good performance on TKPR, it tends to perform well on the others. Hence, we can reduce a multi-objective problem to a single-objective problem, which is rather convenient.

The proposed learning algorithm is useful in:

- 1) the scenarios where the label distribution is highly imbalanced such as medical image classification and remote-sensing image classification. This is because the proposed algorithm can induce better performance on the ranking loss and $AP@K$, which are popular measures in imbalanced learning.
- 2) the scenarios where the ranking of the top- K labels is of interest. The proposed algorithm can effectively optimize the top- K ranking list.
- 3) the scenarios where some ground-truth labels are missing, which is universal in multi-learning since full annotations are rather expensive and time-consuming. As shown in Sec.6.3, the proposed algorithm shows superior performance in such scenarios.

Theoretically, this work focuses on ranking-based measures and does not discuss the connection between TKPR and threshold-based measures such as the Hamming loss, the subset accuracy, and the F-measure. Methodologically, it might be a promising direction to replace the naïve ranking operators in the TKPR objective with differentiable ranking operators [Xie et al \(2020\)](#), such that the loss computation can be more efficient. Additionally, the application of TKPR in other learning tasks such as retrieval and recommendation is also an interesting direction.

Declarations

Availability of data and materials

The datasets that support the experiments in Sec.6.2 are available in Pascal VOC 2007* [Everingham et al \(2010\)](#), MS-COCO† [Lin et al \(2014\)](#), and NUSWDIE‡ [Chua et al \(2009\)](#).

Furthermore, the datasets that support the experiments in Sec.6.3 are also generated from Pascal VOC 2012§ [Everingham et al \(2010\)](#) and MS-COCO [Lin et al \(2014\)](#) based on the protocol described in [Cole et al \(2021\)](#), which we have reviewed in Sec.6.3.1.

Acknowledgment

This work was supported in part by the National Key R&D Program of China under Grant 2018AAA0102000, in part by National Natural Science Foundation of China: 62236008, U21B2038, U23B2051, U2001202, 61931008, 62122075 and 61976202, in part by Youth Innovation Promotion Association CAS, in part by the Strategic Priority Research Program of the Chinese Academy of Sciences, Grant No. XDB0680000, in part by the Innovation Funding of ICT, CAS under Grant No.E000000, in part by the China National Postdoctoral Program for Innovative Talents under Grant BX20240384.

* <http://host.robots.ox.ac.uk/pascal/VOC/voc2007/index.html>

† <https://cocodataset.org>

‡ <https://lms.comp.nus.edu.sg/wp-content/uploads/2019/research/nuswide/NUS-WIDE.html>

§ <http://host.robots.ox.ac.uk/pascal/VOC/voc2012/>

Appendix A Bayes optimality of P@K and R@K Optimization

Menon et al (2019) has presented the Bayes Optimality of P@K and R@K under the no-tie assumption. Here, we extend the results under the with-tie assumption, *i.e.*, Asm.1, which is necessary for the further comparison in Sec.5.1.1.

Proposition 14 (Bayes optimality of P@K and R@K). *Under Asm.1, we have*

$$\begin{aligned} f^* \in \arg \max_f P@K(f) &\Leftrightarrow \forall \mathbf{x} \in \mathcal{X}, \widetilde{\text{Top}}_K(\eta) \subset \text{Top}_K(f^*), \\ \text{Top}_K(f^*) - \widetilde{\text{Top}}_K(\eta) &\subset \text{Tie}_K(\eta), \end{aligned}$$

where $\widetilde{\text{Top}}_K(\eta) := \text{Top}_K(\eta) - \text{Tie}_K(\eta)$, $\text{Top}_K(\eta)$ denotes the indices of the top- K entries of $\eta(\mathbf{x}) \in \mathbb{R}^C$. Meanwhile, let

$$\eta'(\mathbf{x})_i := \eta(\mathbf{x})_i \cdot \mathbb{E}_{\mathbf{y}_{\setminus i} | \mathbf{x}, y_i=1} \left[\frac{1}{1 + N(\mathbf{y}_{\setminus i})} \right], \quad (\text{A1})$$

and $\mathbf{y}_{\setminus i} \in \{0, 1\}^{C-1}$ denotes the vector of all but the i -th label. Then, we have

$$\begin{aligned} f^* \in \arg \max_f R@K(f) &\Leftrightarrow \forall \mathbf{x} \in \mathcal{X}, \widetilde{\text{Top}}_K(\eta') \subset \text{Top}_K(f^*), \\ \text{Top}_K(f^*) - \widetilde{\text{Top}}_K(\eta') &\subset \text{Tie}_K(\eta'). \end{aligned}$$

Proof. Since the sample (\mathbf{x}, \mathbf{y}) is *i.i.d.* sampled from \mathcal{D} , we next consider the following conditional formulations:

$$\begin{aligned} P@K(f | \mathbf{x}) &= \mathbb{E}_{\mathbf{y} | \mathbf{x}} \left[\frac{1}{K} \sum_{k=1}^K y_{\sigma(f,k)} \right], \\ R@K(f | \mathbf{x}) &= \mathbb{E}_{\mathbf{y} | \mathbf{x}} \left[\frac{1}{N(\mathbf{y})} \sum_{k=1}^K y_{\sigma(f,k)} \right]. \end{aligned}$$

For P@K, we have

$$\begin{aligned} P@K(f | \mathbf{x}) &= \frac{1}{K} \sum_{\mathbf{y} \in \mathcal{Y}} \mathbb{P}[\mathbf{y} | \mathbf{x}] \sum_{k=1}^K y_{\sigma(f,k)} \\ &= \frac{1}{K} \sum_{\mathbf{y} \in \mathcal{Y}} \mathbb{P}[\mathbf{y} | \mathbf{x}] \sum_{i \in \mathcal{L}} y_i \cdot \mathbf{1}[i \in \text{Top}_K(f)] \\ &= \frac{1}{K} \sum_{i \in \text{Top}_K(f)} \sum_{\mathbf{y}: y_i=1} \mathbb{P}[\mathbf{y} | \mathbf{x}] \\ &= \frac{1}{K} \sum_{i \in \text{Top}_K(f)} \eta(\mathbf{x})_i \end{aligned}$$

Note that $|\text{Top}_K(\eta) \cup \text{Tie}_K(\eta)|$ might be greater than K . To maximize $P@K(f | \mathbf{x})$, $\text{Top}_K(f)$ must consist of two parts: all the labels in $\widetilde{\text{Top}}_K(\eta)$ and $K - |\widetilde{\text{Top}}_K(\eta)|$ labels from $\text{Tie}_K(\eta)$. That is,

$$\widetilde{\text{Top}}_K(\eta) \subset \text{Top}_K(f^*), \text{Top}_K(f^*) - \widetilde{\text{Top}}_K(\eta) \subset \text{Tie}_K(\eta).$$

For R@K , we have

$$\begin{aligned}
\text{R@K}(f \mid \mathbf{x}) &= \sum_{i \in \text{Top}_K(f)} \mathbb{E}_{\mathbf{y} \mid \mathbf{x}} \left[\frac{y_i}{N(\mathbf{y})} \right] \\
&= \sum_{i \in \text{Top}_K(f)} \mathbb{E}_{y_i} \left[\mathbb{E}_{\mathbf{y}_{\setminus i} \mid \mathbf{x}, y_i} \left[\frac{y_i}{N(\mathbf{y})} \right] \right] \\
&= \sum_{i \in \text{Top}_K(f)} \eta(\mathbf{x})_i \cdot \mathbb{E}_{\mathbf{y}_{\setminus i} \mid \mathbf{x}, y_i=1} \left[\frac{1}{1 + N(\mathbf{y}_{\setminus i})} \right] \\
&= \sum_{i \in \text{Top}_K(f)} \eta'(\mathbf{x})_i
\end{aligned}$$

Then, the proof follows the above analysis of P@K .

As shown in [Menon et al \(2019\)](#), the order of $\eta(\mathbf{x})$ and $\eta'(\mathbf{x})$ are generally inconsistent. Thus, optimizing one measure cannot guarantee the performance on the other one. \square

Appendix B Comparison Between TKPR and Other Metrics

B.1 TKPR v.s. NDCG@K (Proof of Prop.2)

Proposition 2. Given a score function f and $(\mathbf{x}, \mathbf{y}) \in \mathcal{Z}$,

$$\text{TKPR}^\alpha(f, \mathbf{y}) = \begin{cases} \frac{1}{K} \cdot \text{DCG-l@K}(f, \mathbf{y}), & \alpha = \alpha_1, \\ \frac{1}{K} \cdot \text{DCG-ln@K}(f, \mathbf{y}), & \alpha = \alpha_2, \\ \frac{1}{K} \cdot \text{NDCG-l@K}(f, \mathbf{y}), & \alpha = \alpha_3, \end{cases}$$

where DCG-l@K , NDCG-l@K represent the NDCG measures equipped with the linear discount function D_l defined in Eq.(9), respectively;

$$\text{DCG-ln@K}(f, \mathbf{y}) := \frac{1}{N_K(\mathbf{y})} \cdot \text{DCG-l@K}(f, \mathbf{y}). \quad (14)$$

denotes the linear DCG@K with a linear weighting term; $\alpha_1 = 1$, $\alpha_2 := N_K(\mathbf{y})$, $\alpha_3 := N_K(\mathbf{y})\tilde{N}_K(\mathbf{y})$, and

$$\tilde{N}_K(\mathbf{y}) := [2K + 1 - N_K(\mathbf{y})] / 2.$$

Proof. According to the definition of TKPR,

$$\begin{aligned}
\text{TKPR}(f, \mathbf{y}) &= \frac{1}{\alpha K} \sum_{y \in \mathcal{P}(\mathbf{y})} \sum_{k \leq K} \mathbf{1}[\pi_f(y) \leq k] \\
&= \frac{1}{\alpha K} \sum_{k \leq K} \sum_{i \in \mathcal{L}} y_i \mathbf{1}[i \in \text{Top}_k(f)] \\
&= \frac{1}{\alpha K} \sum_{k \leq K} \sum_{i \in \text{Top}_k(f)} y_i \\
&= \frac{1}{\alpha K} \sum_{k \leq K} (K + 1 - k) y_{\sigma(f, k)},
\end{aligned} \quad (\text{B2})$$

where the last equation comes from

$$\begin{aligned}
k = 1, & \quad \sum_{i \in \text{Top}_1(f)} y_i = y_{\sigma(f,1)}, \\
k = 2, & \quad \sum_{i \in \text{Top}_2(f)} y_i = y_{\sigma(f,1)} + y_{\sigma(f,2)}, \\
& \quad \vdots \quad \quad \quad \quad \quad \quad y_{\sigma(f,1)} + y_{\sigma(f,2)} + \cdots + y_{\sigma(f,k)}, \\
k = K, & \quad \sum_{i \in \text{Top}_K(f)} y_i = y_{\sigma(f,1)} + y_{\sigma(f,2)} + \cdots + y_{\sigma(f,k)} + \cdots + y_{\sigma(f,K)}.
\end{aligned}$$

Meanwhile, benefiting from the linear discount function, it is clear that

$$\text{IDCG-1@K}(\mathbf{y}) = \frac{1}{2} \cdot N_K(\mathbf{y})(2K + 1 - N_K(\mathbf{y})) = N_K(\mathbf{y})\tilde{N}_K(\mathbf{y}),$$

which ends the proof. \square

B.2 TKPR v.s. P@K and R@K (Proof of Thm.1)

Theorem 1. *Given $K > 1$, TKPR is statistically more discriminating than P@K and R@K.*

Proof. Without loss of generality, we assume that $\alpha = 1$. Frist of all, the following listwise formulation is useful:

$$\text{TKPR}(f, \mathbf{y}) = \frac{1}{K} \sum_{k \leq K} (K + 1 - k)y_{\sigma(f,k)},$$

whose derivation can be found in the proof of Prop.2. Then, we define the following partition number, where D is written as the sum of b distinct bounded positive integers:

$$pn_K(a, b) := |\{(r_1, r_2, \dots, r_b) \in \mathbb{N}_+^b \mid a = r_1 + r_2 + \cdots + r_b, K \geq r_1 > r_2 > \cdots > r_b \geq 1\}|.$$

Besides, if $a \leq 0$ or $b \leq 0$, $pn_K(a, b) = 0$. Given the input sample (\mathbf{x}, \mathbf{y}) , it is clear that $pn_K(a, b)$ is exactly the number of predictions \mathbf{s} such that

$$\text{P@K}(\mathbf{s}, \mathbf{y}) = b/K, \text{TKPR}(\mathbf{s}, \mathbf{y}) = a/K.$$

On one hand, we have

$$\begin{aligned}
|P| &= |\{(\mathbf{s}, \mathbf{s}') \mid \text{TKPR}(\mathbf{s}, \mathbf{y}) > \text{TKPR}(\mathbf{s}', \mathbf{y}), \text{P@K}(\mathbf{s}, \mathbf{y}) = \text{P@K}(\mathbf{s}', \mathbf{y})\}| \\
&= \sum_{b=0}^K |\{(\mathbf{s}, \mathbf{s}') \mid \text{TKPR}(\mathbf{s}, \mathbf{y}) > \text{TKPR}(\mathbf{s}', \mathbf{y}), \text{P@K}(\mathbf{s}, \mathbf{y}) = \text{P@K}(\mathbf{s}', \mathbf{y}) = b/K\}| \\
&= \sum_{b=0}^K \frac{1}{2} \left[\binom{K}{b}^2 - |\{(\mathbf{s}, \mathbf{s}') \mid \text{TKPR}(\mathbf{s}, \mathbf{y}) = \text{TKPR}(\mathbf{s}', \mathbf{y}), \text{P@K}(\mathbf{s}, \mathbf{y}) = \text{P@K}(\mathbf{s}', \mathbf{y}) = b/K\}| \right] \\
&= \frac{1}{2} \sum_{b=0}^K \binom{K}{b}^2 - \frac{1}{2} \sum_{b=0}^K \sum_{a=0}^{\bar{a}} pn_K(a, b)^2,
\end{aligned}$$

where $\binom{K}{b}$ denotes the combination number, which exactly equals to the number of predictions with $\text{P@K}(f, \mathbf{y}) = b/K$.

On the other hand, let $\bar{a} := \frac{K(K+1)}{2}$ denote the maximum value of $K \cdot \text{TKPR}(f, \mathbf{y})$. And $pn_K(a) := \sum_{b=0}^K pn_K(a, b)$ denotes the number of predictions whose $\text{TKPR}(f, \mathbf{y})$ equals to a/K . Then,

$$\begin{aligned}
|S| &= |\{(s, s') \mid \text{TKPR}(s, \mathbf{y}) = \text{TKPR}(s', \mathbf{y}), \text{P@K}(s, \mathbf{y}) > \text{P@K}(s', \mathbf{y})\}| \\
&= \sum_{a=0}^{\bar{a}} |\{(s, s') \mid \text{TKPR}(s, \mathbf{y}) = \text{TKPR}(s', \mathbf{y}) = a/K, \text{P@K}(s, \mathbf{y}) > \text{P@K}(s', \mathbf{y})\}| \\
&= \sum_{a=0}^{\bar{a}} \frac{1}{2} [pn_K(a)^2 - |\{(s, s') \mid \text{TKPR}(s, \mathbf{y}) = \text{TKPR}(s', \mathbf{y}) = a/K, \text{P@K}(s, \mathbf{y}) = \text{P@K}(s', \mathbf{y})\}|] \\
&= \frac{1}{2} \sum_{a=0}^{\bar{a}} pn_K(a)^2 - \frac{1}{2} \sum_{a=0}^{\bar{a}} \sum_{b=0}^K pn_K(a, b)^2,
\end{aligned}$$

Thus, we have

$$2(|P| - |S|) = \underbrace{\sum_{b=0}^K \binom{K}{b}^2}_{(I)} - \underbrace{\sum_{a=0}^{\bar{a}} pn_K(a)^2}_{(II)}. \quad (\text{B3})$$

Notice that the following number equals to $pn_K(a, b)$, where $t_i = r_i - 1, i \in \{1, 2, \dots, b\}$:

$$|\{(t_1, t_2, \dots, t_b) \in \mathbb{N}^b \mid a - b = t_1 + t_2 + \dots + t_b, K - 1 \geq t_1 > t_2 > \dots > t_b \geq 0\}|.$$

Thus, we have the following recurrence formula:

$$pn_K(a, b) = \underbrace{pn_{K-1}(a-b, b)}_{(a)} + \underbrace{pn_{K-1}(a-b, b-1)}_{(b)},$$

where (a) and (b) correspond to the case where $t_b > 0$ and $t_b = 0$, respectively. Notice that in each recurrence, $K \rightarrow K - 1, a \rightarrow a - b, b \rightarrow \{b, b - 1\}$. Thus, by applying this recurrence iteratively, the coefficients will be exactly the Pascal's triangle:

$$\begin{aligned}
pn_K(a, b) &= 1 \cdot pn_{K-1}(a-b, b) + 1 \cdot pn_{K-1}(a-b, b-1) \\
&= 1 \cdot pn_{K-2}(a-2b, b) + 2 \cdot pn_{K-2}(a-2b, b-1) + 1 \cdot pn_{K-2}(a-2b, b-2) \\
&= 1 \cdot pn_{K-3}(a-3b, b) + 3 \cdot pn_{K-3}(a-3b, b-1) + 3 \cdot pn_{K-3}(a-3b, b-2) + 1 \cdot pn_{K-3}(a-3b, b-3) \\
&\dots \\
&= \sum_{t=0}^{K-1} \binom{K-1}{t} \cdot pn_1(a-b(K-1), b-t).
\end{aligned}$$

Although the last term consists of $K - 1$ combination numbers and $K - 1$ partition numbers, it is fortunate that only when $b - t = 1$, $pn_1(a - b(K - 1), b - t) > 0$. Thus,

$$pn_K(a) = \sum_{b=0}^K pn_K(a, b) = \sum_{b=0}^K \binom{K-1}{b-1} pn_1(a - b(K - 1), 1).$$

Similarly, only when $a - b(K - 1) = 1$, $pn_1(a - b(K - 1), 1) = 1$. Thus, for any a such that $\exists b \in \mathbb{N}_+, a - b(K - 1) = 1$,

$$pn_K(a) = \binom{K-1}{(a-K)/(K-1)}.$$

On top of this, we have

$$(II) = \sum_{a=0}^{\bar{a}} pn_K(a)^2 = \sum_{b=1}^{\lfloor K \rfloor / 2 + 1} \binom{K-1}{b-1}^2,$$

where $\lfloor K \rfloor / 2 + 1$ comes from solve the equation $\bar{a} - b(K-1) = 1$. Finally, since $\binom{K}{b} = \frac{K}{b} \binom{K-1}{b-1} \geq \binom{K-1}{b-1}$, and $K \geq \lfloor K \rfloor / 2 + 1$, we have $(I) \geq (II)$, where the equality holds only if $K = 1$.

Besides, this result is clearly applicable to ROK since the weighting term α does not affect the performance comparison between models. \square

B.3 TKPR v.s. the ranking loss (Proof of Prop.3)

Proposition 3. *Under Asm.2, maximizing TKPR is equivalent to minimizing the TKPR loss*

$$L_K^\alpha(f, \mathbf{y}) := \frac{1}{\alpha K} \sum_{y \in \mathcal{P}(\mathbf{y})} \sum_{k \leq K+1} \ell_{0-1}(s_y - s_{[k]}), \quad (15)$$

Furthermore, the following inequality holds:

$$L_{rank}(f, \mathbf{y}) \leq \frac{\alpha}{N(\mathbf{y})} L_K^\alpha(f, \mathbf{y}). \quad (16)$$

Proof. We consider the following two situations:

- **Case (a):** For each relevant label y that is ranked at $k \leq K$. In this case, we should not punish the term $\ell_{0-1}(s_y - s_{[k]})$:

$$\sum_{k \leq K} \mathbf{1}[\pi_{\mathbf{s}}(y) > k] = -1 + \sum_{k \leq K} \mathbf{1}[s_y \leq s_{[k]}].$$

Note that if $s_{[K]} = s_{[K+1]}$, according to Asm.2, we have $s_y > s_{[K]} = s_{[K+1]}$. And if $s_{[K]} > s_{[K+1]}$, we have $s_y \geq s_{[K]} > s_{[K+1]}$. Hence, we can conclude that $s_y > s_{[K+1]}$ in this case.

- **Case (b):** For each relevant label y that is ranked lower than K , it is clear that

$$\sum_{k \leq K} \mathbf{1}[\pi_{\mathbf{s}}(y) > k] = K = \sum_{k \leq K} \mathbf{1}[s_y \leq s_{[k]}].$$

Note that $s_y \leq s_{[K+1]}$ in this case.

To sum up, we have the following equation for any relevant labels y :

$$\sum_{k \leq K} \mathbf{1}[\pi_{\mathbf{s}}(y) > k] = -1 + \mathbf{1}[s_y \leq s_{[K+1]}] + \sum_{k \leq K} \mathbf{1}[s_y \leq s_{[k]}] = -1 + \sum_{k \leq K+1} \mathbf{1}[s_y \leq s_{[k]}].$$

Thus, we have

$$\sum_{y \in \mathcal{P}(\mathbf{y})} \sum_{k \leq K} \mathbf{1}[\pi_{\mathbf{s}}(y) > k] = -N(\mathbf{y}) + \sum_{y \in \mathcal{P}(\mathbf{y})} \sum_{k \leq K+1} \mathbf{1}[s_y \leq s_{[k]}] = -N(\mathbf{y}) + \sum_{y \in \mathcal{P}(\mathbf{y})} \sum_{k \leq K+1} \ell_{0-1}(s_y - s_{[k]}).$$

Since $N(\mathbf{y})$ is independent with the score function, the two formulations are essentially equivalent.

Furthermore, it is clear that

$$\frac{1}{K} \sum_{k \leq K+1} s_{[k]} \geq \frac{1}{K} \sum_{k \leq K} s_{[k]} \geq \frac{1}{N_-(\mathbf{y})} \sum_{j \in \mathcal{N}(\mathbf{y})} s_j,$$

Since ℓ_{0-1} is non-increasing, we have

$$L_{\text{rank}}(f, \mathbf{y}) \leq \frac{1}{N(\mathbf{y})K} \sum_{y \in \mathcal{P}(\mathbf{y})} \sum_{k \leq K+1} \ell_{0-1}(s_y - s_{[k]}) = \frac{\alpha}{N(\mathbf{y})} L_K^\alpha(f, \mathbf{y}).$$

□

B.4 TKPR v.s. AP@K (Proof of Thm.2)

Lemma 3. For $0 \leq \beta \leq x \leq y$, $\ln y - \ln x \leq \frac{1}{\beta}(y - x)$.

Proof. It is clear that

$$\ln y - \ln x = \ln\left(1 + \frac{y}{x} - 1\right) \leq \frac{y}{x} - 1 = \frac{1}{x} \cdot (y - x) \leq \frac{1}{\beta} \cdot (y - x).$$

□

Theorem 2. Given a score function f and $(\mathbf{x}, \mathbf{y}) \in \mathcal{Z}$, there exists a constant $\rho > 0$ such that

$$\begin{aligned} \rho \cdot \text{TKPR}^{\alpha_2}(f, \mathbf{y}) &\leq \text{AP@K}(f, \mathbf{y}) \\ &\leq K \cdot \text{TKPR}^{\alpha_1}(f, \mathbf{y}), \end{aligned} \tag{17}$$

where the upper bound of ρ is bounded in

$$[1/(K+1), K \ln(K+1)].$$

Proof. For the left inequality, given $(\mathbf{x}, \mathbf{y}) \in \mathcal{Z}$, let $p := K \cdot \text{P@K}(f, \mathbf{y}) > 0$ and $\mathcal{K} := \{k_i\}_{i=1}^p$ such that $1 \leq k_1 < k_2 < \dots < k_p \leq K$ and $\forall k \in \mathcal{K}, y_{\sigma(f,k)} = 1$. Then, we have

$$\begin{aligned} \text{AP@K}(f, \mathbf{y}) &= \frac{1}{N_K(\mathbf{y})} \sum_{k=1}^K \frac{y_{\sigma(f,k)}}{k} \sum_{i=1}^k y_{\sigma(f,i)} \\ &\stackrel{(a)}{=} \frac{1}{N_K(\mathbf{y})} \sum_{k=1}^K \left[\frac{y_{\sigma(f,k)}}{k} + \frac{y_{\sigma(f,k+1)}}{k+1} + \dots + \frac{y_{\sigma(f,K)}}{K} \right] y_{\sigma(f,k)} \\ &\stackrel{(b)}{=} \frac{1}{N_K(\mathbf{y})} \sum_{i=1}^p \sum_{j=k_i}^K \frac{y_{\sigma(f,j)}}{j} \\ &\stackrel{(c)}{=} \frac{1}{N_K(\mathbf{y})} \sum_{i=1}^p \sum_{j=i}^p \frac{1}{k_j} \\ &\stackrel{(d)}{=} \frac{1}{N_K(\mathbf{y})} \sum_{i=1}^p \frac{i}{k_i}, \end{aligned} \tag{B4}$$

where (a) holds since

$$\begin{aligned}
k = 1, & \quad \frac{y_{\sigma(f,1)}}{1} : y_{\sigma(f,1)}, \\
k = 2, & \quad \frac{y_{\sigma(f,2)}}{2} : y_{\sigma(f,1)} + y_{\sigma(f,2)}, \\
& \quad \vdots \quad \quad \quad y_{\sigma(f,1)} + y_{\sigma(f,2)} + \cdots + y_{\sigma(f,k)}, \\
k = K, & \quad \frac{y_{\sigma(f,K)}}{K} : y_{\sigma(f,1)} + y_{\sigma(f,2)} + \cdots + y_{\sigma(f,k)} + \cdots + y_{\sigma(f,K)},
\end{aligned}$$

(b) is induced by replacing $\sum_{k=1}^K y_{\sigma(f,k)}$ with $\sum_{i=1}^p y_{\sigma(f,k_i)}$, (c) is the same as (b), and (d) follows the fact

$$\begin{aligned}
i = 1, & \quad \frac{1}{k_1} + \frac{1}{k_2} + \cdots + \frac{1}{k_j} + \cdots + \frac{1}{k_p}, \\
i = 2, & \quad \frac{1}{k_2} + \cdots + \frac{1}{k_j} + \cdots + \frac{1}{k_p}, \\
& \quad \vdots \quad \quad \quad \frac{1}{k_j} + \cdots + \frac{1}{k_p}, \\
i = p, & \quad \frac{1}{k_p}.
\end{aligned}$$

Meanwhile, we have

$$\begin{aligned}
\text{TKPR}^{\alpha_2}(f, \mathbf{y}) &= \frac{1}{N_K(\mathbf{y})K} \sum_{k=1}^K (K+1-k) y_{\sigma(f,k)} \\
&= \frac{1}{N_K(\mathbf{y})} \sum_{k \in \mathcal{K}} \frac{K+1-k}{K} \\
&= \frac{1}{N_K(\mathbf{y})} \sum_{i=1}^p \frac{K+1-k_i}{K}.
\end{aligned}$$

Since $\text{AP@K}(f, \mathbf{y})$ and $\text{TKPR}^{\alpha_2}(f, \mathbf{y})$ have the same number of bounded summation terms, there must exist a constant $\rho > 0$ such that

$$\text{AP@K}(f, \mathbf{y}) \geq \rho \cdot \text{TKPR}^{\alpha_2}(f, \mathbf{y}).$$

To obtain the range of ρ 's upper bounds, let

$$C_1 := \frac{\sum_{i=1}^p \frac{i}{k_i}}{\sum_{i=1}^p \frac{1}{k_i}} \in [1, p], C_2 := \frac{1}{p} \sum_{i=1}^p k_i \in [k_1, k_p].$$

Then,

$$\begin{aligned}
\text{AP@K}(f, \mathbf{y}) - \rho \cdot \text{TKPR}^{\alpha_2}(f, \mathbf{y}) &= \frac{1}{N_K(\mathbf{y})} \left[C_1 \sum_{i=1}^p \frac{1}{k_i} - \rho \cdot \frac{p(K+1-C_2)}{K} \right] \\
&\geq \frac{1}{N_K(\mathbf{y})} \left[C_1 \sum_{i=1}^p \frac{1}{K+1-i} - \rho \cdot \frac{p(K+1-C_2)}{K} \right] \\
&\stackrel{(a)}{\geq} \frac{1}{N_K(\mathbf{y})} \left[C_1 \ln \frac{K+1}{K+1-p} - \rho \cdot \frac{p(K+1-C_2)}{K} \right],
\end{aligned}$$

where (a) is induced by the fact that for any $1 \leq k \leq K$,

$$\frac{1}{k} + \dots + \frac{1}{K} \geq \int_k^{K+1} \frac{1}{t} dt = \ln(K+1) - \ln k = \ln \frac{K+1}{k}.$$

In other words, when

$$\begin{aligned} \rho &\leq \frac{C_1 \cdot K}{p(K+1-C_2)} \ln \frac{K+1}{K+1-p} \\ &= \underbrace{\frac{C_1}{K+1-C_2}}_{U_1} \cdot \underbrace{\frac{1}{\text{P@K}(f, \mathbf{y})} \ln \frac{1+1/K}{1+1/K-\text{P@K}(f, \mathbf{y})}}_{U_2}, \end{aligned}$$

$\text{AP@K}(f, \mathbf{y}) \geq \rho \cdot \text{TKPR}^{\alpha_2}(f, \mathbf{y})$ will hold. Next, we consider this upper bound from the two parts:

- U_1 is increasing *w.r.t.* C_1 and C_2 that are determined by \mathcal{K} . Since $C_1 \in [1, p]$, $C_2 \in [k_1, k_p]$, we have

$$\frac{1}{K} \leq \frac{1}{K+1-k_1} \leq (II) \leq \frac{p}{K+1-k_p} \leq p \leq K.$$

- U_2 depends on the model performance on P@K . Let

$$g(t) := \frac{1}{t} \ln \frac{1}{1-C_g t}, t \in (0, 1], C_g := \frac{1}{1+\frac{1}{K}} \in [0.5, 1).$$

We have

$$g'(t) = \frac{1}{t^2} \cdot \ln(1-C_g t) + \frac{1}{t} \cdot \frac{C_g}{1-C_g t} = \frac{(1-C_g t) \ln(1-C_g t) + C_g t}{t^2(1-C_g t)}.$$

Let

$$h(t) = (1-t) \ln(1-t) + t, t \in [0, 1].$$

Then, we have

$$h'(t) = -\ln(1-t) - 1 + 1 \geq 0.$$

Hence, $h(t) \geq h(0) = 0$, that is, $g'(t) \geq 0$. In other words, U_2 is increasing *w.r.t.* $\text{P@K}(f, \mathbf{y})$. As $t \rightarrow 0$, $g(t) \rightarrow C_g = \frac{K}{1+K}$. And $g(1) = \ln \frac{1}{1-C_g} = \ln(K+1)$.

To sum up, the upper bound of ρ is bounded in $[1/(K+1), K \ln(K+1)]$.

For the right inequality,

$$\begin{aligned}
\text{AP@K}(f, \mathbf{y}) &= \frac{1}{N_K(\mathbf{y})} \sum_{k=1}^K y_{\sigma(f,k)} \cdot \frac{1}{k} \sum_{i=1}^k y_{\sigma(f,i)} \\
&\leq \frac{1}{N_K(\mathbf{y})} \sum_{k=1}^K \frac{1}{k} \sum_{i=1}^k y_{\sigma(f,i)} \\
&\stackrel{(a)}{=} \frac{1}{N_K(\mathbf{y})} \sum_{k=1}^K \left[\frac{1}{k} + \frac{1}{k+1} + \cdots + \frac{1}{K} \right] y_{\sigma(f,k)} \\
&\stackrel{(b)}{\leq} \frac{1}{N_K(\mathbf{y})} \left[(1 + \ln K) y_{\sigma(f,1)} + \sum_{k=2}^K [\ln K - \ln(k-1)] y_{\sigma(f,k)} \right] \\
&\stackrel{(c)}{\leq} \frac{1}{N_K(\mathbf{y})} \left[K \cdot y_{\sigma(f,1)} + \sum_{k=2}^K [K - (k-1)] y_{\sigma(f,k)} \right] \\
&= \frac{1}{N_K(\mathbf{y})} \left[\sum_{k=1}^K [K+1-k] y_{\sigma(f,k)} \right] \\
&= K \cdot \text{TKPR}^{\alpha_1}(f, \mathbf{y})
\end{aligned} \tag{B5}$$

where (a) follows the derivation of Eq.(B4), (b) comes from the fact that for any $k \in \{2, 3, \dots, K\}$,

$$\begin{aligned}
\frac{1}{k} + \cdots + \frac{1}{K} &\leq \int_{k-1}^K \frac{1}{t} dt = \ln K - \ln(k-1), \\
1 + \frac{1}{2} + \cdots + \frac{1}{K} &\leq 1 + \ln K - \ln(2-1) = 1 + \ln K,
\end{aligned}$$

and (c) is induced by Lem.3 and the fact that $x \geq 1 + \ln x$. \square

Further discussion about the monotonicity of the upper bound of ρ . So far, we have known that U_1 is increasing *w.r.t.* $\text{P@K}(f, \mathbf{y})$. Next, we analyze the monotonicity of U_2 . Note that two factors of \mathcal{K} can affect the value of U_2 : the number of elements p and the value of each k_i . Hence, we next consider the following two orthogonal cases:

- Two score functions share the same ranking performance but difference performances on P@K . Formally, let $\mathcal{K}' := \{k'_i\}_{i=1}^{p+1}$ such that $\forall i \leq p, k_i = k'_i < k'_{p+1}$. On one hand, since $k'_{p+1}/1 = k'_{p+1} > \sum_{i=1}^p k_i/p$,

$$C_2(\mathcal{K}') - C_2(\mathcal{K}) = \frac{k'_{p+1} + \sum_{i=1}^p k_i}{1+p} - \frac{\sum_{i=1}^p k_i}{p} > 0.$$

On the other hand, since $\frac{p+1}{k'_{p+1}} / \frac{1}{k'_{p+1}} = p+1 > \sum_{i=1}^p \frac{i}{k_i} / \sum_{i=1}^p \frac{1}{k_i}$,

$$C_1(\mathcal{K}') - C_1(\mathcal{K}) = \frac{\frac{p+1}{k'_{p+1}} + \sum_{i=1}^p \frac{i}{k_i}}{\frac{1}{k'_{p+1}} + \sum_{i=1}^p \frac{1}{k_i}} - \frac{\sum_{i=1}^p \frac{i}{k_i}}{\sum_{i=1}^p \frac{1}{k_i}} > 0.$$

Since U_2 is increasing *w.r.t.* C_1 and C_2 , we have $U_2(\mathcal{K}') > U_2(\mathcal{K})$. In other words, U_2 is increasing *w.r.t.* $\text{P@K}(f, \mathbf{y})$ under the given ranking performance.

- Two score functions share the same performance on P@K but difference ranking performance. It is a pity that in this case, U_2 is not necessarily increasing *w.r.t.* the ranking performance. For example, assume that $p = 1, K \geq 2$, and let $\mathcal{K}_1 = \{1\}, \mathcal{K}_2 = \{2\}$. It is clear that \mathcal{K}_1 has a better ranking performance. However, we have

$$U_2(\mathcal{K}_1) = \frac{1}{K} < \frac{1}{K-1} = U_2(\mathcal{K}_2).$$

Meanwhile, U_2 is not necessarily decreasing *w.r.t.* the ranking performance. Assume that $p = 2, K = 10$, and let $\mathcal{K}_3 = \{1, 2\}, \mathcal{K}_4 = \{1, 3\}$. It is clear that \mathcal{K}_3 has a better ranking performance. Meanwhile,

$$U_2(\mathcal{K}_3) = \frac{\frac{1}{1} + \frac{2}{2}}{(\frac{1}{1} + \frac{1}{2})(10 + 1 - \frac{1+2}{2})} = \frac{2}{1.5 \cdot 9.5} \approx 0.1404,$$

$$U_2(\mathcal{K}_4) = \frac{\frac{1}{1} + \frac{2}{3}}{(\frac{1}{1} + \frac{1}{3})(10 + 1 - \frac{1+3}{2})} = \frac{5}{36} \approx 0.1389.$$

Thus, we have $U_2(\mathcal{K}_3) > U_2(\mathcal{K}_4)$.

To sum up, as one improves the precision performance, U_2 tends to increase. But when one improves the ranking performance under the given precision performance, U_2 does not necessarily increase.

Appendix C Consistency Analysis of TKPR Optimization

C.1 Bayes Optimality of TKPR (Proof of Prop.4)

Lemma 4 (Rearrangement inequality [Hardy et al \(1952\)](#)). *For any two real number sets $\{a_i\}_{i=1}^n$ and $\{b_i\}_{i=1}^n$,*

$$\sum_{i=1}^n a_{[i]} b_{[i]} \geq \sum_{i=1}^n a_i b_i.$$

Proposition 4 (Bayes optimality of TKPR). *The score function $f : \mathcal{X} \rightarrow \mathbb{R}^C$ is TKPR Bayes optimal if and only if for an input \mathbf{x} , the prediction $f(\mathbf{x})$ is top- K ranking-preserving *w.r.t.* $\Delta(\mathbf{x}) \in \mathbb{R}^C$, where*

$$\Delta(\mathbf{x})_i := \sum_{\mathbf{y}: y_i=1} \frac{\mathbb{P}[\mathbf{y} | \mathbf{x}]}{\alpha}. \quad (24)$$

Proof. We consider the conditional TKPR risk:

$$\begin{aligned}
\mathcal{R}_K^\alpha(f | \mathbf{x}) &:= \mathbb{E}_{\mathbf{y}|\mathbf{x}} \left[\frac{1}{\alpha K} \sum_{i \in \mathcal{L}} \sum_{k=1}^K y_i \mathbf{1}[i \notin \text{Top}_k(f)] \right] \\
&= \mathbb{E}_{\mathbf{y}|\mathbf{x}} \left[\frac{1}{\alpha K} \sum_{i \in \mathcal{L}} \sum_{k=1}^K y_i [1 - \mathbf{1}[i \in \text{Top}_k(f)]] \right] \\
&= \frac{1}{K} \sum_{k=1}^K \sum_{i \in \mathcal{L}} \mathbb{E}_{\mathbf{y}|\mathbf{x}} \left[\frac{y_i}{\alpha} \right] - \frac{1}{K} \mathbb{E}_{\mathbf{y}|\mathbf{x}} \left[\sum_{k=1}^K \sum_{i \in \text{Top}_k(f)} \frac{y_i}{\alpha} \right] \\
&= \sum_{i \in \mathcal{L}} \mathbb{E}_{\mathbf{y}|\mathbf{x}} \left[\frac{y_i}{\alpha} \right] - \frac{1}{K} \sum_{k=1}^K \sum_{i \in \text{Top}_k(f)} \mathbb{E}_{\mathbf{y}|\mathbf{x}} \left[\frac{y_i}{\alpha} \right] \\
&= \sum_{i \in \mathcal{L}} \Delta(\mathbf{x})_i - \frac{1}{K} \sum_{k=1}^K \sum_{i \in \text{Top}_k(f)} \Delta(\mathbf{x})_i \\
&= \sum_{i \in \mathcal{L}} \Delta(\mathbf{x})_i - \frac{1}{K} \sum_{k=1}^K (K+1-k) \Delta(\mathbf{x})_{\sigma(f,k)},
\end{aligned} \tag{C6}$$

where the last equation follows the derivation of Eq.(B2).

Note that $K+1-k$ is decreasing *w.r.t.* k . Thus, when no ties exist in $\Delta(\mathbf{x})_i$, according to Lem.4, it is clear that the optimal solution f^* should satisfy

$$\forall k \leq K, \sigma(f^*, k) = \sigma(\Delta, k).$$

When ties exists, that is, $\exists k \in \mathcal{L}, \Delta(\mathbf{x})_{\sigma(f,k)} = \Delta(\mathbf{x})_{\sigma(f,k+1)}$, f^* can further exchange the value of $f(\mathbf{x})_{[k]}$ and $f(\mathbf{x})_{[k+1]}$. Since $|\text{Top}_K(\Delta) \cup \text{Tie}_K(\Delta)|$ might be greater than K , under Asm.2, f^* should satisfy

$$\forall k \leq K-1, \text{Tie}_k(f^*) = \text{Tie}_k(\Delta), \text{Tie}_K(f^*) \subset \text{Tie}_K(\Delta).$$

□

C.2 Sufficient Condition for TKPR Consistency (Proof of Thm.3)

Theorem 3. *The surrogate loss $\ell(t)$ is TKPR Fisher consistent if it is bounded, differentiable, strictly decreasing, and convex.*

Proof. We first define the conditional risk and the optimal conditional risk of the surrogate loss:

$$\begin{aligned}
\mathcal{R}_K^{\alpha, \ell}(\mathbf{s} | \mathbf{x}) &:= \mathbb{E}_{\mathbf{y}|\mathbf{x}} \left[\frac{1}{\alpha K} \sum_{y \in \mathcal{P}(\mathbf{x})} \sum_{k \leq K+1} \ell(s_y - s_{[k]}) \right], \\
\mathcal{R}_K^{\alpha, \ell, *}(\mathbf{x}) &:= \inf_{\mathbf{s} \in \mathbb{R}^C} \mathcal{R}_K^{\alpha, \ell}(\mathbf{s} | \mathbf{x}).
\end{aligned} \tag{C7}$$

Then, we prove the theorem by the following steps.

Claim 1. If $\mathbf{s}^* \in \arg \inf_{\mathbf{s}} \mathcal{R}_K^{\alpha, \ell}(\mathbf{s} | \mathbf{x})$, then $\text{RPT}(\mathbf{s}^*, \Delta(\mathbf{x}))$.

According to the definition, we have

$$\begin{aligned}
\mathcal{R}_K^{\alpha, \ell}(\mathbf{s} \mid \mathbf{x}) &= \frac{1}{K} \sum_{\mathbf{y} \in \mathcal{Y}} \frac{\mathbb{P}[\mathbf{y} \mid \mathbf{x}]}{\alpha} \sum_{i \in \mathcal{P}(\mathbf{x})} \sum_{k \leq K+1} \ell(s_i - s_{[k]}) \\
&= \frac{1}{K} \sum_{i \in \mathcal{L}} \sum_{k \leq K+1} \ell(s_i - s_{[k]}) \sum_{\mathbf{y}: y_i=1} \frac{\mathbb{P}[\mathbf{y} \mid \mathbf{x}]}{\alpha} \\
&= \frac{1}{K} \sum_{i \in \mathcal{L}} \sum_{k \leq K+1} \Delta_i \ell(s_i - s_{[k]})
\end{aligned} \tag{C8}$$

Next, we show this claim by showing that if $\neg \text{RPT}(\mathbf{s}, \Delta)$, then $\mathcal{R}_K^{\alpha, \ell}(\mathbf{s} \mid \mathbf{x}) > \mathcal{R}_K^{\alpha, \ell, *}(s \mid \mathbf{x})$. Note that $\neg \text{RPT}(\mathbf{s}, \Delta)$ consists of the following cases:

- **Case (1):** Give $\mathbf{s} \in \mathbb{R}^C$ and $i, j \in \mathcal{L}$ such that $\Delta_i = \Delta_j$ but $s_i \neq s_j$, where $\pi_{\mathbf{s}}(i), \pi_{\mathbf{s}}(j) \leq K+1$. Without loss of generality, we assume that $s_i < s_j$. Then, the claim can be obtained by a contradiction. To be specific, we assume that $\mathcal{R}_K^{\alpha, \ell}(\mathbf{s} \mid \mathbf{x}) = \mathcal{R}_K^{\alpha, \ell, *}(s \mid \mathbf{x})$. According to the first-order condition, we have

$$\frac{\partial}{\partial s_i} \mathcal{R}_K^{\alpha, \ell}(\mathbf{s} \mid \mathbf{x}) = \frac{\partial}{\partial s_j} \mathcal{R}_K^{\alpha, \ell}(\mathbf{s} \mid \mathbf{x}) = 0.$$

That is,

$$\begin{aligned}
\underbrace{\Delta_i \sum_{k=1, [k] \neq i}^{K+1} \ell'(s_i - s_{[k]})}_{(I)} &= \underbrace{\sum_{y \neq i} \Delta_y \ell'(s_y - s_i)}_{(II)}; \\
\underbrace{\Delta_j \sum_{k=1, [k] \neq j}^{K+1} \ell'(s_j - s_{[k]})}_{(III)} &= \underbrace{\sum_{y \neq j} \Delta_y \ell'(s_y - s_j)}_{(IV)},
\end{aligned}$$

where $[k] \neq i$ means that the calculation of the derivative will be skipped when $\pi_{\mathbf{s}}(i) = k$. Since $\Delta_i = \Delta_j$, we have

$$\begin{aligned}
(I) &= \Delta_i \ell'(s_i - s_j) + \Delta_i \sum_{k=1, [k] \notin \{i, j\}}^{K+1} \ell'(s_i - s_{[k]}), \\
(II) &= \Delta_i \ell'(s_j - s_i) + \sum_{y \notin \{i, j\}} \Delta_y \ell'(s_y - s_i), \\
(III) &= \Delta_i \ell'(s_j - s_i) + \Delta_i \sum_{k=1, [k] \notin \{i, j\}}^{K+1} \ell'(s_j - s_{[k]}), \\
(IV) &= \Delta_i \ell'(s_i - s_j) + \sum_{y \notin \{i, j\}} \Delta_y \ell'(s_y - s_j).
\end{aligned}$$

Then, since $(I) - (III) = (II) - (IV)$, we have

$$\begin{aligned}
& \underbrace{2\Delta_i \ell'(s_i - s_j)}_{(I')} + \underbrace{\Delta_i \sum_{k=1, [k] \notin \{i, j\}}^{K+1} [\ell'(s_i - s_{[k]}) - \ell'(s_j - s_{[k]})]}_{(II')} \\
&= \underbrace{2\Delta_i \ell'(s_j - s_i)}_{(III')} + \underbrace{\sum_{y \notin \{i, j\}} \Delta_y [\ell'(s_y - s_i) - \ell'(s_y - s_j)]}_{(IV')}.
\end{aligned}$$

Since $\ell'(t)$ is strictly increasing and $s_i < s_j$, it is clear that $(I') < (III')$, $(II') < 0$, and $(IV') > 0$. That is, $(I') + (II') < (III') + (IV')$, which induces contradiction.

- **Case (2):** Give $\mathbf{s} \in \mathbb{R}^C$ and $i, j \in \mathcal{L}$ such that $\Delta_i \neq \Delta_j$ but $s_i = s_j$, where $\pi_{\mathbf{s}}(i), \pi_{\mathbf{s}}(j) \leq K + 1$. The claim can also be obtained by a contradiction. Similarly, According to the first-order condition and $s_i = s_j$, we have

$$\begin{aligned}
(I) &= \Delta_i \ell'(0) + \Delta_i \sum_{k=1, [k] \notin \{i, j\}}^{K+1} \ell'(s_i - s_{[k]}), \\
(II) &= \Delta_j \ell'(0) + \sum_{y \notin \{i, j\}} \Delta_y \ell'(s_y - s_i), \\
(III) &= \Delta_j \ell'(0) + \Delta_j \sum_{k=1, [k] \notin \{i, j\}}^{K+1} \ell'(s_i - s_{[k]}), \\
(IV) &= \Delta_i \ell'(0) + \sum_{y \notin \{i, j\}} \Delta_y \ell'(s_y - s_i).
\end{aligned}$$

Then, since $(I) - (III) = (II) - (IV)$, we have

$$(\Delta_i - \Delta_j) \sum_{k=1, [k] \notin \{i, j\}}^{K+1} \ell'(s_i - s_{[k]}) = 2(\Delta_j - \Delta_i) \ell'(0)$$

which leads to a contradiction since $\ell(t) < 0$ and $\Delta_i \neq \Delta_j$.

- **Case (3):** Give $\mathbf{s}_1 \in \mathbb{R}^C$ and $i, j \in \mathcal{L}$ such that $\Delta_i < \Delta_j$ but $s_{1,i} > s_{1,j}$, where $\pi_{\mathbf{s}}(i), \pi_{\mathbf{s}}(j) \leq K + 1$. Next, we obtain the claim by showing that any swapping breaking the ranking of \mathcal{T}_{Δ} will induce a larger conditional risk. To be specific, let $\mathbf{s}_2 \in \mathbb{R}^C$ such that $s_{2,i} = s_{1,j}$, $s_{2,j} = s_{1,i}$ and $\forall k \notin \{i, j\}, s_{2,k} = s_{1,k}$. Then, we have

$$\begin{aligned}
& K \left[\mathcal{R}_K^{\alpha, \ell}(\mathbf{s}_1 | \mathbf{x}) - \mathcal{R}_K^{\alpha, \ell}(\mathbf{s}_2 | \mathbf{x}) \right] \\
&= \left[\Delta_i \sum_{k=1}^{K+1} \ell(s_{1,i} - s_{1,[k]}) + \Delta_j \sum_{k=1}^{K+1} \ell(s_{1,j} - s_{1,[k]}) \right] - \left[\Delta_i \sum_{k=1}^{K+1} \ell(s_{2,i} - s_{2,[k]}) + \Delta_j \sum_{k=1}^{K+1} \ell(s_{2,j} - s_{2,[k]}) \right] \\
&= \left[\Delta_i \sum_{k=1}^{K+1} \ell(s_{1,i} - s_{1,[k]}) + \Delta_j \sum_{k=1}^{K+1} \ell(s_{1,j} - s_{1,[k]}) \right] - \left[\Delta_i \sum_{k=1}^{K+1} \ell(s_{1,j} - s_{1,[k]}) + \Delta_j \sum_{k=1}^{K+1} \ell(s_{1,i} - s_{1,[k]}) \right] \\
&= (\Delta_j - \Delta_i) \sum_{k=1}^{K+1} [\ell(s_{1,j} - s_{1,[k]}) - \ell(s_{1,i} - s_{1,[k]})] \\
&> 0,
\end{aligned}$$

where the inequality is induced by $\Delta_j > \Delta_i, s_{1,j} < s_{2,j}$ and the surrogate loss ℓ is strictly decreasing.

Given any $\mathbf{a} \in \mathbb{R}^C$, let $\mathcal{T}_{\mathbf{a}} := \{\text{Tie}_k(\mathbf{a})\}_{k=1}^{K+1} = \{\mathcal{T}_1, \mathcal{T}_2, \dots, \mathcal{T}_{|\mathcal{T}_{\mathbf{a}}|}\}$ denote the set of tie sets. Note that $|\mathcal{T}_{\mathbf{a}}| \leq C$ due to the possible ties in \mathbf{a} . From the analysis in **Case (1)** and **Case (2)**, we know that $\mathcal{T}_{\mathbf{s}^*} = \mathcal{T}_{\Delta}$. Without loss of generality, we assume that $\forall i \leq |\mathcal{T}_{\Delta}|, \mathcal{T}_{\Delta,i} = \mathcal{T}_{\mathbf{s}^*,i}$. Define the partial ranking between tie sets as

$$\mathcal{T}_i \prec \mathcal{T}_j \Leftrightarrow \forall y_1 \in \mathcal{T}_i, y_2 \in \mathcal{T}_j, s_{y_1} < s_{y_2}.$$

Then, from the analysis in **Case (3)**, we know that if $\mathcal{T}_{\Delta,1} \prec \mathcal{T}_{\Delta,2} \prec \dots \prec \mathcal{T}_{\Delta,|\mathcal{T}_{\Delta}|}, \mathcal{T}_{\mathbf{s}^*,1} \prec \mathcal{T}_{\mathbf{s}^*,2} \prec \dots \prec \mathcal{T}_{\mathbf{s}^*,|\mathcal{T}_{\mathbf{s}^*|}$, which obtains the claim.

Claim 2.

$$\inf_{\mathbf{s}: \neg \text{RPT}(\mathbf{s}, \mathbf{x})} \mathcal{R}_K^{\alpha, \ell}(\mathbf{s} | \mathbf{x}) > \inf_{\mathbf{s}: \text{RPT}(\mathbf{s}, \mathbf{x})} \mathcal{R}_K^{\alpha, \ell}(\mathbf{s} | \mathbf{x})$$

It is clear that **Claim 2** follows **Claim 1**.

Claim 3. For any sequence $\{\mathbf{s}^{(t)}\}_{t \in \mathbb{N}_+}, \mathbf{s}^{(t)} \in \mathbb{R}^C$,

$$\mathcal{R}_K^{\alpha, \ell}(\mathbf{s}^{(t)} | \mathbf{x}) \rightarrow \inf_{\mathbf{s} \in \mathbb{R}^C} \mathcal{R}_K^{\alpha, \ell}(\mathbf{s} | \mathbf{x}) \Rightarrow \mathcal{R}_K^{\alpha}(\mathbf{s}^{(t)} | \mathbf{x}) \rightarrow \inf_{\mathbf{s} \in \mathbb{R}^C} \mathcal{R}_K^{\alpha}(\mathbf{s} | \mathbf{x}).$$

According to Prop.4 and **Claim 1**, we only need to show that when $t \rightarrow \infty$, $\text{RPT}(\mathbf{s}^{(t)}, \Delta(\mathbf{x}))$. Define

$$\delta := \inf_{\mathbf{s}: \neg \text{RPT}(\mathbf{s}, \Delta(\mathbf{x}))} \mathcal{R}_K^{\alpha, \ell}(\mathbf{s} | \mathbf{x}) - \inf_{\mathbf{s} \in \mathbb{R}^C} \mathcal{R}_K^{\alpha, \ell}(\mathbf{s} | \mathbf{x}).$$

According to **Claim 2**, $0 < \delta < \infty$. Suppose that when $t \rightarrow \infty$, $\neg \text{RPT}(\mathbf{s}^{(t)}, \Delta(\mathbf{x}))$. Then, there exists a large enough T such that

$$\mathcal{R}_K^{\alpha, \ell}(\mathbf{s}^{(t)} | \mathbf{x}) - \inf_{\mathbf{s} \in \mathbb{R}^C} \mathcal{R}_K^{\alpha, \ell}(\mathbf{s} | \mathbf{x}) > \delta,$$

which is contradicts with $\mathcal{R}_K^{\alpha, \ell}(\mathbf{s}^{(t)} | \mathbf{x}) \rightarrow \inf_{\mathbf{s} \in \mathbb{R}^C} \mathcal{R}_K^{\alpha, \ell}(\mathbf{s} | \mathbf{x})$. Thus, we obtain **Claim 3**.

Claim 4. For any sequence of score functions $\{f^{(t)}\}_{t \in \mathbb{N}_+}$,

$$\mathcal{R}_K^{\alpha, \ell}(f^{(t)}) \rightarrow \inf_f \mathcal{R}_K^{\alpha, \ell}(f) \Rightarrow \mathcal{R}_K^{\alpha}(f^{(t)}) \rightarrow \inf_f \mathcal{R}_K^{\alpha}(f).$$

It is clear that **Claim 4** holds with **Claim 3** and

$$\mathcal{R}_K^{\alpha, \ell}(f^{(t)}) = \mathbb{E}_{\mathbf{x}} \left[\mathcal{R}_K^{\alpha, \ell}(f^{(t)} | \mathbf{x}) \right].$$

Then, the proof of Thm.3 ends. □

Appendix D Generalization Analysis for TKPR Optimization

D.1 The Generalization Bound by Traditional Techniques

D.1.1 Lipschitz Property of the TKPR Surrogate Loss (Proof of Prop.5)

Proposition 5. Under Asm.3, the TKPR surrogate loss $L_K^{\alpha, \ell}$ is $\mu_{\ell} \mu_K$ -Lipschitz continuous and bounded by M_K , where

- $\mu_K = \frac{K+1}{\sqrt{K}} + \sqrt{K+1}$, $M_K = (K+1)M_\ell$ when $\alpha = \alpha_1$;
- $\mu_K = \frac{K+1}{\sqrt{K}} + \frac{\sqrt{K+1}}{K}$, $M_K = (K+1)M_\ell$ when $\alpha = \alpha_2$;
- $\mu_K = \frac{K+1}{K^2} + \frac{2}{K\sqrt{K+1}}$, $M_K = \frac{K+1}{K}M_\ell$ when $\alpha = \alpha_3$.

Proof. Given two score functions $f, f' \in \mathcal{F}_K$, then we have

$$\begin{aligned}
& |L_K^{\alpha, \ell}(f, \mathbf{y}) - L_K^{\alpha, \ell}(f', \mathbf{y})| \\
&= \frac{1}{\alpha K} \left| \sum_{y \in \mathcal{P}(\mathbf{x})} \sum_{k \leq K+1} \ell(s_y - s_{[k]}) - \sum_{y \in \mathcal{P}(\mathbf{x})} \sum_{k \leq K+1} \ell(s'_y - s'_{[k]}) \right| \\
&\stackrel{(a)}{=} \frac{1}{\alpha K} \left| \sum_{y \in \mathcal{P}(\mathbf{x})} \sum_{k \leq K+1} \ell(s_y - \mathbf{s}'_{[k]}) - \sum_{y \in \mathcal{P}(\mathbf{x})} \sum_{k \leq K+1} \ell(s'_y - \mathbf{s}'_{[k]}) \right| \\
&\stackrel{(b)}{=} \frac{1}{\alpha K} \left| \sum_{y \in \mathcal{P}(\mathbf{x})} \max_{\substack{\mathcal{K} \subset [C] \\ |\mathcal{K}|=K+1}} \sum_{k \in \mathcal{K}} \ell(s_y - s_k) - \sum_{y \in \mathcal{P}(\mathbf{x})} \max_{\substack{\mathcal{K} \subset [C] \\ |\mathcal{K}|=K+1}} \sum_{k \in \mathcal{K}} \ell(s'_y - s'_k) \right| \\
&\stackrel{(c)}{\leq} \frac{1}{\alpha K} \sum_{y \in \mathcal{P}(\mathbf{x})} \max_{\substack{\mathcal{K} \subset [C] \\ |\mathcal{K}|=K+1}} \left| \sum_{k \in \mathcal{K}} [\ell(s_y - s_k) - \ell(s'_y - s'_k)] \right| \\
&\leq \frac{1}{\alpha K} \sum_{y \in \mathcal{P}(\mathbf{x})} \max_{\substack{\mathcal{K} \subset [C] \\ |\mathcal{K}|=K+1}} \sum_{k \in \mathcal{K}} |\ell(s_y - s_k) - \ell(s'_y - s'_k)|.
\end{aligned}$$

In this process, (a) holds since ℓ is strictly decreasing. (b) holds since

$$\sum_{k=1}^K t_{[k]} = \max_{k \leq K} \sum_{k=1}^K t_k, \forall \mathbf{t} \in \mathbb{R}^C.$$

And (c) holds since

$$|\max\{a_1, \dots, a_K\} - \max\{b_1, \dots, b_K\}| \leq \max\{|a_1 - b_1|, \dots, |a_K - b_K|\}, \quad \forall \mathbf{a}, \mathbf{b} \in \mathbb{R}^K.$$

Furthermore, since ℓ is μ_ℓ -Lipschitz continuous, the last term is bounded by

$$\begin{aligned}
& \frac{\mu_\ell}{\alpha K} \sum_{y \in \mathcal{P}(\mathbf{x})} \max_{\substack{\mathcal{K} \subset [C] \\ |\mathcal{K}|=K+1}} \sum_{k \in \mathcal{K}} |(s_y - s'_y) - (s_k - s'_k)| \\
&\leq \frac{\mu_\ell(K+1)}{\alpha K} \sum_{y \in \mathcal{P}(\mathbf{x})} |s_y - s'_y| + \frac{\mu_\ell N(\mathbf{y})}{\alpha K} \max_{\substack{\mathcal{K} \subset [C] \\ |\mathcal{K}|=K+1}} \sum_{k \in \mathcal{K}} |s_k - s'_k| \\
&\leq \frac{\mu_\ell(K+1)\sqrt{N(\mathbf{y})}}{\alpha K} \left[\sum_{y \in \mathcal{P}(\mathbf{x})} (s_y - s'_y)^2 \right]^{\frac{1}{2}} + \frac{\mu_\ell N(\mathbf{y})\sqrt{K+1}}{\alpha K} \max_{\substack{\mathcal{K} \subset [C] \\ |\mathcal{K}|=K+1}} \left[\sum_{k \in \mathcal{K}} (s_k - s'_k)^2 \right]^{\frac{1}{2}} \\
&\leq \frac{\mu_\ell \left[(K+1)\sqrt{N(\mathbf{y})} + N(\mathbf{y})\sqrt{K+1} \right]}{\alpha K} \left[\sum_{y \in \mathcal{L}} (s_y - s'_y)^2 \right]^{\frac{1}{2}} \\
&= \frac{\mu_\ell \left[(K+1)\sqrt{N(\mathbf{y})} + N(\mathbf{y})\sqrt{K+1} \right]}{\alpha K} \|\mathbf{s} - \mathbf{s}'\|
\end{aligned}$$

When $\alpha = \alpha_1$, it is clear that

$$|L_K^{\alpha, \ell}(f, \mathbf{y}) - L_K^{\alpha, \ell}(f', \mathbf{y})| \leq \mu_\ell \left(\frac{K+1}{\sqrt{K}} + \sqrt{K+1} \right) \|\mathbf{s} - \mathbf{s}'\|,$$

and

$$L_K^{\alpha, \ell}(f, \mathbf{y}) \leq \frac{1}{K} \sum_{\mathbf{y} \in \mathcal{P}(\mathbf{x})} \sum_{k \leq K+1} M_\ell \leq (K+1)M_\ell.$$

When $\alpha = \alpha_2$, it is clear that

$$|L_K^{\alpha, \ell}(f, \mathbf{y}) - L_K^{\alpha, \ell}(f', \mathbf{y})| = \mu_\ell \left(\frac{K+1}{\sqrt{N(\mathbf{y})K}} + \frac{\sqrt{K+1}}{K} \right) \|\mathbf{s} - \mathbf{s}'\| \leq \mu_\ell \left(\frac{K+1}{\sqrt{K}} + \frac{\sqrt{K+1}}{K} \right) \|\mathbf{s} - \mathbf{s}'\|,$$

and

$$L_K^{\alpha, \ell}(f, \mathbf{y}) \leq \frac{1}{N(\mathbf{x})K} \sum_{\mathbf{y} \in \mathcal{P}(\mathbf{x})} \sum_{k \leq K+1} M_\ell \leq (K+1)M_\ell.$$

When $\alpha = \alpha_3$, we have

$$|L_K^{\alpha, \ell}(f, \mathbf{y}) - L_K^{\alpha, \ell}(f', \mathbf{y})| = \frac{2\mu_\ell}{K} \left[\frac{K+1}{\sqrt{N(\mathbf{y})(2K+1-N(\mathbf{y}))}} + \frac{\sqrt{K+1}}{2K+1-N(\mathbf{y})} \right] \|\mathbf{s} - \mathbf{s}'\|.$$

Let $g(t) := \sqrt{t}(2K+1-t)$, $t \in [1, K]$. Then, it is clear that $g'(t) > 0$ when $t \in [1, \frac{2K+1}{3}]$, and $g'(t) < 0$ when $t \in [\frac{2K+1}{3}, K]$. Since $2K \leq \sqrt{K}(K+1)$, we have

$$|L_K^{\alpha, \ell}(f, \mathbf{y}) - L_K^{\alpha, \ell}(f', \mathbf{y})| \leq \frac{2\mu_\ell}{K} \left(\frac{K+1}{2K} + \frac{\sqrt{K+1}}{K+1} \right) \|\mathbf{s} - \mathbf{s}'\| = \mu_\ell \left(\frac{K+1}{K^2} + \frac{2}{K\sqrt{K+1}} \right) \|\mathbf{s} - \mathbf{s}'\|.$$

Meanwhile, we have

$$L_K^{\alpha, \ell}(f, \mathbf{y}) \leq \frac{2}{N(\mathbf{y})(2K+1-N(\mathbf{y}))K} \sum_{\mathbf{y} \in \mathcal{P}(\mathbf{x})} \sum_{k \leq K+1} M_\ell \leq \frac{K+1}{K} M_\ell.$$

□

D.1.2 Generalization Bound of TKPR Optimization (Proof of Prop.6)

Proposition 6. Under Asm.3, for any $\delta \in (0, 1)$, with probability at least $1 - \delta$ over the training set \mathcal{S} , the following generalization bound holds for all the $f \in \mathcal{F}$:

$$\begin{aligned} \mathcal{R}_K^{\alpha, \ell}(f) &\lesssim \Phi(L_K^{\alpha, \ell}, \delta) + \\ &\begin{cases} \mathcal{O}(\sqrt{K}) \cdot \hat{\mathcal{C}}_{\mathcal{S}}(\mathcal{F}), & \alpha \in \{\alpha_1, \alpha_2\}, \\ \mathcal{O}(1/K) \cdot \hat{\mathcal{C}}_{\mathcal{S}}(\mathcal{F}), & \alpha = \alpha_3. \end{cases} \end{aligned}$$

Proof. According to Lem.1, let $\mathcal{G}_K^\ell := \{L_K^{\alpha, \ell} \circ f : f \in \mathcal{F}\}$. Then, with probability at least $1 - \delta$ over the training set \mathcal{S} , the following generalization bound holds for all the $f \in \mathcal{F}$, we have

$$\mathcal{R}_K^{\alpha, \ell}(f) \leq \Phi(L_K^{\alpha, \ell}, \delta) + 2\hat{\mathcal{C}}_{\mathcal{S}}(\mathcal{G}_K^\ell).$$

When $\alpha = \alpha_1$, based on Lem.2 and Prop.5, we have

$$\hat{\mathbf{c}}_{\mathcal{S}}(\mathcal{G}_K^\ell) \leq \sqrt{2}\mu_\ell \left(\frac{K+1}{\sqrt{K}} + \sqrt{K+1} \right) \hat{\mathbf{c}}_{\mathcal{S}}(\mathcal{F}) \sim \mathcal{O}(\sqrt{K}) \cdot \hat{\mathbf{c}}_{\mathcal{S}}(\mathcal{F}).$$

Similarly, when $\alpha = \alpha_2$ we have

$$\hat{\mathbf{c}}_{\mathcal{S}}(\mathcal{G}_K^\ell) \leq \sqrt{2}\mu_\ell \left(\frac{K+1}{\sqrt{K}} + \frac{\sqrt{K+1}}{K} \right) \hat{\mathbf{c}}_{\mathcal{S}}(\mathcal{F}) \sim \mathcal{O}(\sqrt{K}) \cdot \hat{\mathbf{c}}_{\mathcal{S}}(\mathcal{F}).$$

Similarly, when $\alpha = \alpha_3$ we have

$$\hat{\mathbf{c}}_{\mathcal{S}}(\mathcal{G}_K^\ell) \leq \sqrt{2}\mu_\ell \left(\frac{K+1}{K^2} + \frac{2}{K\sqrt{K+1}} \right) \hat{\mathbf{c}}_{\mathcal{S}}(\mathcal{F}) \sim \mathcal{O}\left(\frac{1}{K}\right) \cdot \hat{\mathbf{c}}_{\mathcal{S}}(\mathcal{F}).$$

□

D.1.3 Generalization Bound of the Traditional Ranking Loss (Proof of Prop.7)

Lemma 5. *The following inequality holds:*

$$L_{\text{rank}}^\ell(f, \mathbf{y}) \leq \frac{\alpha}{N(\mathbf{y})} L_K^{\alpha, \ell}(f, \mathbf{y}). \quad (\text{D9})$$

Proof. The proof is similar to that of Prop.3, except that ℓ is strictly decreasing. □

Proposition 7. *Under Asm.3, let*

$$\mathcal{R}_{\text{rank}}^\ell(f) := \mathbb{E}_{(\mathbf{x}, \mathbf{y}) \sim \mathcal{D}} [L_{\text{rank}}^\ell(f, \mathbf{y})] \quad (31)$$

denote the generalization error of the traditional ranking loss. Then, for any $\delta \in (0, 1)$, with probability at least $1 - \delta$ over the training set \mathcal{S} , the following generalization bound holds for all the $f \in \mathcal{F}$:

$$\begin{aligned} & \mathcal{R}_{\text{rank}}^\ell(f) \\ & \lesssim \begin{cases} \Phi(L_K^{\alpha, \ell}, \delta) + \mathcal{O}(\sqrt{K}) \cdot \hat{\mathbf{c}}_{\mathcal{S}}(\mathcal{F}), & \alpha \in \{\alpha_1, \alpha_2\}, \\ K \cdot \Phi(L_K^{\alpha, \ell}, \delta) + \mathcal{O}(1) \cdot \hat{\mathbf{c}}_{\mathcal{S}}(\mathcal{F}), & \alpha = \alpha_3. \end{cases} \end{aligned}$$

Proof. According to Prop.6 and Lem.5, when $\alpha = \alpha_1$, we have

$$\begin{aligned} \mathcal{R}_{\text{rank}}^\ell(f) &= \mathbb{E}_{(\mathbf{x}, \mathbf{y}) \sim \mathcal{D}} [L_{\text{rank}}^\ell(f, \mathbf{y})] \leq \mathbb{E}_{(\mathbf{x}, \mathbf{y}) \sim \mathcal{D}} \left[\frac{1}{N(\mathbf{y})} \cdot L_K^{\alpha, \ell}(f, \mathbf{y}) \right] \\ &\leq \mathbb{E}_{(\mathbf{x}, \mathbf{y}) \sim \mathcal{D}} [L_K^{\alpha, \ell}(f, \mathbf{y})] = \mathcal{R}_K^{\alpha, \ell}(f) \lesssim \Phi(L_K^{\alpha, \ell}, \delta) + \mathcal{O}(\sqrt{K}) \cdot \hat{\mathbf{c}}_{\mathcal{S}}(\mathcal{F}). \end{aligned}$$

Similarly, when $\alpha = \alpha_2$ we have

$$\mathcal{R}_{\text{rank}}^\ell(f) = \mathbb{E}_{(\mathbf{x}, \mathbf{y}) \sim \mathcal{D}} [L_{\text{rank}}^\ell(f, \mathbf{y})] \leq \mathbb{E}_{(\mathbf{x}, \mathbf{y}) \sim \mathcal{D}} [L_K^{\alpha, \ell}(f, \mathbf{y})] = \mathcal{R}_K^{\alpha, \ell}(f) \lesssim \Phi(L_K^{\alpha, \ell}, \delta) + \mathcal{O}(\sqrt{K}) \cdot \hat{\mathbf{c}}_{\mathcal{S}}(\mathcal{F}).$$

Similarly, when $\alpha = \alpha_3$ we have

$$\begin{aligned}\mathcal{R}_{\text{rank}}^\ell(f) &= \mathbb{E}_{(\mathbf{x}, \mathbf{y}) \sim \mathcal{D}} [L_{\text{rank}}^\ell(f, \mathbf{y})] \leq \mathbb{E}_{(\mathbf{x}, \mathbf{y}) \sim \mathcal{D}} [2K + 1 - N(\mathbf{y})] / 2 \cdot L_K^{\alpha, \ell}(f, \mathbf{y}) \\ &\leq K \mathbb{E}_{(\mathbf{x}, \mathbf{y}) \sim \mathcal{D}} [L_K^{\alpha, \ell}(f, \mathbf{y})] = K \cdot \mathcal{R}_K^{\alpha, \ell}(f) \lesssim K \cdot \Phi(L_K^{\alpha, \ell}, \delta) + \mathcal{O}(1) \cdot \hat{\mathcal{C}}_{\mathcal{S}}(\mathcal{F}).\end{aligned}$$

□

D.2 The Generalization Bound by the Data-dependent Contraction Technique

D.2.1 Data-Dependent Contraction Inequality (Proof of Prop.8)

Proposition 8 (Data-dependent contraction inequality). *Under Asm.4, if the loss function $L(f, \mathbf{y})$ is local Lipschitz continuous with a partition \mathcal{S}_Q and constants $\{\mu_q\}_{q=1}^Q$. Let $\pi_q := \frac{N_q}{N}$ be the ratio of \mathcal{S}_q in \mathcal{S} , where $N_q = |\mathcal{S}_q|$. Then,*

$$\hat{\mathcal{C}}_{\mathcal{S}}(\mathcal{G}) \leq \hat{\mathcal{C}}_{\mathcal{S}}(\mathcal{F}) \sum_{q=1}^Q \sqrt{\pi_q} \mu_q. \quad (33)$$

Proof. Let $\{\xi_q\}_{q=1}^Q$ be a partition of ξ such that $\forall q \in \{1, 2, \dots, Q\}, \xi_q \in \{-1, +1\}^{N_q}$. Then, according to the definition of the complexity measure, we have

$$\begin{aligned}\hat{\mathcal{C}}_{\mathcal{S}}(\mathcal{G}) &= \mathbb{E}_{\xi} \left[\sup_{g \in \mathcal{G}} \frac{1}{N} \sum_{n=1}^N \xi^{(n)} g(\mathbf{z}^{(n)}) \right] = \frac{1}{N} \mathbb{E}_{\xi} \left[\sup_{g \in \mathcal{G}} \sum_{q=1}^Q \sum_{n=1}^{N_q} \xi_q^{(n)} g(\mathbf{z}_q^{(n)}) \right] \leq \frac{1}{N} \sum_{q=1}^Q \mathbb{E}_{\xi_q} \left[\sup_{g \in \mathcal{G}} \sum_{n=1}^{N_q} \xi_q^{(n)} g(\mathbf{z}_q^{(n)}) \right] \\ &= \sum_{q=1}^Q \pi_q \hat{\mathcal{C}}_{\mathcal{S}_q}(\mathcal{G}) \stackrel{(a)}{\leq} \sqrt{2} \sum_{q=1}^Q \pi_q \mu_q \hat{\mathcal{C}}_{\mathcal{S}_q}(\mathcal{F}) \stackrel{(b)}{\lesssim} \mathcal{O} \left(\hat{\mathcal{C}}_{\mathcal{S}}(\mathcal{F}) \cdot \sum_{q=1}^Q \mu_q \sqrt{\pi_q} \right),\end{aligned}$$

where (a) comes from Lem.2, and (b) is induced by $\hat{\mathcal{C}}_{\mathcal{S}_q}(\mathcal{F}) \propto \sqrt{\frac{1}{N_q}} = \sqrt{\frac{1}{N\pi_q}} \propto \sqrt{\frac{1}{\pi_q}} \hat{\mathcal{C}}_{\mathcal{S}}(\mathcal{F})$. □

D.2.2 Local Lipschitz Continuity of the TKPR Loss (Proof of Prop.9)

Proposition 9. *Let $\mathcal{S}_q := \{\mathbf{z} \in \mathcal{S} : N(\mathbf{y}) = q\}$. That is, all the samples in \mathcal{S}_q have q relevant labels. Then, under Asm.3, $L_K^{\alpha, \ell}(f, \mathbf{y})$ is local Lipschitz continuous with constants $\{\mu_q\}_{q=1}^Q$ such that*

$$\mu_q = \frac{\mu_\ell [(K+1)\sqrt{q} + q\sqrt{K+1}]}{\alpha(q)K}, \quad (34)$$

where $\alpha(q) \in \{1, q, q(2K+1-q)/2\}$ and $q \leq K$.

Proof. The proof follows that of Prop.5 □

D.2.3 Generalization Bound of $\mathcal{R}_K^{\alpha, \ell}(f)$ Induced by Data-dependent Contraction (Proof of Thm.4)

Theorem 4. *Under Asm.3 and Asm.4, for any $\delta \in (0, 1)$, with probability at least $1 - \delta$ over the training set \mathcal{S} , the following generalization bound holds for all $f \in \mathcal{F}$:*

$$\mathcal{R}_K^{\alpha, \ell}(f) \lesssim \Phi(L_K^{\alpha, \ell}, \delta) + \hat{\mathcal{C}}_{\mathcal{S}}(\mathcal{F}) \mathcal{O}(g(K)), \quad (35)$$

where $\mathfrak{g}(K)$ relies on the distribution of π_q . In Tab.3, we present the results under an exponential distribution and a multinomial distribution, parameterized by λ .

Proof. We can obtain Eq.(35) directly by Lem.1 and Prop.8, and Prop.9. Next, we focus on the two concrete cases.

If $\pi_q \propto e^{-\lambda q}$, since $\mu_q \sim \mathcal{O}(\sqrt{q}/\alpha(q))$, we have

$$\sum_{q=1}^K \mu_q \sqrt{\pi_q} \sim \mathcal{O} \left(\sum_{q=1}^K \frac{\sqrt{q}}{e^{\lambda q/2} \cdot \alpha(q)} \right).$$

When $\alpha(q) = 1$, we have

$$\sum_{q=1}^K \frac{\sqrt{q}}{e^{\lambda q/2}} \leq \sum_{q=1}^K \frac{q}{e^{\lambda q/2}} \leq \int_0^K \frac{t}{e^{\lambda t/2}} dt = \frac{4}{\lambda^2} - \frac{2\lambda K + 4}{\lambda^2 e^{\lambda K/2}} \sim \mathcal{O} \left(\frac{1}{\lambda^2} \right).$$

When $\alpha(q) = q$, we have

$$\begin{aligned} \sum_{q=1}^K \frac{1}{e^{\lambda q/2} \sqrt{q}} &\leq \frac{1}{e^{\lambda/2}} + \int_1^K \frac{1}{e^{\lambda t/2} \sqrt{t}} dt \leq \frac{1}{e^{\lambda/2}} + \int_1^K \frac{1}{e^{\lambda t/2}} dt \\ &= \frac{1}{e^{\lambda/2}} + \frac{2}{\lambda e^{\lambda/2}} - \frac{2}{\lambda e^{\lambda K/2}} \sim \mathcal{O} \left(\frac{1}{e^{\lambda/2}} \right) \end{aligned}$$

When $\alpha(q) = \frac{q(2K+1-q)}{2}$, we have

$$\sum_{q=1}^K \frac{2}{e^{\lambda q/2} \sqrt{q}(2K+1-q)} \leq \frac{1}{K+1} \sum_{q=1}^K \frac{2}{e^{\lambda q/2} \sqrt{q}} \lesssim \mathcal{O} \left(\frac{1}{K e^{\lambda/2}} \right).$$

If $\pi_q \propto q^{-\lambda}$, $\lambda > 0$, since $\mu_q \sim \mathcal{O}(\sqrt{q}/\alpha(q))$, we have

$$\sum_{q=1}^K \mu_q \sqrt{\pi_q} \sim \mathcal{O} \left(\sum_{q=1}^K \frac{1}{q^{(\lambda-1)/2} \cdot \alpha(q)} \right).$$

When $\alpha(q) = 1$, we have

$$\sum_{q=1}^K \mu_q \sqrt{\pi_q} \sim \mathcal{O} \left(\sum_{q=1}^K \frac{1}{q^{(\lambda-1)/2}} \right).$$

Essentially, this bound is a cut-off version of Riemann zeta function [Titchmarsh et al \(1986\)](#). Since the order of Riemann zeta function is out of the scope of this paper, we next provide a coarse-grained result,

and the fine-grained results can be found in [Fokas and Lenells \(2022\)](#).

$$\begin{aligned}\lambda \in (0, 3) &: \sum_{q=1}^K \frac{1}{q^{(\lambda-1)/2}} \leq \int_0^K \frac{1}{t^{(\lambda-1)/2}} dt = \frac{2 \cdot K^{\frac{3-\lambda}{2}} - 2}{3-\lambda} \sim \mathcal{O}\left(K^{\frac{3-\lambda}{2}}\right), \\ \lambda \in [3, 5) &: \sum_{q=1}^K \frac{1}{q^{(\lambda-1)/2}} \leq \sum_{q=1}^K \frac{1}{q} \sim \mathcal{O}(\ln K), \\ \lambda \in [5, \infty) &: \sum_{q=1}^K \frac{1}{q^{(\lambda-1)/2}} \leq \sum_{q=1}^K \frac{1}{q^2} \leq \sum_{q=1}^{\infty} \frac{1}{q^2} = \frac{\pi^2}{6} \sim \mathcal{O}(1).\end{aligned}$$

When $\alpha(q) = q$, we have

$$\sum_{q=1}^K \mu_q \sqrt{\pi_q} \sim \mathcal{O}\left(\sum_{q=1}^K \frac{1}{q^{(\lambda+1)/2}}\right).$$

Similarly,

$$\begin{aligned}\lambda \in (0, 1) &: \sum_{q=1}^K \frac{1}{q^{(\lambda+1)/2}} \leq \int_0^K \frac{1}{t^{(\lambda+1)/2}} dt = \frac{2 \cdot K^{\frac{1-\lambda}{2}} - 2}{1-\lambda} \sim \mathcal{O}\left(K^{\frac{1-\lambda}{2}}\right), \\ \lambda \in [1, 3) &: \sum_{q=1}^K \frac{1}{q^{(\lambda+1)/2}} \leq \sum_{q=1}^K \frac{1}{q} \sim \mathcal{O}(\ln K), \\ \lambda \in [3, \infty) &: \sum_{q=1}^K \frac{1}{q^{(\lambda+1)/2}} \leq \sum_{q=1}^K \frac{1}{q^2} \leq \sum_{q=1}^{\infty} \frac{1}{q^2} = \frac{\pi^2}{6} \sim \mathcal{O}(1).\end{aligned}$$

When $\alpha(q) = \frac{q(2K+1-q)}{2}$, we have

$$\sum_{q=1}^K \mu_q \sqrt{\pi_q} \sim \mathcal{O}\left(\sum_{q=1}^K \frac{1}{(2K+1-q)q^{(\lambda+1)/2}}\right).$$

Similarly,

$$\begin{aligned}\lambda \in (0, 1) &: \sum_{q=1}^K \frac{1}{(2K+1-q)q^{(\lambda+1)/2}} \leq \frac{1}{K+1} \int_0^K \frac{1}{t^{(\lambda+1)/2}} dt \sim \mathcal{O}\left(\frac{1}{K^{(\lambda+1)/2}}\right), \\ \lambda \in [1, 3) &: \sum_{q=1}^K \frac{1}{(2K+1-q)q^{(\lambda+1)/2}} \lesssim \mathcal{O}\left(\frac{\ln K}{K}\right), \\ \lambda \in [3, \infty) &: \sum_{q=1}^K \frac{1}{(2K+1-q)q^{(\lambda+1)/2}} \lesssim \mathcal{O}\left(\frac{1}{K}\right).\end{aligned}$$

□

D.2.4 Generalization Bound of $\mathcal{R}_{\text{rank}}^\ell(f)$ Induced by Data-dependent Contraction (Proof of Prop.10)

Proposition 10. *Let $\tilde{L}_K^\ell(f, \mathbf{y}) := \frac{\alpha}{N(\mathbf{y})} \cdot L_K^{\alpha, \ell}(f, \mathbf{y})$. Then, under Asm.3 and Asm.4, for any $\delta \in (0, 1)$, with probability at least $1 - \delta$ over the training set \mathcal{S} , the following generalization bound holds for all the $f \in \mathcal{F}$:*

- When $\pi_q \propto e^{-\lambda q}$,

$$\mathcal{R}_{\text{rank}}^\ell(f) \lesssim \Phi(\tilde{L}_K^\ell, \delta) + \mathcal{O}(e^{-\lambda/2}) \cdot \hat{\mathfrak{C}}_{\mathcal{S}}(\mathcal{F}).$$

- When $\pi_q \propto q^{-\lambda}$,

$$\begin{aligned} \mathcal{R}_{\text{rank}}^\ell(f) &\lesssim \Phi(\tilde{L}_K^\ell, \delta) \\ &+ \begin{cases} \mathcal{O}(K^{(1-\lambda)/2}) \cdot \hat{\mathfrak{C}}_{\mathcal{S}}(\mathcal{F}), & \lambda \in (0, 1), \\ \mathcal{O}(\ln K) \cdot \hat{\mathfrak{C}}_{\mathcal{S}}(\mathcal{F}), & \lambda \in [1, 3), \\ \mathcal{O}(1) \cdot \hat{\mathfrak{C}}_{\mathcal{S}}(\mathcal{F}), & \lambda \in [3, \infty). \end{cases} \end{aligned}$$

Proof. According to Lem.5, we have

$$\mathcal{R}_{\text{rank}}^\ell(f) = \mathbb{E}_{(\mathbf{x}, \mathbf{y}) \sim \mathcal{D}} [L_{\text{rank}}^\ell(f, \mathbf{y})] \leq \mathbb{E}_{(\mathbf{x}, \mathbf{y}) \sim \mathcal{D}} \left[\frac{\alpha}{N(\mathbf{y})} \cdot L_K^{\alpha, \ell}(f, \mathbf{y}) \right] = \mathbb{E}_{(\mathbf{x}, \mathbf{y}) \sim \mathcal{D}} [\tilde{L}_K^\ell(f, \mathbf{y})]$$

Similar to Prop.9, it is clear that $\tilde{L}_K^\ell(f, \mathbf{y})$ is local Lipschitz continuous with constants $\{\tilde{\mu}_q\}_{q=1}^Q$ such that

$$\tilde{\mu}_q = \frac{\mu_\ell [(K+1)\sqrt{q} + q\sqrt{K+1}]}{qK} \sim \mathcal{O}\left(\frac{1}{\sqrt{q}}\right),$$

Then, let $\tilde{\mathcal{G}}_K^\ell := \{\tilde{L}_K^\ell \circ f : f \in \mathcal{F}\}$. According to Lem.1, with probability at least $1 - \delta$ over the training set \mathcal{S} , the following generalization bound holds for any $f \in \mathcal{F}$, we have

$$\mathcal{R}_{\text{rank}}^\ell(f) \leq \Phi(\tilde{L}_K^\ell, \delta) + 2\hat{\mathfrak{C}}_{\mathcal{S}}(\tilde{\mathcal{G}}_K^\ell).$$

Furthermore, according to Prop.8,

$$\hat{\mathfrak{C}}_{\mathcal{S}}(\tilde{\mathcal{G}}_K^\ell) \lesssim \hat{\mathfrak{C}}_{\mathcal{S}}(\mathcal{F}) \cdot \sum_{q=1}^K \tilde{\mu}_q \sqrt{\pi_q}.$$

If $\pi_q \propto e^{-\lambda q}$, we have

$$\sum_{q=1}^K \tilde{\mu}_q \sqrt{\pi_q} \sim \mathcal{O}\left(\sum_{q=1}^K \frac{1}{e^{\lambda q/2} \sqrt{q}}\right).$$

Following the proof of Thm.4,

$$\sum_{q=1}^K \frac{1}{e^{\lambda q/2} \sqrt{q}} \lesssim \mathcal{O}(e^{-\lambda/2}).$$

Thus, we have

$$\mathcal{R}_{\text{rank}}^\ell(f) \lesssim \Phi(\tilde{L}_K^\ell, \delta) + \mathcal{O}(e^{-\lambda/2}) \cdot \hat{\mathfrak{C}}_{\mathcal{S}}(\mathcal{F}).$$

If $\pi_q \propto q^{-\lambda}$, we have

$$\sum_{q=1}^K \tilde{\mu}_q \sqrt{\pi_q} \sim \mathcal{O}\left(\sum_{q=1}^K \frac{1}{q^{(\lambda+1)/2}}\right).$$

Following the proof of Thm.4,

$$\sum_{q=1}^K \frac{1}{q^{(\lambda+1)/2}} \lesssim \begin{cases} \mathcal{O}\left(K^{\frac{1-\lambda}{2}}\right) \cdot \hat{\mathfrak{C}}_{\mathcal{S}}(\mathcal{F}), & \lambda \in (0, 1), \\ \mathcal{O}(\ln K) \cdot \hat{\mathfrak{C}}_{\mathcal{S}}(\mathcal{F}), & \lambda \in [1, 3), \\ \mathcal{O}(1) \cdot \hat{\mathfrak{C}}_{\mathcal{S}}(\mathcal{F}), & \lambda \in [3, \infty). \end{cases}$$

Thus, we have

$$\mathcal{R}_{\text{rank}}^{\ell}(f) \lesssim \Phi(\tilde{L}_K^{\ell}, \delta) + \begin{cases} \mathcal{O}\left(K^{\frac{1-\lambda}{2}}\right), & \lambda \in (0, 1), \\ \mathcal{O}(\ln K), & \lambda \in [1, 3), \\ \mathcal{O}(1), & \lambda \in [3, \infty). \end{cases}$$

□

D.3 Practical Generalization Bounds

D.3.1 Practical Bounds for Kernel-Based Models (Proof of Prop.11 and Prop.12)

Lemma 6 (The Rademacher complexity of the kernel-based models Wu and Zhu (2020)). *The Rademacher complexity of kernel-based models has the following upper bound:*

$$\hat{\mathfrak{R}}_{\mathcal{S}}(\mathcal{F}_{\mathbb{H}}) \leq \sqrt{\frac{C\Lambda^2 r^2}{N}}. \quad (\text{D10})$$

Proposition 11. *Under Asm.3 and Asm.4, for any $\delta \in (0, 1)$, with probability at least $1 - \delta$ over the training set \mathcal{S} , the following generalization bound holds for all the $f \in \mathcal{F}_{\mathbb{H}}$:*

$$\mathcal{R}_K^{\alpha, \ell}(f) \lesssim \Phi(L_K^{\alpha, \ell}, \delta) + \begin{cases} \mathcal{O}\left(\sqrt{\frac{C\Lambda^2 r^2}{N\lambda^4}}\right), & \alpha = \alpha_1 \\ \mathcal{O}\left(\sqrt{\frac{C\Lambda^2 r^2}{Ne^{\lambda}}}\right), & \alpha = \alpha_2 \\ \mathcal{O}\left(\sqrt{\frac{C\Lambda^2 r^2}{NK^2 e^{\lambda}}}\right), & \alpha = \alpha_3. \end{cases}$$

Proof. The proof completes by Thm.4 and Lem.6. □

Proposition 12. *Under Asm.3 and Asm.4, for any $\delta \in (0, 1)$, with probability at least $1 - \delta$ over the training set \mathcal{S} , the following generalization bound holds for all the $f \in \mathcal{F}_{\mathbb{H}}$:*

$$\mathcal{R}_{\text{rank}}^{\ell}(f) \lesssim \Phi(\tilde{L}_K^{\ell}, \delta) + \mathcal{O}\left(\sqrt{\frac{C\Lambda^2 r^2}{Ne^{\lambda}}}\right).$$

Proof. The proof completes by Prop.10 and Lem.6. □

D.3.2 Practical Bounds for Convolutional Neural Networks (Proof of Prop.13)

Lemma 7 (The Gaussian complexity of Convolutional Neural Networks Long and Sedghi (2020); Wang et al (2023)). *The Rademacher complexity of \mathcal{F}_{ν} has the following upper bound:*

$$\hat{\mathfrak{C}}_{\mathcal{S}}(\mathcal{F}_{\beta, \nu, \chi}) \lesssim \mathcal{O}\left(\frac{d \log(B_{\beta, \nu, \chi} N)}{\sqrt{N}}\right). \quad (\text{D11})$$

Proposition 13. Under Asm.3 and Asm.4, for any $\delta \in (0, 1)$, with probability at least $1 - \delta$ over the training set \mathcal{S} , the following generalization bound holds for all the $f \in \mathcal{F}_{\beta, \nu, \chi}$:

$$\mathcal{R}_K^{\alpha, \ell}(f) \lesssim \Phi(L_K^{\alpha, \ell}, \delta) + \begin{cases} \mathcal{O}\left(\frac{d \log(B_{\beta, \nu, \chi} N)}{\sqrt{N} \lambda^2}\right), & \alpha = \alpha_1, \\ \mathcal{O}\left(\frac{d \log(B_{\beta, \nu, \chi} N)}{\sqrt{N} e^\lambda}\right), & \alpha = \alpha_2, \\ \mathcal{O}\left(\frac{d \log(B_{\beta, \nu, \chi} N)}{\sqrt{N} e^\lambda K}\right), & \alpha = \alpha_3, \end{cases}$$

where $B_{\beta, \nu, \chi} := \chi \beta (1 + \nu + \beta / N_a)^{N_a}$, $N_a := N_c + N_f$.

Proof. Due to the additional term $\log N$ in the upper bound of $\hat{\mathfrak{G}}_{\mathcal{S}}(\mathcal{F}_{\beta, \nu, \chi})$, we need to make minor adjustments to Prop.8. Let $\mathcal{G}_{\beta, \nu, \chi} := \{L_K^\ell \circ f : f \in \mathcal{F}_{\beta, \nu, \chi}\}$. Then, we have

$$\begin{aligned} \hat{\mathfrak{C}}_{\mathcal{S}}(\mathcal{G}_{\beta, \nu, \chi}) &= \sum_{q=1}^Q \pi_q \hat{\mathfrak{C}}_{\mathcal{S}_q}(\mathcal{G}_{\beta, \nu, \chi}) \leq \sqrt{2} \sum_{q=1}^Q \pi_q \mu_q \hat{\mathfrak{C}}_{\mathcal{S}_q}(\mathcal{F}_{\beta, \nu, \chi}) \sim \mathcal{O}\left(\sum_{q=1}^Q \pi_q \mu_q \hat{\mathfrak{C}}_{\mathcal{S}_q}(\mathcal{F}_{\beta, \nu, \chi})\right), \\ &= \mathcal{O}\left(\sum_{q=1}^Q \pi_q \mu_q \frac{d \log(B_{\beta, \nu, \chi} N \pi_q)}{\sqrt{N} \pi_q}\right) \leq \mathcal{O}\left(\sum_{q=1}^Q \sqrt{\pi_q} \mu_q \frac{d \log(B_{\beta, \nu, \chi} N)}{\sqrt{N}}\right) \\ &= \mathcal{O}\left(\hat{\mathfrak{C}}_{\mathcal{S}}(\mathcal{F}_{\beta, \nu, \chi}) \sum_{q=1}^Q \sqrt{\pi_q} \mu_q\right) \end{aligned}$$

Then the proof ends by Prop.10 and Lem.7. □

Appendix E More Implementation Details

Infrastructure. For CNN backbone, we carry out the experiments on an ubuntu 16.04 server equipped with Intel(R) Xeon(R) Silver 4110 CPU and an Nvidia(R) TITAN RTX GPU. The version of CUDA is 10.2 with GPU driver version 440.44. Our codes are implemented via `python` (v-3.8.11) with the main third-party packages including `pytorch` Paszke et al (2019) (v-1.9.0), `numpy` (v-1.20.3), `scikit-learn` (v-0.24.2) and `torchvision` (v-0.10.0).

For transformer backbone, we carry out the experiments on an ubuntu 20.04 server equipped with AMD(R) EPYC(R) 7763 CPU and an Nvidia(R) A100 GPU. The version of CUDA is 11.6 with GPU driver version 510.108.03. The packages are same as those in the CNN backbone.

Warm-up strategy. Note that TKPR focuses on the predictions of top-ranked labels. However, focusing on a few labels at the early training process ignores the learning of the other labels and can bring a high risk of over-fitting. To address this issue, we adopt a warm-up training strategy that encourages the model learning the global information. To be specific, in the first E_w epochs, the models is trained by a global loss. Afterwards, the warm-up loss is replaced with the proposed TKPR losses. The whole learning process is summarized in Alg.1.

In MLC, for the comparison with the ranking-based losses, all the methods adopt the warm-up strategy with the warm-up loss L_{rank} . For the comparison with state-of-the-art methods, the proposed method uses DB-loss/ASL as the warm-up loss for the CNN/transformer backbones, respectively. For the CNN backbones, we set $E = 100, 200$ on Pascal VOC 2007 and MS-COCO, respectively, and E_w is searched in $\{10, 20, 30, 40, 50, 60\}$. For the transformer backbones, we set $E = 80$, and E_w is searched in $\{5, 10, 15, 20, 25\}$.

In MLML, for the comparison with the ranking-based losses, all the methods use L_{rank} as the warm-up loss. For the comparison with state-of-the-art methods, the proposed method uses SPLC as the warm-up loss. We set $E = 80$, and E_w is searched in $\{2, 4, 6, 8, 10\}$.

Implementation of competitors. It is not a trivial task to evaluate the competitors on the proposed TKPR measures due to the significant differences among their settings. In the official setting, $L_{\text{rank}}, L_{u_1}, L_{u_2}, L_{u_3}, L_{u_4}$ and TKML conduct the experiments on traditional datasets such as emotions, bibtex, delicious Tsoumakas et al (2011b), which are no longer popular benchmark datasets for modern backbones. LSEP uses VGG16 as the backbone, which is somewhat outdated. DB-Loss trains the model on a modified version of MS-COCO and Pascal VOC. Fortunately, ASL, CCD, Hill, and SPLC share the same protocols and implementation details, and EM+APL, ROLE, LL-R, LL-Ct, and LL-Cp share the other implementation. Hence, we adopt the following implementation strategy for fair comparison:

- For $L_{\text{rank}}, L_{u_1}, L_{u_2}, L_{u_3}, L_{u_4}$, TKML, LSEP, and DB-Loss, we re-implement the methods based on the code released by ASL (<https://github.com/Alibaba-MIIL/ASL/blob/main/train.py>). For fair comparison, we align the training details with ours, including warm-up, optimizer, batch size, learning rate, input size and so on. The hyperparameters are also searched as suggested in the original paper.
- For ASL, CCD, Hill, SPLC, EM+APL, ROLE, LL-R, LL-Ct, and LL-Cp, we adopt the official implementation and the hyperparameters suggested in the original paper. The mAP performance is also evaluated to guarantee our checkpoints share similar performances as those reported in the original paper.

Besides, as analyzed in (Gao and Zhou, 2013) and (Wu et al, 2021), $\ell_{\text{arc}}(t) = -\arctan(t)$ and ℓ_{exp} are consistent surrogates for the ranking loss and L_{u_2} , respectively. Our implementation follows these theoretical results.

Hyper-parameter search. We withhold 20% of the training set for hyper-parameter search. After this, the model is trained on the full training set with the best hyper-parameters. For fair comparison, the common hyper-parameters, such as learning rate and batch size, are searched for competitors in the same space. The specific hyper-parameters of each method are also searched as suggested in the original paper. If the original paper has provided the optimal hyper-parameters, we will use them directly. Since

the search space is somewhat large, we adopt an early stopping strategy with 5 patience epochs. The hyper-parameters of the warm-up loss follows those of the main loss, requiring no explicit validation set.

Algorithm 1 Learning Algorithm of the ERM Framework

Require: Training set \mathcal{S} , the model parameterized by Θ , the hyperparameters $\{\alpha, \ell, K\}$, the warm-up loss L_w .

- 1: Initialize the model parameters Θ .
 - 2: **for** $e = 1, 2, \dots, E$ **do**
 - 3: $\mathcal{B} \leftarrow \text{SampleMiniBatch}(\mathcal{S}, m)$
 - 4: **if** $e \leq E_w$ **then**
 - 5: Update Θ by minimizing L_w .
 - 6: **else**
 - 7: Update Θ by minimizing $L_K^{\alpha, \ell}$.
 - 8: **end if**
 - 9: Optional: anneal the learning rate η .
 - 10: **end for**
-

Appendix F More Empirical Results

F.1 MLC experiments on Pascal VOC 2007

Overall Performance. Tab.F1 presents the comparison results with the ranking-based losses in the MLC setting, from which we have the following observations:

- The proposed methods demonstrate consistent improvements on mAP@K, NDCG@K, the ranking loss, and the TKPR measures. All these performance gains again validate our theoretical analyses in Sec.4 and Sec.5.2.
- Similar to the results on MS-COCO, the improvement on P@K and R@K is not so significant. This shows that the performance enhancement comes from the improvement on ranking of predictions, which is consistent with the label distributions presented in Fig.3(b).
- The performances of the competitors are inconsistent on different measures. For example, L_{rank} achieve the best NDCG@K and TKPR performance. However, on P@K, mAP@K, and the ranking loss, L_{u_4} and L_{LSEP} are the best. By contrast, the superior performance of TKPR optimization is consistent, which again validates the necessity of the proposed framework.

Tab.F2 presents the comparison results with the state-of-the art loss-oriented methods in the MLC setting, from which we have the following observations:

- Compared with the state-of-the-art methods, the proposed methods achieve the best performances consistently on all the measures, which again validate the effectiveness of the proposed learning framework.
- The DB-Loss and ASL are competitive in this setting. Their success might come from the emphasis on inherent imbalanced label distributions in multi-label learning. However, the proposed methods still outperform the two methods, as the analysis in Sec.5.2 show that the proposed method can also generalize well on imbalanced label distributions.
- Similarly, performances of the competitors are inconsistent on different measures while the proposed methods achieve the best performances consistently.

Sensitivity Analysis. In Fig.F1, we present the sensitivity of the proposed framework *w.r.t.* hyperparameter K on Pascal VOC 2007 with $E_w = 50$. From the results, we have the following observations:

- The model tends to achieve the best median performance with $K \in \{3, 4, 5\}$, which suggests that an appropriately larger K is necessary for the proposed framework.
- The performance degeneration under $K = 2$ is more significant when $\alpha = \alpha_3$. In other words, TKPR optimization with $\alpha = \alpha_3$ is more sensitive than those with $\alpha \in \{\alpha_1, \alpha_2\}$.

Table F1 The empirical results of the ranking-based losses and TKPR on Pascal VOC 2007, where the backbone is ResNet101. The best and runner-up results on each metric are marked with red and blue, respectively. The best competitor on each measure is marked with underline.

Type	Metrics	P@K		R@K		mAP@K		NDCG@K		TKPR $^{\alpha_1}$		TKPR $^{\alpha_2}$		TKPR $^{\alpha_3}$		Ranking
	K	3	5	3	5	3	5	3	5	3	5	3	5	3	5	Loss
Ranking Loss	L_{rank}	.444	.278	.959	.989	.613	.625	.826	.840	<u>1.045</u>	<u>1.181</u>	.762	.850	.273	.177	.043
	L_{u_1}	.443	.278	.960	.989	.653	.665	.766	.780	.985	1.144	.708	.818	.255	.171	.041
	L_{u_2}	.443	<u>.278</u>	.958	.988	.652	.665	.764	.778	.984	1.144	.707	.817	.255	.171	.041
	L_{u_3}	.443	.279	.956	<u>.991</u>	.650	.664	.796	.812	1.008	1.160	.730	.832	.262	.174	.040
	L_{u_4}	<u>.446</u>	.278	<u>.965</u>	.989	<u>.674</u>	<u>.683</u>	.785	.796	1.015	1.162	.733	.833	.264	.174	<u>.038</u>
	L_{LSEP}	.442	<u>.279</u>	.959	<u>.991</u>	.626	.641	.817	.833	1.033	1.175	.752	.845	.270	.176	.042
	L_{TKML}	.422	.272	.915	.972	.614	.634	.788	.815	.998	1.138	.729	.823	.262	.171	.052
TKPR (Ours)	α_1	.437	.272	.945	.969	.912	.921	.930	.941	1.154	1.233	.864	.904	.308	.188	.021
	α_2	<u>.450</u>	.277	<u>.970</u>	.987	<u>.947</u>	<u>.954</u>	<u>.960</u>	<u>.968</u>	<u>1.190</u>	<u>1.267</u>	<u>.892</u>	<u>.928</u>	<u>.318</u>	<u>.193</u>	<u>.010</u>
	α_3	<u>.447</u>	.277	.948	.965	<u>.985</u>	<u>.947</u>	.953	.963	1.185	1.262	.886	.924	.316	.192	.011

Table F2 The empirical results of state-of-the-art MLC methods and TKPR on Pascal VOC 2007, where the backbone is ResNet101. The best and runner-up results on each metric are marked with red and blue, respectively. The best competitor on each measure is marked with underline.

Type	Metrics	P@K		R@K		mAP@K		NDCG@K		TKPR $^{\alpha_1}$		TKPR $^{\alpha_2}$		TKPR $^{\alpha_3}$		Ranking
	K	3	5	3	5	3	5	3	5	3	5	3	5	3	5	Loss
Loss Oriented	ASL \dagger	.452	.278	<u>.973</u>	.989	<u>.956</u>	<u>.963</u>	.966	.973	1.203	1.277	.899	.933	.321	.194	.008
	DB-Loss	<u>.453</u>	<u>.279</u>	.973	.988	.956	.962	<u>.966</u>	<u>.973</u>	<u>1.205</u>	<u>1.278</u>	<u>.900</u>	<u>.933</u>	<u>.321</u>	<u>.195</u>	<u>.008</u>
	CCD \dagger	.451	.279	.969	<u>.990</u>	.948	.956	.960	.970	1.194	1.272	.893	.930	.319	.194	.009
	Hit \dagger	.446	.276	.960	.981	.932	.940	.948	.957	1.179	1.256	.881	.919	.315	.192	.014
	SPLC \dagger	.451	.278	.969	.986	.947	.954	.959	.967	1.195	1.271	.892	.928	.319	.193	.010
TKPR (Ours)	α_1	<u>.455</u>	<u>.281</u>	.975	.989	<u>.961</u>	<u>.967</u>	<u>.971</u>	<u>.977</u>	<u>1.210</u>	<u>1.283</u>	.903	<u>.937</u>	<u>.322</u>	<u>.196</u>	<u>.007</u>
	α_2	.454	.279	<u>.976</u>	<u>.990</u>	.961	.966	.971	.977	1.208	1.282	<u>.904</u>	.936	.322	.196	.007
	α_3	<u>.455</u>	<u>.279</u>	<u>.977</u>	.989	<u>.962</u>	<u>.967</u>	<u>.972</u>	<u>.977</u>	<u>1.211</u>	<u>1.283</u>	<u>.905</u>	<u>.937</u>	<u>.322</u>	<u>.196</u>	<u>.007</u>

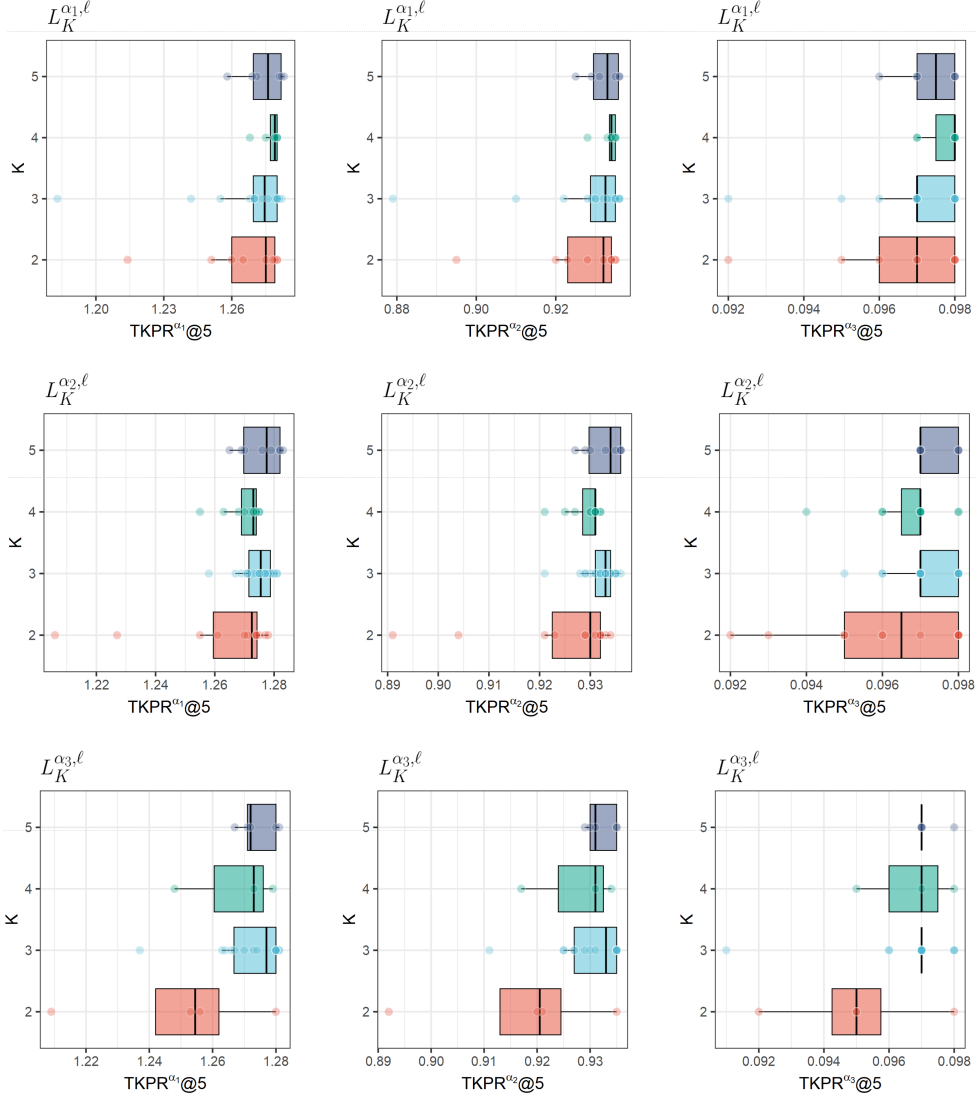


Fig. F1 Sensitivity analysis of the proposed methods on Pascal VOC 2007. The y-axis denotes the values of the hyperparameter K , and the x-axis represents the value of TKPR@5 under the corresponding K .

F.2 MLC experiments with Transformer Backbone

Overall Performance. Tab.F3 and Tab.F4 present the comparison results with the state-of-the-art loss-oriented methods with the swin-transformer backbone in the MLC setting, from which we have the following observations:

- The proposed methods still outperform the competitors consistently on all the measures, which validates the robustness of the proposed framework.
- Compared with the improvements with the CNN backbone, the performance gains on the transformer backbone are more significant on MS-COCO. This phenomenon shows that the proposed framework can better exploit the potential of powerful pre-trained backbones.
- Benefiting from the powerful backbones, CCD achieves the best performance among the competitors. However, its performances on the ranking-based measures with $K = 3$ are comparable/inferior to ASL. In other words, CDD pay more attention to the whole ranking list, rather than the top-ranked ones.

Case study. Fig.F2 and Fig.F3 present visual results on the MS-COCO and NUS-WIDE datasets, respectively, where the proposed methods perform better than all the competitors. For each input image, we present the ground-truth labels and the top-5 predicted labels of the proposed methods and the competitors. All the ground-truth labels are marked with **green**. From the results, we have the following observations:

- TKPR tends to rank the ground-truth labels higher than the competitors. This improvement brings the enhancement on mAP@K, NDCG@K, TKPR, and the ranking loss, which is consistent with the Bayes optimality of TKPR and again validates the effectiveness of the proposed framework.
- For some cases, TKPR ranks all the ground-truth labels in the top-5 list, which brings the improvement on P@K and R@K.

Table F3 The empirical results of state-of-the-art MLC methods and TKPR on MS-COCO, where the backbone is swin-transformer. The best and runner-up results on each metric are marked with **red** and **blue**, respectively. The best competitor on each measure is marked with underline.

Type	Metrics	P@K		R@K		mAP@K		NDCG@K		TKPR ^{α1}		TKPR ^{α2}		TKPR ^{α3}		Ranking Loss
	K	3	5	3	5	3	5	3	5	3	5	3	5	3	5	
Loss Oriented	ASL [†]	.705	.496	.838	.917	.932	.919	.951	.947	1.606	1.928	.754	.786	.318	.189	.0096
	DB-Loss	.698	.489	.831	.907	.924	.908	.944	.938	1.595	1.908	.749	.779	.316	.187	.0125
	CCD [†]	<u>.705</u>	<u>.498</u>	<u>.839</u>	<u>.920</u>	<u>.933</u>	<u>.921</u>	<u>.951</u>	<u>.948</u>	<u>1.606</u>	<u>1.930</u>	<u>.754</u>	<u>.787</u>	<u>.318</u>	<u>.189</u>	<u>.0094</u>
	Hill [†]	.696	.493	.832	.915	.918	.909	.940	.940	1.585	1.909	.745	.780	.314	.187	.0101
	SPLC [†]	.676	.487	.815	.909	.883	.883	.914	.922	1.532	1.862	.724	.765	.305	.183	.0116
TKPR (Ours)	α ₁	.712	.503	.847	.928	.940	.929	.956	.953	1.616	1.953	.759	.798	.321	.192	.0096
	α ₂	.710	.501	.844	.925	.937	.926	.955	.952	1.612	1.941	.756	.790	.319	.190	.0092
	α ₃	.707	.499	.842	.922	.935	.923	.953	.950	1.609	1.935	.755	.788	.319	.189	.0096

Table F4 The empirical results of state-of-the-art MLC methods and TKPR on NUS-WIDE, where the backbone is swin-transformer. The best and runner-up results on each metric are marked with **red** and **blue**, respectively. The best competitor on each measure is marked with underline.

Type	Metrics	P@K		R@K		mAP@K		NDCG@K		TKPR ^{α1}		TKPR ^{α2}		TKPR ^{α3}		Ranking Loss
		K	3	5	3	5	3	5	3	5	3	5	3	5		
Loss Oriented	ASL [†]	.573	.420	.799	.906	<u>.817</u>	.830	<u>.855</u>	.876	<u>1.318</u>	1.601	<u>.708</u>	.757	<u>.284</u>	.175	.0132
	DB-Loss	.572	.419	.798	.904	.815	.828	.853	.875	1.316	1.597	.707	.756	.283	.174	.0149
	CCD [†]	<u>.574</u>	<u>.422</u>	<u>.801</u>	<u>.910</u>	.816	<u>.831</u>	.854	<u>.877</u>	1.317	<u>1.602</u>	.707	<u>.758</u>	.284	<u>.175</u>	<u>.0127</u>
	Hill [†]	.570	.420	.798	.908	.803	.820	.844	.869	1.299	1.589	.699	.753	.280	.174	.0132
	SPLC [†]	.564	.420	.793	.908	.789	.810	.833	.862	1.278	1.574	.689	.747	.276	.172	.0137
TKPR (Ours)	α ₁	<u>.579</u>	<u>.424</u>	<u>.807</u>	<u>.914</u>	<u>.824</u>	<u>.838</u>	<u>.861</u>	<u>.883</u>	<u>1.328</u>	<u>1.613</u>	<u>.713</u>	<u>.763</u>	<u>.286</u>	<u>.176</u>	<u>.0126</u>
	α ₂	<u>.581</u>	<u>.425</u>	<u>.809</u>	<u>.916</u>	<u>.827</u>	<u>.840</u>	<u>.864</u>	<u>.885</u>	<u>1.336</u>	<u>1.617</u>	<u>.716</u>	<u>.767</u>	<u>.287</u>	<u>.177</u>	<u>.0122</u>
	α ₃	.578	.423	.806	.912	.824	.837	.861	.882	1.328	1.612	.713	.762	.286	.176	.0128

GT: [person, remote, chair, couch, laptop]
 Top-5 predictions:
 TKPR (Ours): [chair, laptop, remote, couch, person]
 ASL: [dining table, laptop, couch, remote, person]
 CCD: [kite, couch, keyboard, laptop, remote]
 Hill: [bowl, laptop, person, remote, couch]
 SPLC: [bowl, chair, person, couch, remote]



GT: [oven, bowl, sink, bottle]
 Top-5 predictions:
 TKPR (Ours): [oven, sink, microwave, bowl, bottle]
 ASL: [sink, spoon, bowl, oven, microwave]
 CCD: [bowl, sandwich, donut, bottle, oven]
 Hill: [bottle, spoon, microwave, bowl, oven]
 SPLC: [bottle, microwave, bowl, spoon, oven]



GT: [person, handbag, pizza]
 Top-5 predictions:
 TKPR (Ours): [pizza, handbag, sandwich, dining table, person]
 ASL: [handbag, hot dog, dining table, sandwich, person]
 CCD: [pizza, banana, orange, person, sandwich]
 Hill: [orange, bottle, pizza, sandwich, person]
 SPLC: [handbag, hot dog, sandwich, pizza, person]



GT: [person, book, bed, laptop]
 Top-5 predictions:
 TKPR (Ours): [laptop, bed, keyboard, person, book]
 ASL: [tv, cell phone, keyboard, person, book]
 CCD: [bed, book, laptop, keyboard, mouse]
 Hill: [laptop, cell phone, keyboard, person, book]
 SPLC: [teddy bear, laptop, keyboard, person, book]



GT: [person, cup, fork, knife, sandwich, hot dog, dining table]
 Top-5 predictions:
 TKPR (Ours): [hot dog, dining table, bowl, fork, person]
 ASL: [bowl, dining table, hot dog, fork, person]
 CCD: [cake, hot dog, apple, pizza, sandwich]
 Hill: [bowl, fork, person, dining table, hot dog]
 SPLC: [spoon, person, fork, hot dog, dining table]



GT: [person, oven, sink, refrigerator, vase, potted plant]
 Top-5 predictions:
 TKPR (Ours): [sink, refrigerator, bottle, oven, person]
 ASL: [bottle, refrigerator, sink, person, oven]
 CCD: [orange, sink, toilet, refrigerator, oven]
 Hill: [microwave, person, sink, bottle, oven]
 SPLC: [microwave, refrigerator, sink, oven, bottle]

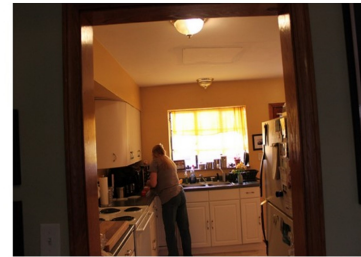


Fig. F2 Case study on the COCO dataset with the swin-transformer backbone, where the proposed methods rank the relevant labels higher than the competitors do.

GT: [sky, animal, water, whales, ocean]
 Top-5 predictions:
 TKPR (Ours): [sky, ocean, whales, animal, water]
 ASL: [lake, sky, water, whales, animal]
 CCD: [mountain, surf, lake, animal, whales]
 Hill: [clouds, whales, sky, water, animal]
 SPLC: [clouds, water, sky, animal, whales]



GT: [buildings, cityscape]
 Top-5 predictions:
 TKPR (Ours): [lake, cityscape, bridge, buildings, water]
 ASL: [sky, bridge, lake, buildings, water]
 CCD: [bridge, airport, plane, buildings, sign]
 Hill: [snow, bridge, lake, buildings, water]
 SPLC: [lake, sky, cityscape, water, buildings]



GT: [road, sky, tree, grass]
 Top-5 predictions:
 TKPR (Ours): [grass, road, plants, sky, tree]
 ASL: [road, plants, clouds, sky, tree]
 CCD: [tree, flowers, grass, sign, plants]
 Hill: [road, plants, sky, grass, tree]
 SPLC: [road, frost, sky, plants, tree]



GT: [running, animal, dog]
 Top-5 predictions:
 TKPR (Ours): [toy, running, snow, dog, animal]
 ASL: [sand, toy, snow, dog, animal]
 CCD: [toy, mountain, running, animal, snow]
 Hill: [toy, sky, snow, animal, dog]
 SPLC: [toy, cat, snow, dog, animal]



GT: [sky, lake, beach]
 Top-5 predictions:
 TKPR (Ours): [lake, beach, clouds, sky, water]
 ASL: [sky, rocks, lake, beach, water]
 CCD: [lake, rocks, beach, grass, flowers]
 Hill: [lake, ocean, clouds, sky, water]
 SPLC: [beach, ocean, sky, clouds, water]



GT: [plants, sunset, grass]
 Top-5 predictions:
 TKPR (Ours): [sand, sunset, sky, plants, grass]
 ASL: [mountain, sand, sky, plants, grass]
 CCD: [garden, sand, sign, flowers, grass]
 Hill: [mountain, sand, plants, sky, grass]
 SPLC: [sand, clouds, plants, sky, grass]



Fig. F3 Case study on the NUS-WIDE dataset with the swin-transformer backbone, where the proposed methods rank the relevant labels higher than the competitors do.

F.3 More MLML experiments on Pascal VOC 2012

In Tab.F5 and Tab.F6, we present the results on Pascal VOC 2012 in the MLML setting. From these results, we have the following observations:

- Compared with the ranking-based losses, the proposed methods also demonstrate significant improvements on mAP@K, NDCG@K, the ranking loss, and the TKPR measures. Note that for the competitors, the performance degeneration induced by missing labels seems insignificant. This phenomenon is not surprising since the relevant labels are inherently sparse in Pascal VOC 2012.
- Compared with state-of-the-art methods, the proposed methods achieve consistent improvements on all the measures. Note that these performance gains are not so impressive than those in MS-COCO, *i.e.*, Tab.8, which might again comes from the sparse property of the dataset.
- The best competitors differ on different measures, which again validates the necessity of the proposed framework.

Table F5 The empirical results of the ranking-based losses and TKPR on Pascal VOC 2012-MLML, where the backbone is ResNet50. The best and runner-up results on each metric are marked with red and blue, respectively. The best competitor on each measure is marked with underline.

Type	Metrics	P@K		R@K		mAP@K		NDCG@K		TKPR ^{α1}		TKPR ^{α2}		TKPR ^{α3}		Ranking Loss
	K	3	5	3	5	3	5	3	5	3	5	3	5	3	5	
Ranking loss	L_{rank}	.438	.277	.943	.976	.893	.906	.917	.932	1.131	1.227	.850	.897	.304	.187	.0199
	L_{u1}	.444	.279	.955	.983	<u>.926</u>	<u>.938</u>	<u>.944</u>	<u>.957</u>	<u>1.166</u>	<u>1.253</u>	<u>.877</u>	<u>.916</u>	<u>.313</u>	<u>.191</u>	<u>.0136</u>
	L_{u2}	.444	.279	.955	.983	.926	.937	.944	.956	1.166	1.253	.877	.916	.313	.191	.0137
	L_{u3}	<u>.445</u>	<u>.280</u>	<u>.956</u>	<u>.984</u>	.919	.930	.939	.951	1.160	1.251	.871	.913	.311	.191	.0139
	L_{u4}	.444	.279	.955	.983	.926	.937	.944	.956	1.166	1.253	.877	.916	.313	.191	.0137
	L_{LSEP}	.444	.280	.954	.983	.915	.927	.936	.949	1.157	1.249	.869	.911	.310	.190	.0148
	L_{TKML}	.443	.280	.951	.983	.910	.923	.931	.946	1.149	1.244	.863	.908	.308	.189	.0158
TKPR (Ours)	α_1	<u>.450</u>	<u>.282</u>	<u>.963</u>	<u>.987</u>	<u>.939</u>	<u>.947</u>	<u>.954</u>	<u>.963</u>	<u>1.181</u>	<u>1.266</u>	<u>.886</u>	<u>.924</u>	<u>.317</u>	<u>.193</u>	<u>.0112</u>
	α_2	<u>.448</u>	<u>.280</u>	<u>.961</u>	<u>.985</u>	<u>.938</u>	<u>.948</u>	<u>.953</u>	<u>.964</u>	<u>1.180</u>	<u>1.264</u>	<u>.887</u>	<u>.923</u>	<u>.317</u>	<u>.193</u>	<u>.0116</u>
	α_3	.447	.280	.961	.985	.938	.947	.953	.963	1.180	1.264	.886	.923	.316	.192	.0117

Table F6 The empirical results of state-of-the-art MLML methods and TKPR on Pascal VOC 2012-MLML, where the backbone is ResNet50. The best and runner-up results on each metric are marked with red and blue, respectively. The best competitor on each measure is marked with underline.

Type	Metrics	P@K		R@K		mAP@K		NDCG@K		TKPR ^{α1}		TKPR ^{α2}		TKPR ^{α3}		Ranking Loss
	K	3	5	3	5	3	5	3	5	3	5	3	5	3	5	
Loss Oriented	ROLE [†]	.443	.276	.955	.978	.935	.944	.951	.961	1.175	1.254	.885	.920	.316	.192	.0163
	EM+APL [†]	.446	.277	.959	.979	<u>.937</u>	<u>.944</u>	<u>.952</u>	<u>.961</u>	<u>1.179</u>	<u>1.259</u>	<u>.886</u>	.920	<u>.316</u>	.192	.0157
	Hill [†]	.444	.279	.956	.984	.924	.935	.942	.955	1.165	1.253	.876	.916	.313	.191	.0137
	SPLC [†]	<u>.446</u>	<u>.280</u>	.958	.984	.929	.939	.947	.958	1.170	1.257	.879	.918	.314	<u>.192</u>	.0137
	LL-R [†]	.427	.266	.962	.986	.924	.934	.942	.954	1.132	1.207	.883	.922	.311	.191	.0131
	LL-C [†]	.427	.266	.962	<u>.987</u>	.925	.937	.943	.956	1.134	1.209	.884	<u>.924</u>	.312	.191	<u>.0128</u>
	LL-Cp [†]	.428	.265	<u>.963</u>	.986	.926	.936	.944	.955	1.137	1.210	.885	.924	.312	.191	.0131
TKPR (Ours)	α_1	<u>.451</u>	<u>.281</u>	<u>.965</u>	<u>.987</u>	<u>.942</u>	<u>.950</u>	<u>.957</u>	<u>.966</u>	<u>1.183</u>	<u>1.268</u>	<u>.887</u>	<u>.925</u>	<u>.318</u>	<u>.193</u>	<u>.0112</u>
	α_2	<u>.450</u>	<u>.280</u>	<u>.966</u>	.986	<u>.941</u>	<u>.949</u>	<u>.956</u>	<u>.965</u>	<u>1.183</u>	<u>1.267</u>	<u>.888</u>	<u>.925</u>	<u>.317</u>	<u>.193</u>	<u>.0114</u>
	α_3	.450	.280	.965	.986	.941	.949	.956	.965	1.183	<u>1.268</u>	.887	.924	.317	.192	.0114

References

- Aljundi R, Patel Y, Sulc M, et al (2023) Contrastive classification and representation learning with probabilistic interpretation. In: AAAI Conference on Artificial Intelligence, pp 6675–6683
- Andrews GE (1998) *The Theory of Partitions*. Cambridge University Press
- Baruch EB, Ridnik T, Friedman I, et al (2022) Multi-label classification with partial annotations using class-aware selective loss. In: IEEE/CVF Conference on Computer Vision and Pattern Recognition, pp 4754–4762
- Boutell MR, Luo J, Shen X, et al (2004) Learning multi-label scene classification. *Pattern Recognit* 37:1757–1771
- Brown A, Xie W, Kalogeiton V, et al (2020) Smooth-ap: Smoothing the path towards large-scale image retrieval. In: European Conference on Computer Vision, pp 677–694
- Carneiro G, Chan AB, Moreno PJ, et al (2007) Supervised learning of semantic classes for image annotation and retrieval. *IEEE Trans Pattern Anal Mach Intell* 29:394–410
- Chen C, Zhao Y, Li J (2023) Semantic contrastive bootstrapping for single-positive multi-label recognition. *Int J Comput Vis* 131:3289–3306
- Chen Z, Wei X, Wang P, et al (2019) Multi-label image recognition with graph convolutional networks. In: IEEE Conference on Computer Vision and Pattern Recognition, pp 5177–5186
- Chua T, Tang J, Hong R, et al (2009) NUS-WIDE: a real-world web image database from national university of singapore. In: ACM International Conference on Image and Video Retrieval
- Clare A, King RD (2001) Knowledge discovery in multi-label phenotype data. In: European Conference on Principles of Data Mining and Knowledge Discovery, pp 42–53
- Cole E, Aodha OM, Lorieul T, et al (2021) Multi-label learning from single positive labels. In: IEEE Conference on Computer Vision and Pattern Recognition, pp 933–942
- Dai S, Xu Q, Yang Z, et al (2023) DRAUC: an instance-wise distributionally robust AUC optimization framework. In: Annual Conference on Neural Information Processing Systems, pp 44658–44670
- Davis J, Goadrich M (2006) The relationship between precision-recall and ROC curves. In: International Conference on Machine Learning, pp 233–240
- Dembczynski K, Cheng W, Hüllermeier E (2010) Bayes optimal multilabel classification via probabilistic classifier chains. In: International Conference on Machine Learning, pp 279–286
- Dembczynski K, Kotowski W, Hüllermeier E (2012a) Consistent multilabel ranking through univariate losses. In: International Conference on Machine Learning, pp 1–8
- Dembczynski K, Waegeman W, Cheng W, et al (2012b) On label dependence and loss minimization in multi-label classification. *Mach Learn* 88:5–45
- Deng J, Dong W, Socher R, et al (2009) Imagenet: A large-scale hierarchical image database. In: IEEE Conference on Computer Vision and Pattern Recognition, pp 248–255

- Ding Z, Wang A, Chen H, et al (2023) Exploring structured semantic prior for multi label recognition with incomplete labels. In: IEEE/CVF Conference on Computer Vision and Pattern Recognition, pp 3398–3407
- Elisseff A, Weston J (2001) A kernel method for multi-labelled classification. In: Annual Conference on Neural Information Processing Systems, pp 681–687
- Everingham M, Gool LV, Williams CKI, et al (2010) The pascal visual object classes (VOC) challenge. *International Journal of Computer Vision* 88:303–338
- Fokas AS, Lenells J (2022) On the asymptotics to all orders of the riemann zeta function and of a two-parameter generalization of the riemann zeta function. *Mem Amer Math Soc* 275:1–62
- Fürnkranz J, Hüllermeier E, Mencía EL, et al (2008) Multilabel classification via calibrated label ranking. *Mach Learn* 73:133–153
- Gao W, Zhou Z (2013) On the consistency of multi-label learning. *Artif Intell* 199-200:22–44
- Gerych W, Hartvigsen T, Buquicchio L, et al (2021) Recurrent bayesian classifier chains for exact multi-label classification. In: Annual Conference on Neural Information Processing Systems, pp 15981–15992
- Golowich N, Rakhlin A, Shamir O (2018) Size-independent sample complexity of neural networks. In: Conference On Learning Theory, pp 297–299
- Goodfellow I, Bengio Y, Courville A (2016) Deep learning. MIT press
- Hardy GH, Littlewood JE, Pólya G, et al (1952) Inequalities. Cambridge university press
- He K, Zhang X, Ren S, et al (2016) Deep residual learning for image recognition. In: IEEE Conference on Computer Vision and Pattern Recognition, pp 770–778
- Hu S, Ying Y, Wang X, et al (2020) Learning by minimizing the sum of ranked range. In: Annual Conference on Neural Information Processing Systems, pp 1–11
- Huang W, Wu Z, Liang C, et al (2015) A neural probabilistic model for context based citation recommendation. In: AAAI Conference on Artificial Intelligence, pp 2404–2410
- Ibrahim KM, Epure EV, Peeters G, et al (2020) Confidence-based weighted loss for multi-label classification with missing labels. In: International Conference on Multimedia Retrieval, pp 291–295
- Jernite Y, Choromanska A, Sontag DA (2017) Simultaneous learning of trees and representations for extreme classification and density estimation. In: International Conference on Machine Learning, pp 1665–1674
- Kalina J, Krzysztof D (2018) Bayes optimal prediction for ndcg@k in extreme multi-label classification. In: Workshop on Multiple Criteria Decision Aid to Preference Learning, pp 1–4
- Khosla P, Teterwak P, Wang C, et al (2020) Supervised contrastive learning. In: Annual Conference on Neural Information Processing Systems, pp 18661–18673
- Kim Y, Kim J, Akata Z, et al (2022) Large loss matters in weakly supervised multi-label classification. In: IEEE/CVF Conference on Computer Vision and Pattern Recognition

- Kim Y, Kim J, Jeong J, et al (2023) Bridging the gap between model explanations in partially annotated multi-label classification. In: IEEE/CVF Conference on Computer Vision and Pattern Recognition, pp 3408–3417
- Lapin M, Hein M, Schiele B (2015) Top-k multiclass SVM. In: Annual Conference on Neural Information Processing Systems, pp 325–333
- Lapin M, Hein M, Schiele B (2016) Loss functions for top-k error: Analysis and insights. In: IEEE Conference on Computer Vision and Pattern Recognition, pp 1468–1477
- Lapin M, Hein M, Schiele B (2018) Analysis and optimization of loss functions for multiclass, top-k, and multilabel classification. *IEEE Trans Pattern Anal Mach Intell* 40:1533–1554
- Li T, Gao S, Xu Y (2017a) Deep multi-similarity hashing for multi-label image retrieval. In: ACM Conference on Information and Knowledge Management, pp 2159–2162
- Li Y, Song Y, Luo J (2017b) Improving pairwise ranking for multi-label image classification. In: IEEE Conference on Computer Vision and Pattern Recognition, pp 1837–1845
- Lin T, Maire M, Belongie SJ, et al (2014) Microsoft COCO: common objects in context. In: European Conference on Computer Vision, pp 740–755
- Ling CX, Huang J, Zhang H (2003) AUC: a statistically consistent and more discriminating measure than accuracy. In: International Joint Conference on Artificial Intelligence, pp 519–526
- Liu B, Xu N, Lv J, et al (2023) Revisiting pseudo-label for single-positive multi-label learning. In: International Conference on Machine Learning, pp 22249–22265
- Liu J, Chang W, Wu Y, et al (2017) Deep learning for extreme multi-label text classification. In: International ACM SIGIR Conference on Research and Development in Information Retrieval, pp 115–124
- Liu R, Liu H, Li G, et al (2022a) Contextual debiasing for visual recognition with causal mechanisms. In: IEEE/CVF Conference on Computer Vision and Pattern Recognition, pp 12745–12755
- Liu T (2009) Learning to rank for information retrieval. *Found Trends Inf Retr* 3:225–331
- Liu W, Wang H, Shen X, et al (2022b) The emerging trends of multi-label learning. *IEEE Trans Pattern Anal Mach Intell* 44:7955–7974
- Liu Z, Lin Y, Cao Y, et al (2021) Swin transformer: Hierarchical vision transformer using shifted windows. In: IEEE/CVF International Conference on Computer Vision, pp 9992–10002
- Long PM, Sedghi H (2020) Generalization bounds for deep convolutional neural networks. In: International Conference on Learning Representations, pp 1–15
- Maurer A (2016) A vector-contraction inequality for rademacher complexities. In: International Conference on Algorithmic Learning Theory, pp 3–17
- Menon AK, Rawat AS, Reddi SJ, et al (2019) Multilabel reductions: what is my loss optimising? In: Annual Conference on Neural Information Processing Systems, pp 10599–10610

- Mohapatra P, Rolínek M, Jawahar CV, et al (2018) Efficient optimization for rank-based loss functions. In: IEEE Conference on Computer Vision and Pattern Recognition, pp 3693–3701
- Mohri M, Rostamizadeh A, Talwalkar A (2012) Foundations of Machine Learning. The MIT Press
- Paszke A, Gross S, Massa F, et al (2019) Pytorch: An imperative style, high-performance deep learning library. In: Annual Conference on Neural Information Processing Systems, pp 8024–8035
- Prabhu Y, Varma M (2014) Fastxml: a fast, accurate and stable tree-classifier for extreme multi-label learning. In: ACM SIGKDD International Conference on Knowledge Discovery and Data Mining, pp 263–272
- Qiu Z, Hu Q, Zhong Y, et al (2022) Large-scale stochastic optimization of NDCG surrogates for deep learning with provable convergence. In: International Conference on Machine Learning, pp 18122–18152
- Radlinski F, Craswell N (2010) Comparing the sensitivity of information retrieval metrics. In: ACM SIGIR Conference on Research and Development in Information Retrieval, pp 667–674
- Ramzi E, Thome N, Rambour C, et al (2021) Robust and decomposable average precision for image retrieval. In: Annual Conference on Neural Information Processing Systems, pp 23569–23581
- Ridnik T, Baruch EB, Zamir N, et al (2021) Asymmetric loss for multi-label classification. In: IEEE/CVF International Conference on Computer Vision, pp 82–91
- Russakovsky O, Deng J, Su H, et al (2015) Imagenet large scale visual recognition challenge. *Int J Comput Vis* 115:211–252
- Sun Y, Zhang Y, Zhou Z (2010) Multi-label learning with weak label. In: AAAI Conference on Artificial Intelligence, pp 593–598
- Sutskever I, Martens J, Dahl GE, et al (2013) On the importance of initialization and momentum in deep learning. In: International Conference on Machine Learning, pp 1139–1147
- Swezey RME, Grover A, Charron B, et al (2021) Pirank: Scalable learning to rank via differentiable sorting. In: Annual Conference on Neural Information Processing Systems, pp 21644–21654
- Tang P, Jiang M, Xia BN, et al (2020) Multi-label patent categorization with non-local attention-based graph convolutional network. In: AAAI Conference on Artificial Intelligence, pp 9024–9031
- Titchmarsh EC, Heath-Brown DR, Titchmarsh ECT, et al (1986) The theory of the Riemann zeta-function. Oxford university press
- Tsoumakas G, Katakis I, Vlahavas IP (2011a) Random k-labelsets for multilabel classification. *IEEE Trans Knowl Data Eng* 23:1079–1089
- Tsoumakas G, Xioufis ES, Vilcek J, et al (2011b) MULAN: A java library for multi-label learning. *J Mach Learn Res* 12:2411–2414
- Waegeman W, Dembczynski K, Jachnik A, et al (2014) On the bayes-optimality of f-measure maximizers. *J Mach Learn Res* 15:3333–3388
- Wang J, Yang Y, Mao J, et al (2016) CNN-RNN: A unified framework for multi-label image classification. In: IEEE Conference on Computer Vision and Pattern Recognition, pp 2285–2294

- Wang Y, Wang L, Li Y, et al (2013) A theoretical analysis of NDCG type ranking measures. In: Annual Conference on Learning Theory, pp 25–54
- Wang Z, Chen T, Li G, et al (2017) Multi-label image recognition by recurrently discovering attentional regions. In: IEEE International Conference on Computer Vision, pp 464–472
- Wang Z, Xu Q, Yang Z, et al (2022) Openauc: Towards auc-oriented open-set recognition. In: Annual Conference on Neural Information Processing Systems, pp 25033–25045
- Wang Z, Xu Q, Yang Z, et al (2023) Optimizing partial area under the top-k curve: Theory and practice. *IEEE Trans Pattern Anal Mach Intell* 45:5053–5069
- Wei T, Mao Z, Shi J, et al (2022) A survey on extreme multi-label learning. *CoRR* abs/2210.03968
- Wen P, Xu Q, Yang Z, et al (2022a) Exploring the algorithm-dependent generalization of auprc optimization with list stability. In: Annual Conference on Neural Information Processing Systems
- Wen P, Xu Q, Yang Z, et al (2022b) Exploring the algorithm-dependent generalization of AUPRC optimization with list stability. In: Annual Conference on Neural Information Processing Systems, pp 28335–28349
- Wen P, Xu Q, Yang Z, et al (2024) Algorithm-dependent generalization of AUPRC optimization: Theory and algorithm. *IEEE Trans Pattern Anal Mach Intell* 46:5062–5079
- Wu B, Liu Z, Wang S, et al (2014) Multi-label learning with missing labels. In: International Conference on Pattern Recognition, pp 1964–1968
- Wu B, Jia F, Liu W, et al (2018) Multi-label learning with missing labels using mixed dependency graphs. *Int J Comput Vis* 126:875–896
- Wu G, Zhu J (2020) Multi-label classification: do hamming loss and subset accuracy really conflict with each other? In: Annual Conference on Neural Information Processing Systems, pp 1–11
- Wu G, Li C, Xu K, et al (2021) Rethinking and reweighting the univariate losses for multi-label ranking: Consistency and generalization. In: Annual Conference on Neural Information Processing Systems, pp 14332–14344
- Wu G, Li C, Yin Y (2023) Towards understanding generalization of macro-auc in multi-label learning. In: International Conference on Machine Learning, pp 37540–37570
- Wu T, Huang Q, Liu Z, et al (2020) Distribution-balanced loss for multi-label classification in long-tailed datasets. In: European Conference on Computer Vision, pp 162–178
- Wu X, Zhou Z (2017) A unified view of multi-label performance measures. In: International Conference on Machine Learning, pp 3780–3788
- Wydmuch M, Jasinska K, Kuznetsov M, et al (2018) A no-regret generalization of hierarchical softmax to extreme multi-label classification. In: Bengio S, Wallach HM, Larochelle H, et al (eds) Annual Conference on Neural Information Processing Systems, pp 6358–6368
- Xie M, Huang S (2022) Partial multi-label learning with noisy label identification. *IEEE Trans Pattern Anal Mach Intell* 44:3676–3687

- Xie Y, Dai H, Chen M, et al (2020) Differentiable top-k with optimal transport. In: Annual Conference on Neural Information Processing Systems, pp 20520–20531
- Xu B, Bu J, Chen C, et al (2012) An exploration of improving collaborative recommender systems via user-item subgroups. In: International World Wide Web Conference, pp 21–30
- Xu J, Li H (2007) Adarank: a boosting algorithm for information retrieval. In: ACM SIGIR Conference on Research and Development in Information Retrieval, pp 391–398
- Xu N, Lv J, Geng X (2019) Partial label learning via label enhancement. In: AAAI Conference on Artificial Intelligence, pp 5557–5564
- Xu Q, Xiong J, Huang Q, et al (2014) Online hodgerank on random graphs for crowdsourcable qoe evaluation. *IEEE Trans Multim* 16:373–386
- Yang F, Koyejo S (2020) On the consistency of top-k surrogate losses. In: International Conference on Machine Learning, pp 10727–10735
- Yang T, Ying Y (2023) AUC maximization in the era of big data and AI: A survey. *ACM Comput Surv* 55:172:1–172:37
- Yang Z, Xu Q, Bao S, et al (2022) Learning with multiclass AUC: theory and algorithms. *IEEE Trans Pattern Anal Mach Intell* 44:7747–7763
- Yang Z, Xu Q, Bao S, et al (2023) Optimizing two-way partial AUC with an end-to-end framework. *IEEE Trans Pattern Anal Mach Intell* 45:10228–10246
- Ye J, He J, Peng X, et al (2020) Attention-driven dynamic graph convolutional network for multi-label image recognition. In: European Conference on Computer Vision, pp 649–665
- Ye N, Chai KMA, Lee WS, et al (2012) Optimizing f-measure: A tale of two approaches. In: International Conference on Machine Learning, pp 1–8
- You R, Guo Z, Cui L, et al (2020) Cross-modality attention with semantic graph embedding for multi-label classification. In: AAAI Conference on Artificial Intelligence, pp 12709–12716
- Zhang M, Zhou Z (2014) A review on multi-label learning algorithms. *IEEE Trans Knowl Data Eng* 26:1819–1837
- Zhang Y, Cheng Y, Huang X, et al (2021) Simple and robust loss design for multi-label learning with missing labels. *CoRR* abs/2112.07368
- Zhou D, Chen P, Wang Q, et al (2022) Acknowledging the unknown for multi-label learning with single positive labels. In: European Conference on Computer Vision, pp 423–440